8-18-2014 12:00 AM

Size-dependent Electroelastic Properties of Piezoelectric Nanoplates

Zhengrong Zhang, *The University of Western Ontario*

Supervisor: Liying Jiang, *The University of Western Ontario*

A thesis submitted in partial fulfillment of the requirements for the Master of Engineering Science degree in Mechanical and Materials Engineering

Size-dependent Electroelastic Properties of Piezoelectric Nanoplates

(Thesis format: Integrated Article)

by

Zhengrong Zhang

Graduate Program in Mechanical and Materials Engineering

A thesis submitted in partial fulfillment
of the requirements for the degree of
Master of Engineering Science

The School of Graduate and Postdoctoral Studies
The University of Western Ontario
London, Ontario, Canada

Abstract

With the development of nanotechnology, piezoelectric nanostructures have attracted a surge of interests in research communities for the potential applications as transistors, sensors, actuators, resonators and energy harvesters in nanoelectromechanical systems (NEMS) due to their high electromechanical coupling and unique features at the nano-scale. Piezoelectric nanomaterials have been characterized to possess size-dependent electromechanical coupling properties from both experimental and theoretical perspectives. Therefore it is of great importance to investigate the physical mechanisms of these distinct nano-scale structure features in order to fulfill the design and application of those piezoelectricity-based nanodevices.

Due to large surface to volume ratio and manifest strain gradients typically present in nanostructures, surface effects and flexoelectricity are commonly believed to be responsible for the size-dependent electromechanical properties of piezoelectric nanomaterials. This thesis aims to develop modified continuum mechanics models with the consideration of the surface effects and the flexoelectricity to theoretically investigate such size effects. Based on the classical Kirchhoff plate model and the extended linear piezoelectricity theory, the influence of flexoelectricity on the static bending and the transverse vibration of a piezoelectric nanoplate (PNP) is firstly examined. Then the surface effects including the residual surface stress, the surface elasticity and the surface piezoelectricity are further incorporated to develop a more comprehensive modified Kirchhoff plate model in addition to the flexoelectricity. Variational principle is adopted to derive the governing equations and the corresponding boundary conditions for a clamped PNP.

Ritz approximate solutions for the static bending and the free vibration of the PNP indicate that the influence of the flexoelectricity and the surface effects is more prominent for thinner plates with smaller thickness. The simulation results also demonstrate that such size effects on the electromechanical coupling behaviors of the PNP are sensitive to the surface material properties, the applied electrical load and the plate dimensions. Moreover, it also suggests that the possible frequency tuning of PNP-based resonators through the applied electric voltage could be modified by either the flexoelectricity or the surface effects.

The current work is claimed to provide increased understanding on the fundamental physics of the size-dependent electromechanical coupling properties of piezoelectric nanostructures and thus benefit the design and applications of PNP-based nanodevices.

Keywords

Flexoelectricity; Surface effects; Piezoelectric nanoplates; Size-dependent properties

Co-Authorship Statement

Title: Flexoelectric effect on the electroelastic responses and vibrational behaviors of a piezoelectric nanoplate (Chapter 2)

Authors: Z. R. Zhang, Z. Yan and L. Y. Jiang

Dr. L. Y. Jiang initiated the idea of the work. The derivation of formulations was conducted by the candidate under the guidance of Z. Yan and Dr. L. Y. Jiang. The simulation results were interpreted by the candidate under the constructive suggestions of Dr. L. Y. Jiang. The candidate wrote the first draft of the manuscript and Dr. L. Y. Jiang reviewed and modified this paper. This paper was published by Journal of Applied Physics, Vol. 116, 014307, (2014).

Title: Size effects on electromechanical coupling fields of a bending piezoelectric nanoplate due to surface effects and flexoelectricity (Chapter 3)

Authors: Z. R. Zhang and L. Y. Jiang

Dr. L. Y. Jiang initiated the topic of the work. The derivation of formulations was conducted by the candidate. The simulation results were interpreted by the candidate under the constructive suggestions of Dr. L. Y. Jiang. The candidate wrote the first draft of the manuscript and Dr. L. Y. Jiang reviewed and modified the draft chapters. This manuscript has been submitted for publication.

Acknowledgments

I would like to express my greatest gratitude to my supervisor Professor Liying Jiang for giving me this valuable opportunity to study at The University of Western Ontario. Her guidance, patience and constructive suggestions throughout my Master study not only helped me gain knowledge but also taught me the required attitude for research.

Much appreciation would be expressed to my advisory committee members Dr. Asokanthan and Dr. Sun for their help.

I would like to thank the assistance and guidance from the faculty and staff members in the Department of Mechanical and Materials Engineering at The University of Western Ontario. Much appreciation would also be expressed to my colleagues in Professor Liying Jiang's research group for their help and support.

I also appreciated the financial support from Natural Sciences and Engineering Research Council of Canada (NSERC).

Finally, my special grateful thanks would be expressed to my parents for their unending love and support and to my friends for their help and encouragement.

Table of Contents

List of Figures

Chapter 1

1 Introduction

1.1 Piezoelectric nanomaterials and their size-dependent properties

Piezoelectric materials represent a particularly interesting class of smart materials, possessing highly efficient electromechanical coupling, i.e., piezoelectricity, which is a unique feature for non-centrosymmetric dielectric materials. For such kind of crystals, the center of the positive charge coincides with the center of the negative charge without any applied force, resulting in zero polarization. However, when an external force is applied, the centers of the positive and negative charges undergo relative displacement with respect to each other and induce a dipole moment. Those dipole moments give rise to the polarization. In contrast, for centrosymmetric crystals, the centers of the positive and negative charges still coincide with each other even under uniform strains. Thus no polarization is induced in the crystals, indicating no piezoelectricity for centrosymmetric dielectrics. The direct piezoelectric effect is defined as the change in electric field with the applied mechanical stress or strain and the generation of the stress or strain in response to the applied electric field is accordingly referred as the converse piezoelectric effect (Cady, 1946; Lew *et al*., 2011). With the development of nanotechnology and synthesis techniques, a variety of piezoelectric nanomaterials have been synthesized under different growth conditions. In general, nanostructured materials are defined as materials with morphological features on the nano-scale, which are smaller than one tenth

of a micrometer in at least one direction (Mishra and Sethy, 2013). Those nanostructures can be classified into three groups based on their dimensions (Fang *et al.*, 2013), including zero-dimensional (0D) nanoparticles (Capsal *et al.,* 2011); one-dimensional (1D) piezoelectric nanostructures such as nanowires (Wang *et al.*, 2006), nanotubes (She *et al*., 2007), nanobelts (Wang *et al*., 2007), and *etc*.; and two-dimensional (2D) piezoelectric nanostructures such as nanofilms (Yamano *et al*., 2012) and nanoribbons (Qi *et al*., 2010). Such nanostructured materials may possess special physical and mechanical properties stemming from their nano-scale features. In particular, the enhanced electromechanical coupling of piezoelectric nanomaterials makes them attractive for the potential applications as generators, sensors and transducers. (Wang *et al.*, 2006; Sun *et al*., 2010; Lew *et al*., 2011; Fang *et al.*, 2013) in nanoelectromechanical systems (NEMS). In order to further explore the piezoelectric nanomaterials and apply them commercially, it is of great importance to get a thorough and comprehensive understanding of their electromechanical coupling properties at the nano-scale.

It was reported from the existing experimental observations that the physical properties of piezoelectric nanostructures are different from their bulk counterparts when their characteristic size scales down to the nano-scale. For example, the elastic moduli of ZnO nanowires were found to increase pronouncedly with the decreasing diameter of the nanowires when the nanowire size was reduced to a certain small value, demonstrating the size-dependent features of nanomaterials (Stan *et al*., 2007; Agrawal *et al.*, 2008; Chen *et al*., 2006). The effective piezoelectric coefficient of ZnO nanobelts was experimentally determined through a piezoresponse force microscopy by Zhao *et al*. (2004) and it was demonstrated to be significantly larger than that of the bulk ZnO. In

addition to the experimental work, computational methods have also been adopted to capture the size-dependent properties of piezoelectric nanomaterials. For example, Kulkarni *et al.* (2005) conducted molecular dynamic simulations to investigate the ultimate tensile stress and the Young's modulus of the ZnO nanobelts when subjected to tensile loadings. It was found in this work that the elastic response was dependent on the orientation and size of the nanobelts. Agrawal and Espinosa (2011) also found the giant size dependence of the piezoelectric coefficient of ZnO and GaN nanowires by performing the first principle-based density function theory calculation. In order to fulfill the potential applications of the piezoelectric nanomaterials, it is essential to understand the origins and underlying physics of such size dependency of the electromechanical coupling.

1.2 Literature review

1.2.1 Size-dependence attributes: flexoelectricity and surface effects

Due to the manifest strain gradients and large surface to volume ratio typically presented in the nanostructured materials, flexoelectricity and surface effects are commonly believed to be responsible for the size-dependent properties of nanostructured materials.

Flexoelectricity is defined as a spontaneous polarization in dielectrics in response to strain gradients or nonuniform strain fields. In contrast to the traditional electromechanical coupling, i.e., piezoelectricity which only exists in the non-centrosymmetric dielectrics, flexoelectricity is a universal effect present in all dielectric materials since the strain gradients locally break the inversion symmetry of the material structure and thus lead to polarization even in the centrosymmetric dielectrics

(Maranganti and Sharma, 2009). Phenomenologically, the polarization induced by the flexoelectricity is proportional to the strain gradients and the flexoelectric coefficients. In general, such flexoelectric effect is less significant compared to the piezoelectric effect for macro-scale piezoelectric materials due to the relative small values of the flexoelectric coefficients. However, the flexoelectricity may become comparable when the characteristic size of the structure scales down to the nano-scale (Majdoub e*t al*., 2008) since the strain gradients are inversely proportional to the structure characteristic size. Therefore it is necessary to incorporate the size-dependent flexoelectric effect in investigating the electromechanical coupling behaviors of piezoelectric nanomaterials. A thorough and comprehensive review of the fundamental physics, influences and potential applications of the flexoelectricity in solids has been conducted by Nguyen *et al.* (2013), Yudin and Tagantsev (2013) and Zubko *et al.* (2013).

In parallel to the flexoelectricity, surface effects also play a significant role in characterizing the size effects of piezoelectric materials at nano-scale. Due to the different constraints of the surface atoms and the bulk ones, the energy associated with the atoms at and near the surface is different from the atoms in the bulk (Streitz *et al*., 1994) rendering the formation of the free surface energy in the solids. The concept of the surface stress was introduced by Gibbs (1906) as the work-conjugate to surface strain with respect to surface energy. Since the effect of surfaces on the nearby atoms generally extends to a few atomic layers acting like a transition interphase, the Gibbs idealization ascribes the surface energy and the surface stress to a “mathematical surface” with zero thickness. The effect of surface stress is generally not considered in the conventional continuum solid mechanics theories (Wang *et al.*, 2011). However, neglecting such effect

will no longer be accurate when the characteristic size of the materials scales down to the nanometers due to the large surface to volume ratio typically present in the nanostructures. Such surface effects may significantly contribute to the size-dependent properties of nanomaterials. For elastic nanomaterials, a general continuum model incorporating the surface effects was elaborated by Gurtin and Murdoch (1975). Under a reasonable assumption, a surface can be regarded as a thin layer with negligible thickness adhered to the bulk without slipping (Cammarata, 1994; Miller and Shenoy, 2000). The constitutive and equilibrium equations for the surface layer are different from those in the bulk of the solid.

The size effects on the electromechanical coupling behaviors of piezoelectric nanostructures have recently stimulated a surge of interests in the research communities. This literature review will elaborate the current state of art research about the size-dependent surface effects and the flexoelectricity in the following sections.

1.2.2 Characterization and influence of the flexoelectricity

Tagantsev (1985) developed a phenomenological description of the flexoelectricity and suggested that the flexoelectric coefficients might be proportional to the dielectric susceptibility. This perception was later justified by a series of experimental work conducted by Ma and Cross (2001; 2002; 2005; 2006). Additionally, the flexoelectric coefficients of some dielectrics such as $BaTiO_3$ and $SrTiO_3$ were computed via the first principle theory and the *ab initio* calculation (Hong and Vanderbilt 2013; Xu *et al*., 2013; Yin and Qu, 2014). These investigations provide basis for further quantitatively characterizing the flexoelectric effect in dielectrics.

It was reported in the literature that the flexoelectricity opens new avenues for tuning the physical properties of nanoferroelectrics. For example, Lee *et al*. (2011) has demonstrated that the flexoelectricity can modify the domain configurations and the hysteresis loop of the ferroelectric epitaxial thin films. The dielectric constants of the ferroelectric epitaxial thin films were found to reduce due to the flexoelectricity (Gatalan *et al*., 2004). It was explained by Majdoub e*t al*. (2009) that the dead layer effect caused by the flexoelectricity was responsible for the lower capacity of the nanocapacitors. Moreover, the apparent piezoelectric coefficients of piezoelectric nanostructures were found to be magnified by the flexoelectricity (Majdoub e*t al*., 2008). Due to this enhanced electromechanical coupling induced by the flexoelectricity, it was also proposed by Fousek *et al*. (1999) and Sharma *et al*. (2010) that the mechanism of flexoelectricity allows the possibility of creating piezoelectric materials by using non-piezoelectric constituents. Eliseev *et al*. (2009) studied the property changes for the ferroelectric thin pills and nanowires with Landau-Ginsburg-Devonshire phenomenological approach and demonstrated that the flexoelectricity alters unit-cell symmetry and renormalizes all the polar, piezoelectric, and dielectric properties of the nanostructures. Chen and Soh (2012) also adopted the Landau-Ginsburg-Devonshire phenomenological model to capture the influence of the flexoelectricity upon the electric polarization in bilayer nanocomposite thin films and pointed out that the flexoelectricity induced polarization becomes more prominent with the decreasing film thickness. Tagantsev and Yurkov (2012) phenomenologically suggested that the standard mechanical boundary conditions of the nanostructures might be modified by the flexoelectricity.

In order to further explore the flexoelectric effect, it is essential to establish theoretical frameworks with the consideration of this nano-scale structure feature. Some efforts have been devoted in this aspect. Based on the linear piezoelectricity theory developed by Toupin (1956), Maranganti *et al*. (2006) proposed a mathematical framework for nonpiezoelectric dielectrics accounting for the flexoelectricity and provided explicit analytical solutions for the general embedded mismatched inclusion problem. Shen and Hu (Hu and Shen, 2010; Shen and Hu, 2010) established a more comprehensive theoretical model incorporating the flexoelectricity, surface effects and electrostatic force for the nanosized dielectrics. Based on these theoretical fundamentals, the influence of the flexoelectricity on the physical and mechanical properties of piezoelectric nanostructures has been theoretically investigated. For example, Majdoub *et al*. (2008) reported the giant enhancement of the apparent piezoelectric coefficient of piezoelectric and nonpiezoelectric nanobeams by using a modified Euler beam model with the incorporation of the flexoelectric effect, which was also validated by atomistic simulation results. The effect of flexoelectricity on the electric potential generated in bent ZnO nanowires has been investigate by Liu *et al*. (2012). The simulation results suggest that the consideration of the flexoelectricity may bridge the gap between the results from the classical piezoelectricity theory and the experimental measurements for nano-scale dielectrics. Based on the modified Euler-Bernoulli beam and Timoshenko beam theories with the consideration of the flexoelectricity, the electroelastic responses and the vibrational behaviors of one-dimensional bending piezoelectric nanostructures have been studied by Yan and Jiang (2013a; 2013b) and it was found that the flexoelectric effect is more manifest for the thinner beams with smaller thickness. However, the theoretical modeling of the effect of the flexoelectricity upon the electromechanical coupling

behaviors of piezoelectric nanostructures is far from complete and sufficient. Therefore it is necessary to further uncover the flexoelectric effect on the size-dependent properties of piezoelectric nanomaterials with modified continuum modeling methods.

1.2.3 Investigation on the surface effects

Pioneered by Gurtin and Murdoch (1975), an underlying framework addressing the surface elasticity theory was developed to incorporate the surface effects. According to the surface elasticity theory, the nanostructure is decomposed into a bulk part and a surface part, in which the surface can be modeled as a thin layer with negligible thickness. The material properties and constitutive equations for the surface are different from those of the corresponding bulk counterpart. It is worth mentioning that the distinct surface material parameters can be obtained by experiment measurements and atomistic simulations. For example, Izumi *et al*. (2004) have successfully calculated the residual surface stress and the surface elastic constants of the crystal and amorphous silicon by molecular dynamics method. Shenoy (2005) also developed a method for the determination of the surface elastic constants of some metallic crystals based on the embedded atom simulations. Dai *et al*. (2011) have highlighted the concept of surface piezoelectricity and calculated the surface piezoelectric constants of ZnO, $SrTiO_3$ and $BaTiO_3$ by using a combination of a theoretical framework and atomistic calculations.

The size-dependent properties of nanostructures have been extensively investigated from both experimental measurements (Zhao *et al*., 2004; Tabib-Azar *et al*., 2005; Chen *et al*., 2006; Jing *et al*., 2006; Ni and Li, 2006; Stan *et al*., 2007) and atomistic simulations (Zhang *et al*., 2008; Kulkarni *et al*., 2005; Makeev *et al*., 2006; Rudd and Lee, 2008; Agrawal *et al*., 2009; Hu and Pan, 2009). However, due to the extreme difficulty of

experiments performed on nanostructures and the computing expensiveness of the atomistic simulations, it is natural to resort to the modified continuum theories with the incorporation of structure features for modeling the size-dependent physical properties of nanostructured materials due to the efficiency of such a method.

The size-dependent properties of elastic nanomaterials are commonly believed to attribute to the surface effects. Based on the linear surface elasticity model developed by Gurtin and Murdoch (1975), the size-dependent properties of nanostructures due to the surface effects have been widely explored by the modified continuum models from both the static and dynamic aspects. Miller and Shenoy (2000) characterized the difference of the effective stiffness of nanosized structural elements from the model incorporating the surface effects and the standard continuum mechanics approach. It was found that such difference depends on the size of the structures which was in good agreement with the direct atomistic simulations. Based on the modified Euler-Bernoulli beam model and the generalized Young-Laplace equations, the effects of surface elasticity and surface stress upon the elastic properties of static bending nanowires with different boundary conditions have been investigated by He and Lilley (2008). Wang and Feng (2007; 2009) addressed the effects of the residual surface stress and the surface elasticity upon the buckling and vibrational behavior of the nanowires. Moreover, some attention has also been paid to investigate the surface effects upon the mechanical properties of the two dimensional nanostructures. For example, Lu *et al*. (2006) proposed a modified plate theory and accordingly derived the governing equations for both the Kirchhoff plate model and Mindlin plate model with the consideration of the surface effects. This work provided a theoretical basis for performing the size-dependent static and dynamic analysis of the

plate-like nanostructures. Later Assadi *et al*. (2010) conducted the dynamic analysis of the nanoplate with surface effects based on the modified Kirchhoff plate model. It was reported that the discrepancy between the dynamic characteristics obtained from the modified continuum model and those from the classical continuum theory increases significantly for the plates with smaller thicknesses and larger aspect ratios.

Nevertheless, the surface elasticity model may be insufficient to accurately predict the size-dependent properties of piezoelectric nanomaterials due to the exclusion of the surface piezoelectricity. By extending from the surface elasticity model, Huang and Yu (2006) established the fundamental framework for the surface piezoelectricity model with the consideration of the surface piezoelectricity in addition to the residual surface stress and the surface elasticity. Their work demonstrated that the surface piezoelectricity significantly influences the stress and electric fields of a piezoelectric ring when the ring size scales down to nanometers. Based on this surface piezoelectricity model, Zhang *et al.* (2012) examined the surface effects on the buckling of piezoelectric nanofilms subjected to the electrical loading. The results in their work indicated that such influence on the critical buckling voltage of the piezoelectric nanofilm is sensitive to the film thickness, the length-to-thickness ratio and the sign of the residual surface stress. The surface effects on the wrinkling of a piezoelectric nanofilm on a compliant substrate were analytically investigated by Li *et al.* (2011) which revealed that such effects are dependent on the film thickness. Moreover, Yan and Jiang (2011a; 2011b; 2012a; 2012b) have systematically conducted modified continuum mechanics modeling to predict the static and dynamic behaviors of piezoelectric nanobeams/nanowires and nanoplates with the consideration of the surface effects. It was reported from their simulation work that the electromechanical

responses, bending, vibrational and buckling behaviors of the piezoelectric nanostructures are size-dependent and are prominently influenced by the surface effects. Accordingly, it is of great importance to take the effects of the residual surface stress, surface elasticity and the surface piezoelectricity into account in investigating the electromechanical coupling of the piezoelectric nanostructures.

1.3 Objectives

Both the experimental measurements and theoretical studies unambiguously present the size-dependence of the electromechanical coupling properties of piezoelectric nanomaterials. A full understanding on such characteristic nano-scale features is necessary for better design and applications of piezoelectricity-based nanodevices. Since plate structure is one of the fundamental building blocks for the device applications, the current work will focus on a piezoelectric nanoplate. The main objective of this thesis is to provide a fundamental understanding of the physics governing the size-dependent electromechanical coupling behaviors of a clamped piezoelectric nanoplate based on a modified Kirchhoff plate model with the incorporation of the nano-scale features of the structure. Specific work includes:

(1) Investigating the flexoelectric effect on the electroelastic responses and vibrational behaviors of a piezoelectric nanoplate.

(2) Investigating the size effects on the electromechanical coupling fields of a bending piezoelectric nanoplate due to surface effects and flexoelectricity.

1.4 Thesis outline

Chapter 1 presents a general introduction to the piezoelectric nanomaterials and their size-dependent properties and reviews existing studies on the flexoelectricity and the surface effects.

In Chapter 2, a modified Kirchhoff plate model with the consideration of the flexoelectricity is developed. Simulation results will be presented and interpreted to show how the flexoelectricity influences the static bending and free vibrational behaviors of a clamped piezoelectric nanoplate.

A more comprehensive model with the consideration of both the surface effects and the flexoelectricity is proposed in Chapter 3. Simulation results are demonstrated to show the combined influences of flexoelectricity and surface on the electromechanical coupling properties of a clamped bending piezoelectric nanoplate.

Chapter 4 summarizes and concludes the thesis and provides some recommendations for the future work.

References

Agrawal, R., Espinosa, H. D., 2011. Giant piezoelectric size effects in Zinc Oxide and Gallium Nitride nanowires. A First principles investigation. Nano Lett. **11** 786 – 790.

Agrawal, R., Peng, B. and Espinosa, H. D., 2009. Experimental-computational investigation of ZnO nanowires strength and fracture. Nano Lett. **9** 4177-4183.

Agrawal, R., Peng, B., Gdoutos, E. E. and Espinosa, H. D., 2008. Elasticity size effects in

ZnO nanowires-a combined experimental-computational approach. Nano Lett. **8** 3668-3674.

Assadi, A., Farshi, B. and Alinia-Ziazi, A., 2010. Size dependent dynamic analysis of nanoplates. J. Appl. Phys. **107** 124310.

Cady, W. G., 1946. Piezoelectricity, New York: McGraw-Hill.

Cammarata, R. C., 1994. Surface and interface stress effects in thin films. Prog. Surf. Sci. **46** 1-38.

Capsal, J. F., Dantras, E., Dandurand, J. and Lacabanne, C., 2011. Molecular mobility in piezoelectric hybrid nanocomposites with 0–3 connectivity: volume fraction influence. J. Non-Cryst. Solids **358** 3410-3415.

Catalan, G., Sinnamon, L. J.and Gregg, J. M., 2004. The effect of flexoelectricity on the dielectric properties of inhomogeneously strained ferroelectric thin films. J. Phys.: Condens. Matter **16** 2253-2264.

Chen, C. Q., Shi, Y., Zhang, Y. S., Zhu, J. and Yan, Y. J., 2006. Size dependence of Young's modulus in ZnO nanowires. Phys.Rev. Lett. **96** 075505.

Chen, H. T. and Soh, A. K., 2012. Influence of flexoelectric effects on multiferroic nanocomposite thin bilayer films. J. Appl. Phys. **112** 074104.

Chen, Y. X., Dorgan, B. L., McIlroy, D. N. and Aston, D. E., 2006. On the importance of boundary conditions on nanomechanical bending behavior and elastic modulus determination of silver nanowires. J. Appl. Phys **100** 104301.

Eliseev, E. A., Morozovska, A. N., Glinchuk, M. D. and Blinc, R., 2009. Spontaneous flexoelectric/flexomagnetic effect in nanoferroics. Phys. Rev. B **79** 165433.

Fang, X. Q., Liu, J. X. and Gupta, V., 2013. Fundamental formulations and recent achievements in piezoelectric nano-structures: a review. Nanoscale. **5** 1716-1726.

Fousek, J., Cross, L. E. and Litvin, D. B., 1999. Possible piezoelectric composites based on the flexoelectric effect. Mater. Lett. **39** 287-291.

Gibbs, J. W., 1906. The scientific papers of J. Willard Gibbs, Vol. 1. London: Longmans-Green.

Gurtin, M. E. and Murdoch, A. I., 1975. A continuum theory of elastic material surfaces. Arch. Ration. Mech. Anal. **57** 291-323.

He, J. and Lilley, C. M., 2008. Surface effect on the elastic behavior of static bending nanowires. Nano Lett. **8** 1798-1802.

Hong, J. W. and Vanderbilt, D., 2013. First-principles theory and calculation of flexoelectricity. Phys. Rev. B **88** 174107.

Hu, J. and Pan, B. C., 2009. Surface effect on the size- and orientation-dependent elastic properties of singlecrystal ZnO nanostructures. J. Appl. Phys. **105** 034302.

Hu, S. L. and Shen, S. P., 2010. Variational principles and governing equations in nano-dielectrics with the flexoelectric effect. Sci. China, Ser. G **53** 1497-1504.

Huang, G. Y. and Yu, S. W., 2006. Effect of surface piezoelectricity on the electromechanical behavior of a piezoelectric ring. Phys. Status Solidi B—Basic Solid State Phys. **243** R22-R24.

Izumi, S., Hara, S., Kumagai, T. and Sakai, S., 2004. A method for calculating surface stress and surface elastic constants by molecular dynamics: application to the surface of crystal and amorphous silicon. Thin Solid Films **467** 253-260.

Jing, G.Y., Duan, H. L., Sun, X. M., Zhang, Z. S., Xu, J., Li, Y. D., Wang, J. X. and Yu, D. P., 2006. Surface effects on elastic properties of silver nanowires: contact atomic-force microscopy. Phys. Rev. B **73** 235409.

Kulkarni, A. J., Zhou, M. and Ke, F. J., 2005. Orientation and size dependence of the elastic properties of zinc oxide nanobelts. Nanotechnology **16** 2749-2756.

Lee, D., Yoon, A., Jang, S.Y., Yoon, J. G., Chung, J. S., Kim, M., Scott, J. F. and Noh, T. W., 2011. Giant flexoelectric effect in ferroelectric epitaxial thin films. Phys. Rev. Lett. **107** 057602.

Lew, L.C., Voon,Y. and Willatzen, M., 2011. Electromechanical phenomena in semiconductor nanostructures. J. Appl. Phys. **109** 031101.

Li, Y. H., Fang, B., Zhang, J. Z. and Song, J. Z., 2011. Surface effects on the wrinkling of piezoelectric films on compliant substrates. J. Appl. Phys. **110** 114303.

Liu, C. C., Hu, S. L. and Shen, S. P., 2012. Effect of flexoelectricity on electrostatic potential in a bent piezoelectric nanowire. Smart Mater. Struct. **21** 115024.

Lu, P., He, L. H., Lee, H. P. and Lu, C., 2006. Thin plate theory including surface effects. Int. J. Solids Struct. **43** 4631-4647.

Ma, W. H. and Cross, L. E., 2001. Observation of the flexoelectric effect in relaxor Pb (Mg 1/3 Nb 2/3) O 3 ceramics. Appl. Phys. Lett. **78** 2920-2921.

Ma, W. H. and Cross, L. E., 2002. Flexoelectric polarization of barium strontium titanate in the paraelectric state. Appl. Phys. Lett. **81** 3440-3442.

Ma, W. H. and Cross, L. E., 2005. Flexoelectric effect in ceramic lead zirconate titanate. Appl. Phys. Lett. **86** 072905.

Ma, W. H. and Cross, L. E., 2006. Flexoelectricity of barium titanate. Appl. Phys. Lett. **88** 232902.

Majdoub, M. S., Maranganti, R. and Sharma, P., 2009. Understanding the origins of the intrinsic dead layer effect in nanocapacitors. Phys. Rev. B **79** 115412.

Majdoub, M. S., Sharma, P. and Cagin, T., 2008. Enhanced size-dependent piezoelectricity and elasticity in nanostructures due to the flexoelectric effect. Phys. Rev. B **77** 125424.

Makeev, M. A., Srivastava, D. and Menon, M., 2006. Silicon carbide nanowires under external loads: An atomistic simulation study. Phys. Rev. B **74** 165303.

Maranganti, R. and Sharma, P., 2009. Atomistic determination of flexoelectric properties of crystalline dielectrics. Phys. Rev. B **80** 054109.

Maranganti, R., Sharma, N. D. and Sharma, P., 2006. Electromechanical coupling in

nonpiezoelectric materials due to nanoscale nonlocal size effects: Green's function solutions and embedded inclusions. Phys. Rev. B **74** 014110.

Miller, R. E. and Shenoy, V. B., 2000. Size-dependent elastic properties of nanosized structural elements. Nanotechnology **11** 139-147.

Mishra, S. and Sethy, B. K., 2013. Nano-indentation of Copper – Nickel thin films-a molecular dynamics simulation study. National Institute of Technology Rourkela.

Ni, H. and Li, X. D., 2006. Young's modulus of ZnO nanobelts measured using atomic force microscopy and nanoindentation techniques. Nanotechnology **17** 3591.

Nguyen, T. D., Mao, S., Yeh, Y. W., Purohit, P. K. and McAlpine, M. C., 2013. Nanoscale flexoelectricity. Adv. Mater. **25** 946-974.

Qi, Y., Jafferis, N. T., Lyons, K., Lee, C. M., Ahmad, H. and McAlpine, M. C., 2010. Piezoelectric ribbons printed onto rubber for flexible energy conversion. Nano Lett. **10** 524-528.

Rudd, R. E. and Lee, B., 2008. Mechanics of silicon nanowires: size-dependent elasticity from first principles. Mol. Simul. **34** 1-8.

Sharma, N.D., Landis, C. M. and Sharma, P. 2010, Piezoelectric thin-film superlattices without using piezoelectric materials. J. Appl. Phys. **108** 024304.

She, G. W., Zhang, X. H., Shi, W. S., Fan, X. and Chang, J. C., 2007. Electrochemical/chemical synthesis of highly-oriented single-crystal ZnO nanotube arrays on transparent conductive substrates. Electrochem. Commun. **9** 2784-2788.

Shen, S. P. and Hu, S. L., 2010. A theory of flexoelectricity with surface effect for elastic dielectrics. J. Mech. Phys. Solids **58** 665-677.

Shenoy, V. B., 2005. Atomistic calculations of elastic properties of metallic fcc crystal surfaces. Phys. Rev. B **71** 094104.

Stan, G., Ciobanu, C. V., Parthangal, P. M. and Cook, R. F., 2007. Diameter-dependent radial and tangential elastic moduli of ZnO nanowires. *Nano Lett.* **7** 3691-3697.

Streitz, F. H., Cammarata, R. C. and Sieradzki, K., 1994. Surface-stress effects on elastic properties. I. Thin metal films. Phys. Rev. B **49** 10699-10706.

Sun, C. L., Shi, J. and Wang, X. D., 2010. Fundamental study of mechanical energy harvesting using piezoelectric nanostructures. J. Appl. Phys. **108** 034309.

Tabib-Azar, M., Nassirou, M., Wang, R., Sharma, S., Kamins, T.I., Islam, M.S. and Williams, R. S., 2005. Mechanical properties of self-welded silicon nanobridges. Appl. Phys. Lett. **87**113102.

Tagantsev, A. K., 1985. Theory of flexoelectric effect in crystals. Sov. Phys. JETP **61** 1246-1254.

Tagantsev, A. K. and Yurkov, A. S., 2012. Flexoelectric effect in finite samples. J. Appl. Phys. **112** 044103.

Toupin, R. A., 1956. The elastic dielectric. J. Ration. Mech. Anal. **5** 849-915.

Wang, G. F. and Feng, X. Q., 2007. Effects of surface elasticity and residual surface tension on the natural frequency of microbeams. Appl. Phys. Lett. **90** 231904.

Wang, G. F. and Feng, X. Q., 2009. Surface effects on buckling of nanowires under uniaxial compression. Appl. Phys. Lett. **94** 141913.

Wang, J. X., Huang, Z. P., Duan, H. L., Yu, S. W., Feng, X. Q., Wang, G. F., Zhang, W. X. and Wang, T. J., 2011. Surface stress effect in mechanics of nanostructured materials. Acta Mech. Solida Sin. **24** 52-82.

Wang, X. D., Song, J. H. and Wang, Z. L., 2007. Nanowire and nanobelt arrays of zinc oxide from synthesis to properties and to novel devices. J. Mater. Chem. **17** 711-720.

Wang, Z. L. and Song, J. H., 2006. Piezoelectric nanogenerators based on zinc oxide nanowire arrays. Science **312** 242-246.

Xu, T., Wang, J., Shimada, T. and Kitamura, T., 2013. Direct approach for flexoelectricity from first-principles calculations: cases for SrTiO3 and BaTiO3. J. Phys.: Condens. Matter **25** 415901.

Yamano, A., Takata K. and Kozuka, H., 2012. Ferroelectric domain structures of 0.4-m-thick Pb(Zr,Ti)O3 films prepared by polyvinylpyrrolidone-assisted Sol-Gel method. J. Appl. Phys. **111** 054109.

Yan, Z. and Jiang, L. Y., 2011a. Surface effects on the electromechanical coupling and bending behaviours of piezoelectric nanowires. J. Phys. D: Appl. Phys. **44** 075404.

Yan, Z. and Jiang, L.Y., 2011b. The vibrational and buckling behaviors of piezoelectric nanobeams with surface effects. Nanotechnology **22** 245703.

Yan, Z. and Jiang, L. Y., 2012a. Surface effects on the electroelastic responses of a thin

piezoelectric plate with nanoscale thickness. J. Phys. D: Appl. Phys. **45** 255401.

Yan, Z. and Jiang, L. Y., 2012b. Surface effects on the vibration and buckling of piezoelectric nanoplates. *EPL* **99** 27007.

Yan, Z. and Jiang, L. Y., 2013a. Flexoelectric effect on the electroelastic responses of bending piezoelectric nanobeams. J. Appl. Phys. **113** 194102.

Yan, Z. and Jiang, L. Y., 2013b. Size-dependent bending and vibration behaviour of piezoelectric nanobeams due to flexoelectricity. J. Phys. D: Appl. Phys. **46** 355502.

Yin, B. L. and Qu, S. X., 2014. An ab initio investigation of flexoelectric effect in ultrathin BaTiO3 nanotubes. J. Appl. Phys. **115** 074102.

Yudin, P. V. and Tagantsev, A. K., 2013. Fundamentals of flexoelectricity in solids. Nanotechnology **24** 432001.

Zhang, J., Wang, C. Y. and Adhikari, S., 2012. Surface effect on the buckling of piezoelectric nanofilms. J. Phys. D: Appl. Phys. **45** 285301.

Zhang, T. Y., Luo, M., Chan, W. K., 2008. Size-dependent surface stress, surface stiffness, and Young's modulus of hexagonal prism [111] - Si C nanowires. J. Appl. Phys. **103** 104308.

Zhao, M. H., Wang, Z. L. and Mao, S. X., 2004. Piezoelectric characterization of individual Zinc Oxide nanobelt probed by piezoresponse force microscope. Nano Lett. **4** 587-590.

Zubko, P., Catalan, G. and Tagantsev, A. K., 2013. Flexoelectric effect in solids. Annu.

Rev. Mater. Res. **43** 387-421.

Chapter 2

2 Flexoelectric effect on the electroelastic responses and vibrational behaviors of a piezoelectric nanoplate

2.1 Introduction

Electromechanical coupling, referring to the interplay between electric fields and mechanical fields, has been widely explored in the development of piezoelectricity-based devices in transduction technology, including transducers, sensors, resonators and energy harvesters (Yang, 2006). Such a conventional electromechanical coupling, in particular between the electric polarization and a uniform strain, is a unique feature for non-centrosymmetric dielectric materials, such as piezoelectric materials. In contrast, flexoelectricity, referring to the spontaneous polarization in response to a nonuniform strain or a strain gradient, is a universal effect in all classes of dielectric materials even in the centrosymmetric crystals. A rational physical interpretation of this phenomenon is the local breaking of inversion symmetry of the material structure caused by the strain gradient, rendering the formation of dipole moments and thus the induced polarization (Maranganti and Sharma, 2009). Recently, Zubko *et al*. (2013), Nguyen *et al*. (2013), Yudin and Tagantsev (2013) have conducted a thorough and comprehensive review elaborating the fundamentals of the flexoelectricity in solids, its consequences in the physical properties of nano-scale systems and the potential applications of this electromechanical phenomenon. For example, it was interpreted in the literature that the flexoelectricity is responsible for modifying some physical characteristics of

ferroelectrics, including the shifts of domain configurations and the ferroelectric hysteresis loop (Lee *et al*., 2011), the reduction of dielectric constant (Catalan *et al*., 2004; 2005), the vanishing of switchable spontaneous polarization (Chu *et al*., 2004), and the degradation of capacitance of ferroelectric capacitors due to the formation of a non-switchable dead layer (Majdoub *et al*., 2009). Since the flexoelectricity induced electric polarization may enable the effective electromechanical coupling responses in non-piezoelectric dielectric materials, it is promising to create piezoelectric composite materials without using any piezoelectric constituents, which was first proposed by Fousek *et al*. (1999) and further explored by the same group and others (Fu *et al*., 2007; Zhu *et al*., 2006; Sharma *et al*., 2007; 2010). The essence of the design concept in these works is to create inhomogeneous strain field in the active constituent dispersed in the matrix material of the composites, inducing the electric polarization due to the flexoelectricity. As a net effect, a piezoelectricity is achieved for the composites in response to either a mechanical load or an electrical load. It was also found in the literature that the flexoelectricity could be exploited for polarization control mechanically instead of electrically for the potential applications in non-volatile memory devices (Lu *et al*., 2012).

Phenomenologically, this strain gradient induced polarization due to the flexoelectricity is proportional to the flexoelectric coefficient and the magnitude of the strain gradient. Pioneered by Ma and Cross, a series of experiments were conducted on a variety of bulk ferroelectric ceramics to quantitatively estimate the flexoelectric effect by measuring their flexoelectric coefficients (Ma and Cross, 2001; 2002; 2005; 2006). It was revealed in their work that the flexoelectric coefficient of ferroelectrics scales with their

dielectric permittivity. Ponomareva *et al*. (2012) further elucidated that the flexoelectric coefficient is also temperature dependent. In general, such a flexoelectric effect is rather insignificant relative to the piezoelectric effect in macro-scale piezoelectric materials. However, due to the fact that the strain gradient is inversely proportional to the characteristic size of the structures (Majdoub, 2008), the flexoelectricity triggered by the strain gradient is expected to become more prominent for the piezoelectrics at the nano-scale. Thus the size-dependent flexoelectricity may contribute significantly to the electromechanical coupling of piezoelectric materials at the nano-scale and it is necessary to incorporate such an effect when investigating the static and dynamic behaviors of those nanostructured materials.

With the development of nanotechnology, flexoelectricity has re-stimulated a surge of scientific interests in research communities recently, as the large strain gradients often present in nano-scale materials may result in strong flexoelectric effect. It was found in the literature that the electromechanical coupling of piezoelectric nanomaterials could be enhanced by the flexoelectric effect (Majdoub, 2008; Ma and Cross, 2003), which may open new avenues for the design considerations and potential applications of piezoelectric nanostructures in NEMS devices (Wang, 2007). In order to fulfill the potential applications of those piezoelectric nanostructures as nanodevices, it is essential to build theoretical frameworks with the consideration of nano-scale structure features to understand the fundamental physics governing the electromechanical coupling of materials at the nano-scale. Extending from the linear piezoelectricity theory developed by Toupin (1956), Maranganti *et al.* (2006) established a mathematical framework for dielectrics including the effects of both the strain gradient and polarization gradient based

on the variational principle. Later, a more comprehensive theoretical framework incorporating the flexoelectricity, surface effects and electrostatic force was developed by Hu and Shen (Hu and Shen, 2010; Shen and Hu, 2010). Owing to those pioneering studies, the influence of the flexoelectricity upon the electromechanical coupling of piezoelectric nanomaterials could be characterized to some extent. For example, Majdoub *et al*. (2008) applied those theoretical frameworks on the Euler-Bernoulli beam model and found that the apparent piezoelectric coefficient of both piezoelectric and nonpiezoelectric nanobeams was dramatically enhanced by the flexoelectricity. The effect of the flexoelectricity upon the electric potential distribution in a bending ZnO nanowire was analytically predicted by Liu *et al*. (2012) which was in good agreement with experimental data. Based on the modified Euler-Bernoulli beam and Timoshenko beam models with the incorporation of the flexoelectric effect, the size-dependent electroelastic responses and dynamic behaviors of one-dimensional piezoelectric nanostructures were investigated by Yan and Jiang (2013a; 2013b).

Except for such a few theoretical studies of modeling the flexoelectric effect upon the static and dynamic behaviors of one-dimensional dielectric nanostructures as mentioned above, investigation on the size-dependent properties of two-dimensional piezoelectric nanostructures induced by the flexoelectricity is even more limited. Until recently, Chen and Soh (2012) characterized the influence of the flexoelectricity upon the distribution of the electric polarization in a bending bilayer nanocomposites and it was found that the flexoelectricity induced polarization is dependent on the film thickness. In order to further uncover the flexoelectric effect on two-dimensional piezoelectric nanostructures, such as the piezoelectric nanoplate (PNP), the objective of the current

work is to develop a modified plate model based on the conventional Kirchhoff plate theory and the extended linear piezoelectricity theory by incorporating the flexoelectric effect. Simulation results will be demonstrated to show how the static bulk flexoelectricity influences the electroelastic responses and the vibrational behaviors of the piezoelectric nanoplate. It should be mentioned that the surface effects and the dynamic bulk flexoelectricity are ignored in this paper (Yudin and Tagantsev, 2013). Therefore, the current model could be claimed only to represent the trend of the influence of the static bulk flexoelectricity. A more comprehensive model with consideration of those complete structure scale features may be the future concentration.

2.2 Formulation and solution of the problem

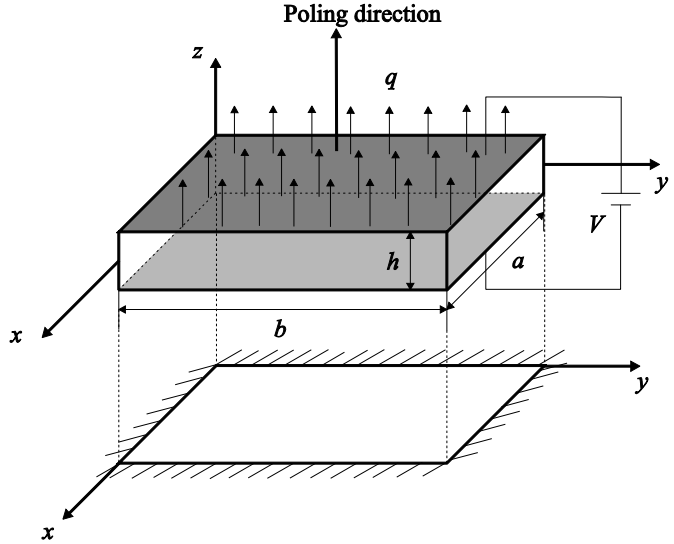

Figure 2.1: Schematic of a clamped piezoelectric nanoplate under applied mechanical and electrical loads.

In the current work, the electroelastic responses and the vibration of a clamped piezoelectric plate with length *a*, width *b* and thickness *h* as shown in figure 2.1 will be

investigated. A Cartesian coordinate system is adopted to describe the plate with *xy* plane being the undeformed midplane of the plate and *z* axis along the thickness direction. The plate is polarized in the *z* direction and subjected to an electric voltage *V* between the electrodes coated on the upper and lower surfaces of the plate. For static bending analysis, the plate is also subjected to a uniformly distributed load with density *q*. The Kirchhoff plate theory is adopted in the current work for modeling purpose. Correspondingly, the displacements of the plate can be described as

$$u(x,y,z,t) = u^0(x,y,t) - z\frac{\partial w(x,y,z,t)}{\partial x}, \tag{2.1a}$$

$$v(x,y,z,t) = v^0(x,y,t) - z\frac{\partial w(x,y,z,t)}{\partial y}, \tag{2.1b}$$

$$w(x,y,z,t) = w(x,y,t), \tag{2.1c}$$

where $w(x, y, t)$ is the transverse displacement in the plate thickness direction; $u(x,y,z,t)$ and $v(x,y,z,t)$ are the displacements along the *x* and *y* directions, respectively; $u^0(x,y,t)$ and $v^0(x,y,t)$ are the displacements of the midplane along the *x* and *y* directions, which in general are induced by the applied voltage due to the electromechanical coupling of the piezoelectric plate. For a clamped plate with four edges fixed, it is reasonable to assume $u^0(x,y,t) = 0$ and $v^0(x,y,t) = 0$ as adopted in Zhao *et al.* 's work (2007) for a traditional piezoelectric plate, which means that the midplane displacements induced by electromechanical coupling are trivial according to the Kirchhoff plate theory. Thus the non-zero strain components can be expressed as

$$\varepsilon_{xx} = -z\frac{\partial^2 w}{\partial x^2}, \tag{2.2a}$$

$$\varepsilon_{yy} = -z\frac{\partial^2 w}{\partial y^2}, \tag{2.2b}$$

$$\varepsilon_{xy} = -z\frac{\partial^2 w}{\partial x \partial y}. \tag{2.2c}$$

Since $h<<a$, b for a Kirchhoff plate, the strain gradients along the x and y directions (for example, $\varepsilon_{xx,x} = -z\frac{\partial^3 w}{\partial x^3}$ and $\varepsilon_{xx,\mathrm{y}} = -z\frac{\partial^3 w}{\partial x^2 \partial y}$) can be ignored as compared to the strain gradients along the thickness direction (for example, $\varepsilon_{xx,z} = -\frac{\partial^2 w}{\partial x^2}$ and $\varepsilon_{yy,z} = -\frac{\partial^2 w}{\partial y^2}$). Such an assumption was also adopted by Yan and Jiang for an Euler beam (Yan and Jiang, 2013a). In the following analysis, we will only consider the flexoelectricity induced by the strain gradients along the thickness direction, which are expressed as

$$\varepsilon_{xx,z} = -\frac{\partial^2 w}{\partial x^2}, \tag{2.3a}$$

$$\varepsilon_{yy,z} = -\frac{\partial^2 w}{\partial y^2}, \tag{2.3b}$$

$$\varepsilon_{xy,z} = -\frac{\partial^2 w}{\partial x \partial y}. \tag{2.3c}$$

In order to incorporate the flexoelectric effect, the extended linear theory of piezoelectricity is used in the current work. It includes the coupling between the strain gradient and the polarization, and the coupling between the polarization gradient and the strain(Yudin and Tagantsev, 2013; Sharma *et al*., 2010; Majdoub *et al*., 2008; Yan and Jiang, 2013a). For simplicity, the higher-order couplings between the strain and the strain gradient, the strain gradient and the strain gradient, and the strain gradient and the polarization gradient are ignored in the current work as in the existing studies (Zubko *et*

al., 2013; Sharma *et al*., 2010; Majdoub *et al*., 2008; Yan and Jiang, 2013a). Under this assumption, the expression of the internal energy density function U is given as,

$$U_b = \frac{1}{2}a_{kl}P_kP_l + \frac{1}{2}c_{ijkl}\varepsilon_{ij}\varepsilon_{kl} + d_{ijk}\varepsilon_{ij}P_k + \frac{1}{2}b_{ijkl}P_{i,j}P_{k,l} + f_{ijkl}u_{i,jk}P_l + e_{ijkl}\varepsilon_{ij}P_{k,l} \ , \tag{2.4}$$

where P_i and ε_{ij} are the components for the polarization tensor and strain tensor, respectively. The strain tensor is defined as $\varepsilon_{ij} = \frac{1}{2}(u_{i,j} + u_{j,i})$ with u_{i} being the displacement components. a_{kl} , c_{ijkl} and d_{ijk} stand for the elements of the reciprocal dielectric susceptibility, elastic constant and piezoelectric constant tensors, which are exactly the same as those in the linear piezoelectricity theory. The other terms in equation (2.4) represent the higher-order couplings between the electric polarization and the strain fields, i.e., the interaction of polarization gradient and polarization gradient (represented by tensor b_{ijkl}), the strain gradient and polarization coupling (represented by tensor f_{ijkl}), the strain and polarization gradient coupling (represented by tensor e_{ijkl}) . It was justified by Sharma *et al*. (2010) and Shen and Hu (2010) that the flexocoupling coefficient tensor $f_{ijkl} = -e_{ijkl}$.

Thus the constitutive equations can be derived from the extended linear theory of piezoelectricity as (Hu and Shen, 2010),

$$\sigma_{ij} = \frac{\partial U_b}{\partial \varepsilon_{ij}} = c_{ijkl}\varepsilon_{kl} + d_{ijk}P_k + e_{ijkl}P_{k,l}, \tag{2.5a}$$

$$\sigma_{ijm} = \frac{\partial U_b}{\partial u_{i,jm}} = f_{ijmk}P_k, \tag{2.5b}$$

$$E_i = \frac{\partial U_b}{\partial P_i} = a_{ij} P_j + d_{jki} \varepsilon_{jk} + f_{jkli} u_{j,kl} \quad , \tag{2.5c}$$

$$E_{ij} = \frac{\partial U_b}{\partial P_{i,j}} = b_{ijkl} P_{k,l} + e_{klij} \varepsilon_{kl} \tag{2.5d}$$

where σ_{ij} and E_{i} represent the traditional stress and electrical field tensors as in linear piezoelectricity theory, while σ_{ijm} is defined as the higher order stress tensor (or moment stress tensor) induced by the flexoelectricity and E_{ij} can be considered as the higher order local electrical force, which are all ignored in the classical piezoelectricity theory. In addition, the direct flexoelectricity contributes to the electric field E_i as demonstrated by the last term in equation (2.5c), while the inverse flexoelectric effect contributes to the stress field as evidenced by the last term in equation (2.5a). In the following formulation, the contracted notation for the subscripts of the conventional material constant tensors is adopted for simplicity purpose, i.e., c_{11}=c_{1111}, c_{66}=$c_{1212,}$ d_{31}=$d_{311,}$ a_{3333}=a_{33} and b_{3333}=b_{33}. From Refs. (Sharma *et al*., 2010; Yan and Jiang, 2013a), it is concluded that the flexocoupling coefficient tensor is related to the flexoelectric coefficient tensor μ_{ijkl}, i.e., $f_{ijkl} = a_{lm}(\mu_{ijkm} + \mu_{ikjm} - \mu_{jkim})$. These two tensors have the same symmetry and the same number of independent components. Le Quang and He (2011) explicitly solved the fundamental problem to determine the number of independent components in the flexoelectric coefficient tensor for a given symmetry class of materials. The non-zero and independent flexoelectric coefficient elements μ_{ijkl} for the example material tetragonal $BaTiO_3$ (point group 4mm) were given in Shu *et al*.'s work (2011). Thus the corresponding flexocoupling coefficient tensor of the tetragonal $BaTiO_3$ can be obtained. Following the same convention of subscript transformation in Ref. (Shu *et al*., 2011),

$f_{1133} = f_{2233}$ can be represented by f_{19}. Accordingly, the electric field in equation (2.5c) can be expressed for a transversely isotropic piezoelectric material as

$$E_z = a_{33} P_z + d_{31}(\varepsilon_{xx} + \varepsilon_{yy}) + f_{19}(\varepsilon_{xx,z} + \varepsilon_{yy,z}) . \tag{2.6}$$

When the PNP is subjected to an electric potential Φ across the plate thickness, the electric field is assumed to exist only along the thickness direction as adopted by Zhao *et al.* (2007), which is expressed in terms of the electric potential Φ and the higher order local electrical force E_{ij} (Hu and Shen, 2010), as

$$E_z = -\frac{\partial \Phi}{\partial z} + E_{zx,x} + E_{zy,y} + E_{zz,z} , \tag{2.7}$$

With the consideration of the so-called background permittivity for ferroelectrics (Hlinka and Marton, 2006; Tagantsev and Gerra, 2006), the Gauss's law is expressed in the absence of free electric charges as,

$$-\kappa_0 \kappa_b \Phi_{,zz} + P_{z,z} = 0 , \tag{2.8}$$

where $\kappa_0 = 8.85 \times 10^{-12} C \cdot V^{-1} \cdot m^{-1}$ is the permittivity of the vacuum or the air, and the background permittivity $\kappa_b = 6.62$ is taken for $BaTiO_3$ when the electric field is parallel to the polarization (Tagantsev and Gerra, 2006). In the following formulation, $\kappa = \kappa_0 \kappa_b$ is adopted for simplicity. Combining equations (2.6)-(2.8) and the electric boundary conditions, i.e., $E_{ij} n_j = 0$ and $\Phi(\frac{h}{2}) = V$ and $\Phi(-\frac{h}{2}) = 0$ when the plate is subjected to an electrical voltage V across the plate thickness, the electric potential, the polarization and the electric field can be derived in terms of the plate transverse displacement w and the applied voltage V as

$$\Phi = \frac{d_{31}}{2(1+a_{33}\kappa)}(\frac{\partial^2 w}{\partial x^2}+\frac{\partial^2 w}{\partial y^2})(z^2-\frac{1}{4}h^2)+\frac{V}{h}z+\frac{V}{2}$$
$$+\frac{f_{19}}{1+a_{33}\kappa}(\frac{\partial^2 w}{\partial x^2}+\frac{\partial^2 w}{\partial y^2})z-\frac{f_{19}h}{2(1+a_{33}\kappa)}(\frac{\partial^2 w}{\partial x^2}+\frac{\partial^2 w}{\partial y^2})\frac{e^{\lambda z}-e^{-\lambda z}}{e^{\frac{h}{2}\lambda}-e^{-\frac{h}{2}\lambda}}, \tag{2.9a}$$

$$E_z = -\frac{d_{31}}{1+a_{33}\kappa}(\frac{\partial^2 w}{\partial x^2}+\frac{\partial^2 w}{\partial y^2})z-\frac{V}{h}+\frac{a_{33}\kappa f_{19}}{1+a_{33}\kappa}(\frac{\partial^2 w}{\partial x^2}+\frac{\partial^2 w}{\partial y^2})$$
$$-\frac{a_{33}f_{19}h}{2\lambda b_{33}}(\frac{\partial^2 w}{\partial x^2}+\frac{\partial^2 w}{\partial y^2})\frac{e^{\lambda z}+e^{-\lambda z}}{e^{\frac{h}{2}\lambda}-e^{-\frac{h}{2}\lambda}}, \tag{2.9b}$$

$$P_z = \frac{d_{31}\kappa}{1+a_{33}\kappa}(\frac{\partial^2 w}{\partial x^2}+\frac{\partial^2 w}{\partial y^2})z-\frac{V}{a_{33}h}+\frac{f_{19}(1+2a_{33}\kappa)}{a_{33}(1+a_{33}\kappa)}(\frac{\partial^2 w}{\partial x^2}+\frac{\partial^2 w}{\partial y^2})$$
$$-\frac{f_{19}h}{2\lambda b_{33}}(\frac{\partial^2 w}{\partial x^2}+\frac{\partial^2 w}{\partial y^2})\frac{e^{\lambda z}+e^{-\lambda z}}{e^{\frac{h}{2}\lambda}-e^{-\frac{h}{2}\lambda}}, \tag{2.9c}$$

where $\lambda = \sqrt{\frac{1+\kappa a_{33}}{\kappa b_{33}}}$. It should be noted that without the consideration of the effects of the strain gradient and the polarization gradient, the expressions for the electric fields reduces to the classical ones.

Substituting equation (2.9c) into equations (2.5a) and (2.5b), both the traditional stresses and the higher order stresses can be determined. Therefore, the electroelastic fields of the PNP are completely solved if the transverse displacement *w* is determined under the applied mechanical and electrical loads. For example, the traditional stresses are determined in terms of the transverse displacement *w* and the applied voltage *V* as

$$\sigma_{xx} = (-c_{11} + \frac{d_{31}^2\kappa}{1+a_{33}\kappa})z\frac{\partial^2 w}{\partial x^2} + (-c_{12} + \frac{d_{31}^2\kappa}{1+a_{33}\kappa})z\frac{\partial^2 w}{\partial y^2} - \frac{d_{31}V}{a_{33}h}$$
$$+(\frac{d_{31}f_{19}}{a_{33}} - \frac{d_{31}f_{19}h}{2\lambda b_{33}}\frac{e^{\lambda z}+e^{-\lambda z}}{e^{\frac{h}{2}\lambda} - e^{-\frac{h}{2}\lambda}} + \frac{f_{19}^2 h}{2b_{33}}\frac{e^{\lambda z}-e^{-\lambda z}}{e^{\frac{h}{2}\lambda} - e^{-\frac{h}{2}\lambda}})(\frac{\partial^2 w}{\partial x^2} + \frac{\partial^2 w}{\partial y^2}), \quad (2.10a)$$

$$\sigma_{yy} = (-c_{12} + \frac{d_{31}^2\kappa}{1+a_{33}\kappa})z\frac{\partial^2 w}{\partial x^2} + (-c_{11} + \frac{d_{31}^2\kappa}{1+a_{33}\kappa})z\frac{\partial^2 w}{\partial y^2} - \frac{d_{31}V}{a_{33}h}$$
$$+(\frac{d_{31}f_{19}}{a_{33}} - \frac{d_{31}f_{19}h}{2\lambda b_{33}}\frac{e^{\lambda z}+e^{-\lambda z}}{e^{\frac{h}{2}\lambda} - e^{-\frac{h}{2}\lambda}} + \frac{f_{19}^2 h}{2b_{33}}\frac{e^{\lambda z}-e^{-\lambda z}}{e^{\frac{h}{2}\lambda} - e^{-\frac{h}{2}\lambda}})(\frac{\partial^2 w}{\partial x^2} + \frac{\partial^2 w}{\partial y^2}), \quad (2.10b)$$

$$\sigma_{xy} = -2c_{66}z\frac{\partial^2 w}{\partial x \partial y}. \quad (2.10c)$$

In order to determine the transverse displacement of the PNP, Hamilton's principle is adopted in the current work to derive the governing equation and the mechanical boundary conditions of the plate (Yan and Jiang, 2013b; Rao, 2007), i.e.,

$$\delta\int_{t_1}^{t_2}(-\int_{\Omega} H d\Omega + K + W)dt = 0, \quad (2.11)$$

where Ω is the entire volume of the plate. $H = U - \frac{1}{2}\kappa\Phi_{,z}\Phi_{,z} + \Phi_{,z}P_z$ (Toupin, 1956) is the electric enthalpy density with U being the internal energy density defined by equation (2.4). Manipulating equations (2.5a), (2.5b), (2.5c) and (2.5d) and equation (2.4), the expression of the internal energy density can be reduced to $U = \frac{1}{2}(\sigma_{xx}\varepsilon_{xx} + \sigma_{yy}\varepsilon_{yy} + 2\sigma_{xy}\varepsilon_{xy} + \sigma_{xxz}\varepsilon_{xx,z} + \sigma_{yyz}\varepsilon_{yy,z} + E_z P_z + \mathrm{E}_{zz}\mathrm{P}_{z,z})$. K is the kinetic energy defined as $K = \frac{1}{2}\iint[\rho\frac{h^3}{12}\left(\left(\frac{\partial\dot{w}}{\partial x}\right)^2 + \left(\frac{\partial\dot{w}}{\partial y}\right)^2\right) + \rho h\dot{w}^2]dxdy$ for the plate, where ρ is the mass density and the dot "." represents the derivation with respect to time *t*. It should be mentioned that the so-called dynamic flexoelectric effect, which has been

phenomenologically described by Tagantsev (1986) and Yudin and Tagantsev (2013) is not considered here. In addition, for a clamped PNP with in-plane displacement constraint, the work done by external forces is defined as $W = \iint qwdxdy - \frac{1}{2}\iint [N_{xx}(\frac{\partial w}{\partial x})^2 + N_{yy}(\frac{\partial w}{\partial y})^2 + 2N_{xy}(\frac{\partial w}{\partial x}\frac{\partial w}{\partial y})]dxdy$ with N_{xx}, N_{yy} and N_{xy} being the resultant in-plane forces due to the electromechanical coupling. These in-plane forces are defined as $N_{xx} = \int_{-\frac{h}{2}}^{\frac{h}{2}} \sigma_{xx} dz = \frac{d_{31} f_{19} h}{a_{33}(1+\kappa a_{33})}(\frac{\partial^2 w}{\partial x^2} + \frac{\partial^2 w}{\partial y^2}) - \frac{d_{31}}{a_{33}} V,$

$N_{yy} = \int_{-\frac{h}{2}}^{\frac{h}{2}} \sigma_{yy} dz = \frac{d_{31} f_{19} h}{a_{33}(1+\kappa a_{33})}(\frac{\partial^2 w}{\partial x^2} + \frac{\partial^2 w}{\partial y^2}) - \frac{d_{31}}{a_{33}} V$ and $N_{xy} = \int_{-\frac{h}{2}}^{\frac{h}{2}} \sigma_{xy} dz = 0.$ Obviously, the flexoelectricity also contributes to these forces as indicated by the first term in their expressions. It should be noticed that if the applied voltage is positive and sufficient large, the resultant in-plane forces may become compressive and result in the mechanical buckling of the plate.

Applying the variational principle of equation (2.11), the governing equation of the PNP with the consideration of the flexoelectric effect is derived as

$$D_{11}(\frac{\partial^4 w}{\partial x^4} + \frac{\partial^4 w}{\partial y^4}) + 2(D_{12} + 2D_{66})\frac{\partial^4 w}{\partial^2 x \partial^2 y} + \frac{d_{31}}{a_{33}} V(\frac{\partial^2 w}{\partial x^2} + \frac{\partial^2 w}{\partial y^2}) + 2\frac{d_{31} f_{19} h}{a_{33}(1+\kappa a_{33})}(\frac{\partial^2 w}{\partial x \partial y})^2$$
$$-2\frac{d_{31} f_{19} h}{a_{33}(1+\kappa a_{33})}\frac{\partial^2 w}{\partial x^2}\frac{\partial^2 w}{\partial y^2} - \frac{\rho h^3}{12}(\frac{\partial^2 \ddot{w}}{\partial x^2} + \frac{\partial^2 \ddot{w}}{\partial y^2}) + \rho h \ddot{w} - q = 0, \tag{2.12}$$

with

$$D_{11} \equiv (c_{11} - \frac{d_{31}^2 \kappa}{(1+\kappa a_{33})})\frac{h^3}{12} - \frac{f_{19}^2 h}{a_{33}(1+\kappa a_{33})} - \frac{f_{19}^2 h^2}{2\lambda b_{33}}\frac{e^{\frac{h}{2\lambda}} + e^{-\frac{h}{2\lambda}}}{e^{\frac{h}{2\lambda}} - e^{-\frac{h}{2\lambda}}} + \frac{b_{33} d_{31}^2 \kappa^2 h}{(1+\kappa a_{33})^2}, \tag{2.13a}$$

$$D_{12} \equiv (c_{12} - \frac{d_{31}^2 \kappa}{(1+\kappa a_{33})}) \frac{h^3}{12} - \frac{f_{19}^2 h}{a_{33}(1+\kappa a_{33})} - \frac{{f_{19}}^2 h^2}{2\lambda b_{33}} \frac{e^{\frac{h}{2\lambda}} + e^{-\frac{h}{2\lambda}}}{e^{\frac{h}{2\lambda}} - e^{-\frac{h}{2\lambda}}} + \frac{b_{33} d_{31}^2 \kappa^2 h}{(1+\kappa a_{33})^2}, \tag{2.13b}$$

$$D_{66} \equiv \frac{c_{66}}{12} h^3 . \tag{2.13c}$$

If the flexoelectric effect is excluded, the governing equation (2.12) reduces to equation (2.16) in Yan and Jiang's work (2012a) without the consideration of the surface effects, which represents the transverse motion equation of a conventional piezoelectric plate based on the Kirchhoff plate theory. It is identified from the expressions of D_{11} and D_{12} that the flexoelectricity decreases the effective bending rigidity as compared to the conventional piezoelectric plate. When the plate thickness scales down to nanometers, according to the values of the flexoelectric coefficients provided in the work of Ponomareva *et al*. (2012), Yan and Jiang (2013a), Chen and Soh (2012) and Eliseev *et al*. (2009), the reduction of the bending rigidity due to the flexoelectricity becomes comparable to the values of traditional D_{11} and D_{12}. Therefore, it is necessary to incorporate the flexoelectricity to investigate the static and dynamic behaviors of the piezoelectric plates with nano-scale thickness. However, D_{11} and D_{12} must be ensured positive to keep the mechanical stability of the plate. It should be mentioned that the current model ignore the surface elasticity and surface piezoelectricity which have been demonstrated to increase the bending rigidity of the piezoelectric nanostructures prominently (Yan and Jiang, 2011; Li *et al*., 2011). In addition, the current model also neglects the effect of surface flexoelectricity (Yudin and Tagantsev, 2013; Tagantsev, 2012; Stengel, 2013) to make the analysis more mathematically tractable. Without considering those surface effects and the higher order gradient terms (the coupling between strain gradient and strain gradient for example), the current model aims to

provide a theoretical prediction on the trend of the effect of pure bulk flexoelectricity upon the static and dynamic bending behaviors of a PNP.

In addition, the corresponding mechanical boundary conditions for the clamped PNP are also derived from the variational principle as $w=0$ and $\frac{\partial w}{\partial n}=0$ at the four edges, which yields

$$w=0 \text{ and } \frac{\partial w}{\partial x}=0 \quad \text{at } x=0 \text{ and } x=a; \tag{2.14a}$$

$$w=0 \text{ and } \frac{\partial w}{\partial y}=0 \quad \text{at } y=0 \text{ and } y=b. \tag{2.14b}$$

Thus the static and dynamic responses of the bending PNP will be determined by solving the nonlinear partial differential governing equation (2.12) with the consideration of the mechanical boundary conditions (2.14a) and (2.14b).

2.2.1 Electroelastic responses of a static bending PNP

For the static bending of a PNP, the governing equation is reduced from equation (2.12) by ignoring the inertial terms, i.e.,

$$\begin{aligned} &D_{11}\left(\frac{\partial^4 w}{\partial x^4}+\frac{\partial^4 w}{\partial y^4}\right)+2(D_{12}+2D_{66})\frac{\partial^4 w}{\partial^2 x\partial^2 y}+\frac{d_{31}}{a_{33}}V\left(\frac{\partial^2 w}{\partial x^2}+\frac{\partial^2 w}{\partial y^2}\right) \\ &+2\frac{d_{31}f_{19}h}{a_{33}(1+\kappa a_{33})}\left(\frac{\partial^2 w}{\partial x\partial y}\right)^2-2\frac{d_{31}f_{19}h}{a_{33}(1+\kappa a_{33})}\frac{\partial^2 w}{\partial x^2}\frac{\partial^2 w}{\partial y^2}-q=0, \end{aligned} \tag{2.15}$$

In order to perform bending analysis of the PNP, Ritz method (Reddy, 2007) is adopted to get the approximate solution of equation (2.15). In this solution scheme, the weak form of the variational statement of equation (2.15) is expressed as

$$\iint \{D_{11}[\frac{\partial^2 w}{\partial x^2}\frac{\partial^2(\delta w)}{\partial x^2}+\frac{\partial^2 w}{\partial y^2}\frac{\partial^2(\delta w)}{\partial y^2}]+D_{12}[\frac{\partial^2 w}{\partial x^2}\frac{\partial^2(\delta w)}{\partial y^2}+\frac{\partial^2 w}{\partial y^2}\frac{\partial^2(\delta w)}{\partial x^2}]$$
$$+4D_{66}\frac{\partial^2 w}{\partial x\partial y}\frac{\partial^2(\delta w)}{\partial x\partial y}-\frac{d_{31}}{a_{33}}V[\frac{\partial w}{\partial x}\frac{\partial(\delta w)}{\partial x}+\frac{\partial w}{\partial y}\frac{\partial(\delta w)}{\partial y}]$$
$$+\frac{d_{31}f_{19}h}{2a_{33}(1+\kappa a_{33})}\left[\frac{\partial^2(\delta w)}{\partial y^2}\left(\frac{\partial w}{\partial x}\right)^2+2\frac{\partial^2 w}{\partial y^2}\frac{\partial w}{\partial x}\frac{\partial(\delta w)}{\partial x}\right] \tag{2.16}$$
$$+\frac{d_{31}f_{19}h}{2a_{33}(1+\kappa a_{33})}\left[\frac{\partial^2(\delta w)}{\partial x^2}\left(\frac{\partial w}{\partial y}\right)^2+2\frac{\partial^2 w}{\partial x^2}\frac{\partial w}{\partial y}\frac{\partial(\delta w)}{\partial y}\right]-q(\delta w)\}dxdy=0.$$

According to the Ritz method, the solution of the transverse displacement of the PNP is approximated in the form of (Reddy, 2007),

$$w(x,y)\approx\sum_{i=1}^{m}\sum_{j=1}^{n}A_{ij}X_i(x)Y_j(y), \tag{2.17}$$

where A_{ij} are the constants to be determined, and $X_i(x)$ and $Y_j(y)$ are coordinate functions satisfying the plate boundary conditions. For the clamped plate, the expressions of $X_i(x)$ and $Y_j(y)$ are given as (Reddy, 2007)

$$X_i(x)=\left(\frac{x}{a}\right)^{i+1}-2\left(\frac{x}{a}\right)^{i+2}+\left(\frac{x}{a}\right)^{i+3}, \tag{2.18a}$$

$$Y_j(y)=\left(\frac{y}{b}\right)^{j+1}-2\left(\frac{y}{b}\right)^{j+2}+\left(\frac{y}{b}\right)^{j+3}. \tag{2.18b}$$

Obviously, these coordinate functions satisfy the mechanical boundary conditions of the clamped plate. Substituting equation (2.17) into equation (2.16) results in,

$$[R]\{A\}+[M]\{A^2\}=\{F\} \tag{2.19}$$

With

$$
\begin{aligned}
R_{(ij)(kl)} = \iint \Bigg[& D_{11}\left(\frac{\partial^2 X_i}{\partial x^2} Y_j \frac{\partial^2 X_k}{\partial x^2} Y_l + \frac{\partial^2 Y_j}{\partial y^2} X_i \frac{\partial^2 Y_l}{\partial y^2} X_k\right) \\
& + D_{12}\left(\frac{\partial^2 X_i}{\partial x^2} Y_j \frac{\partial^2 Y_l}{\partial y^2} X_k + \frac{\partial^2 Y_j}{\partial y^2} X_i \frac{\partial^2 X_k}{\partial x^2} Y_l\right) \\
& + 4D_{66} \frac{\partial X_i}{\partial x}\frac{\partial Y_j}{\partial y}\frac{\partial X_k}{\partial x}\frac{\partial Y_l}{\partial y} \\
& - \frac{d_{31}}{a_{33}} V\left(\frac{\partial X_i}{\partial x} Y_j \frac{\partial X_k}{\partial x} Y_l + \frac{\partial Y_j}{\partial y} X_i \frac{\partial Y_l}{\partial y} X_k\right)\Bigg] dxdy,
\end{aligned}
\tag{2.20}
$$

$$
\begin{aligned}
M_{(ij)(kl)} = \iint \Bigg\{ & \frac{d_{31} f_{19} h}{2a_{33}(1+\kappa a_{33})}\Bigg[\left(\frac{\partial X_i}{\partial x} Y_j\right)^2 \frac{\partial^2 Y_l}{\partial y^2} X_k + \left(\frac{\partial Y_j}{\partial y} X_i\right)^2 \frac{\partial^2 X_k}{\partial x^2} Y_l \\
& + 2\frac{\partial^2 Y_j}{\partial y^2} X_i \frac{\partial X_i}{\partial x} Y_j \frac{\partial X_k}{\partial x} Y_l + 2\frac{\partial^2 X_i}{\partial x^2} Y_j \frac{\partial Y_j}{\partial y} X_i \frac{\partial Y_l}{\partial y} X_k\Bigg]\Bigg\} dxdy
\end{aligned}
\tag{2.21}
$$

and $$F_{kl} = \iint q X_k Y_l dxdy\,. \tag{2.22}$$

Solving the nonlinear algebraic equation (2.19), the unknown constants A_{ij} in the vector A can be determined. Correspondingly, the electroelastic fields are determined by substituting equation (2.17) into equations (2.9) and (2.10).

For the considered range of the material properties, the plate dimensions and applied mechanical and electrical loads, the plate undergoes infinitesimal deformation. The distribution of the nonlinear terms $2\frac{d_{31} f_{19} h}{a_{33}(1+\kappa a_{33})}(\frac{\partial^2 w}{\partial x \partial y})^2$ and $2\frac{d_{31} f_{19} h}{a_{33}(1+\kappa a_{33})}\frac{\partial^2 w}{\partial x^2}\frac{\partial^2 w}{\partial y^2}$ in equation (2.15) is checked and it was found that these terms could be neglected as compared with the other terms. Therefore, the governing equation for the static bending of the PNP is simplified as a linear partial differential equation, i.e.,

$$D_{11}(\frac{\partial^4 w}{\partial x^4}+\frac{\partial^4 w}{\partial y^4})+2(D_{12}+2D_{66})\frac{\partial^4 w}{\partial^2 x\partial^2 y}+\frac{d_{31}}{a_{33}}V(\frac{\partial^2 w}{\partial x^2}+\frac{\partial^2 w}{\partial y^2})-q=0\,, \tag{2.23}$$

and its weak form of the variational statement is expressed as

$$\begin{aligned}&\iint\{D_{11}[\frac{\partial^2 w}{\partial x^2}\frac{\partial^2(\delta w)}{\partial x^2}+\frac{\partial^2 w}{\partial y^2}\frac{\partial^2(\delta w)}{\partial y^2}]+D_{12}[\frac{\partial^2 w}{\partial x^2}\frac{\partial^2(\delta w)}{\partial y^2}+\frac{\partial^2 w}{\partial y^2}\frac{\partial^2(\delta w)}{\partial x^2}]\\&+4D_{66}\frac{\partial^2 w}{\partial x\partial y}\frac{\partial^2(\delta w)}{\partial x\partial y}-\frac{d_{31}}{a_{33}}V[\frac{\partial w}{\partial x}\frac{\partial(\delta w)}{\partial x}+\frac{\partial w}{\partial y}\frac{\partial(\delta w)}{\partial y}]-q(\delta w)\}dxdy=0.\end{aligned} \tag{2.24}$$

Similarly, by applying the Ritz method, the unknown constants A_{ij} in equation (2.17) can be determined from the following linear algebraic equations,

$$[R]\{A\}=\{F\}, \tag{2.25}$$

with $R_{(ij)(kl)}$ and F_{kl} given before.

2.2.2 Free vibration of a PNP

For the free vibration of a PNP without the applied mechanical load q, the governing equation (2.12) can be simplified by neglecting the nonlinear terms as

$$\begin{aligned}&D_{11}(\frac{\partial^4 w}{\partial x^4}+\frac{\partial^4 w}{\partial y^4})+2(D_{12}+2D_{66})\frac{\partial^4 w}{\partial^2 x\partial^2 y}+\frac{d_{31}}{a_{33}}V(\frac{\partial^2 w}{\partial x^2}+\frac{\partial^2 w}{\partial y^2})\\&-\frac{\rho h^3}{12}(\frac{\partial^2 \ddot{w}}{\partial x^2}+\frac{\partial^2 \ddot{w}}{\partial y^2})+\rho h\ddot{w}=0.\end{aligned} \tag{2.26}$$

The harmonic solution of equation (2.26) takes the form of

$$w(x,y,t)=W(x,y)e^{i\omega t}\,, \tag{2.27}$$

where ω is the resonant frequency and W represents the mode shape of the vibration. Substituting equation (2.27) into equation (2.26) results in

$$D_{11}(\frac{\partial^4 W}{\partial x^4}+\frac{\partial^4 W}{\partial y^4})+2(D_{12}+2D_{66})\frac{\partial^4 W}{\partial^2 x\partial^2 y}+\frac{\rho h^3}{12}\omega^2(\frac{\partial^2 W}{\partial x^2}+\frac{\partial^2 W}{\partial y^2}) \\ +\frac{d_{31}}{a_{33}}V(\frac{\partial^2 W}{\partial x^2}+\frac{\partial^2 W}{\partial y^2})-\rho h\omega^2 W=0. \tag{2.28}$$

Similar to the static bending analysis of the PNP, Ritz method is also adopted to get the approximate solution and the same procedure is conducted. The weak form of variational statement of equation (2.28) is presented as

$$\iint\left\{D_{11}\left[\frac{\partial^2 W}{\partial x^2}\frac{\partial^2(\delta W)}{\partial x^2}+\frac{\partial^2 W}{\partial y^2}\frac{\partial^2(\delta W)}{\partial y^2}\right]+D_{12}\left[\frac{\partial^2 W}{\partial x^2}\frac{\partial^2(\delta W)}{\partial y^2}+\frac{\partial^2 W}{\partial y^2}\frac{\partial^2(\delta W)}{\partial x^2}\right]\right. \\ +4D_{66}\frac{\partial^2 W}{\partial x\partial y}\frac{\partial^2(\delta W)}{\partial x\partial y}-\rho h\omega^2 W\delta W-\frac{\rho h^3}{12}\omega^2\left[\frac{\partial W}{\partial x}\frac{\partial(\delta W)}{\partial x}+\frac{\partial W}{\partial y}\frac{\partial(\delta W)}{\partial y}\right] \\ \left.-\frac{d_{31}}{a_{33}}V\left[\frac{\partial W}{\partial x}\frac{\partial(\delta W)}{\partial x}+\frac{\partial W}{\partial y}\frac{\partial(\delta W)}{\partial y}\right]\right\}dxdy=0. \tag{2.29}$$

Similarly, the transverse vibration mode shape $W(x,y)$ is approximated as

$$W(x,y)\approx\sum_{i=1}^{m}\sum_{j=1}^{n}A_{ij}X_i(x)Y_j(y), \tag{2.30}$$

with $X_i(x)$ and $Y_j(y)$ given in the previous section, which satisfy the mechanical boundary conditions of the clamped PNP. Substituting equation (2.30) into equation (2.29), we get:

$$([R]-\omega^2[B])\{A\}=\{0\}, \tag{2.31}$$

with $R_{(ij)(kl)}$ derived in the previous section and

$$B_{(ij)(kl)} = \iint \left[\rho h X_i Y_j X_k Y_l + \frac{\rho h^3}{12} \left(\frac{\partial X_i}{\partial x} Y_j \frac{\partial X_k}{\partial x} Y_l + \frac{\partial Y_j}{\partial y} X_i \frac{\partial Y_l}{\partial y} X_k \right) \right] dxdy. \tag{2.32}$$

The resonant frequency can thus be determined by solving the characteristic equation of equation (2.31).

In the following section, the effect of the flexoelectricity on the elelctroelastic responses and the dynamic behaviors of the PNP will be further demonstrated through case studies. It is worth mentioning that without the consideration of the flexoelectricity, all the equations can be reduced to the corresponding equations from the conventional piezoelectric plate.

2.3 Results and discussions

In this section, in order to demonstrate the effect of the flexoelectricity on the static and dynamic responses of a piezoelectric nanoplate (PNP), $BiTiO_3$ is taken as an example material as the case study. The bulk elastic, piezoelectric and dielectric constants for the plate under the plane strain condition are calculated as c_{11}=167.55GPa, c_{12}=78.15 GPa, $c_{66} = 44.7$ GPa, $a_{33} = 0.79 \times 10^8$ V·m/C and d_{31}=3.5×10^8 V/m based on the information provided in Ref. (Giannakopoulos and Suresh, 1999). $b_{33} = 1 \times 10^{-9} Jm^3 / C^2$ is taken according to Refs. (Maranganti *et al*., 2006; Eliseev *et al*., 2009). Due to the lack of the exact value for the flexocoupling constant in the literature, f_{19}=10 V is adopted in the current calculation for illustration purpose according to Refs. (Zubko *et al*., 2013; Ponomareva *et al*., 2012; Tagantsev, 1986). The distributed load q is set as 0.1 pN/nm^2 to ensure that the plate undergoes small deformation. In current work, three terms for the

coordinate functions are used in the Ritz method to approximate the transverse displacement (e.g. $m = 3$, $n = 3$) to ensure the convergence of the solution.

Firstly, the effect of the flexoelectricity upon the static bending of a PNP is examined. For a nanoplate with fixed dimension ratio $a = b = 50h$ under both electrical and mechanical loads, the variation of the normalized maximum deflection (w / w_0^V) at the middle of the plate ($x = 0.5a,\ y = 0.5b$) with the plate thickness h is plotted in figure 2.2, where w_0^V is the maximum deflection of the plate under the same applied loads without the consideration of the flexoelectric effect. As shown in this figure, the flexoelectricity results in a softer elastic behavior of the plate since a larger deflection is induced in the plate with the incorporation of the flexoelectric effect. In addition, the flexoelectric effect is size-dependent and more prominent for the thinner plate with smaller thickness. With the increase of the plate thickness h, the flexoelectric effect diminishes with all the curves approaching unity as expected. It is interesting to see from this figure that the applied electric potential V alters the flexoelctric effect upon the bending behavior of the PNP. For example, when a positive voltage is applied, the effect of the flexoelectricity upon the static bending of the PNP is magnified with the increase of the magnitute of the applied voltage. However, such a flexoelectric effect is reduced with the increase of the magnitute of an electrical voltage applied in the opposite direction .

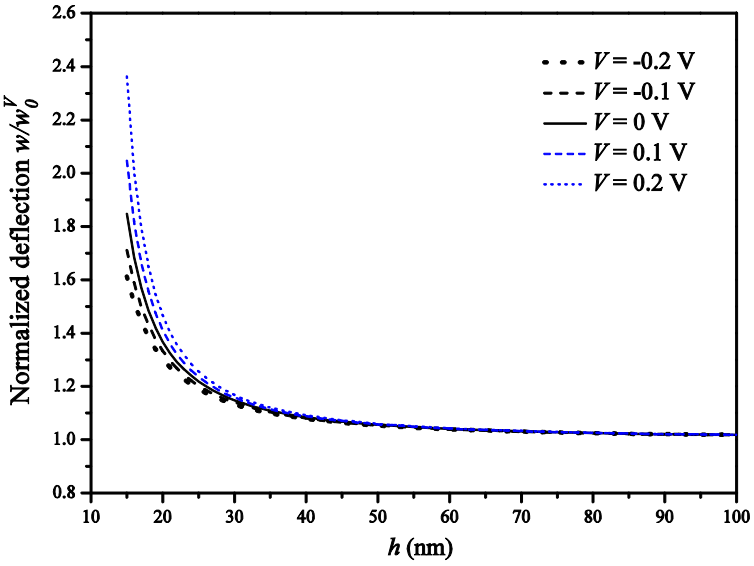

Figure 2.2: Variation of normalized maximum deflection with plate thickness under different voltage ($a = b = 50h$).

In order to see how the flexoelectric effect changes with the plate length to thickness ratio, figure 2.3 depicts the variation of the normalized maximum deflection of a square PNP ($a = b$) with length to thickness ratio (a/h) under different voltage. The thickness of the PNP is set as $h = 20\,\text{nm}$. From this figure, it is concluded that length to thickness ratio a/h, in combination with the applied voltage, also influences the effect of the flexoelectricity upon the static bending of the plate. For example, the effect of the flexoelectricity is independent of the length to thickness ratio (a/h) without the applied voltage as indicated by the straight line for the case of $V = 0\,\text{V}$. However, when a positive voltage is applied, the effect of the flexoelectricity is enhanced by increasing the length to thickness ratio a/h, while an opposite trend is observed under a negative applied voltage. The reason behind this phenomenon is that the applied voltage induces

in-plane forces for the midplane of the plate due to the electromechanical coupling, which in turn affect the stiffness of the plate and the strain gradient, resulting in a varying flexoelectric effect. The results shown in figure 2.2 and figure 2.3 clearly demonstrate that the flexoelectric effect upon the elastic field of a PNP depends on the plate thickness, length to thickness ratio and the applied electrical load, indicating the significance of considering flexoelectricity in predicting the PNP static bending behavior.

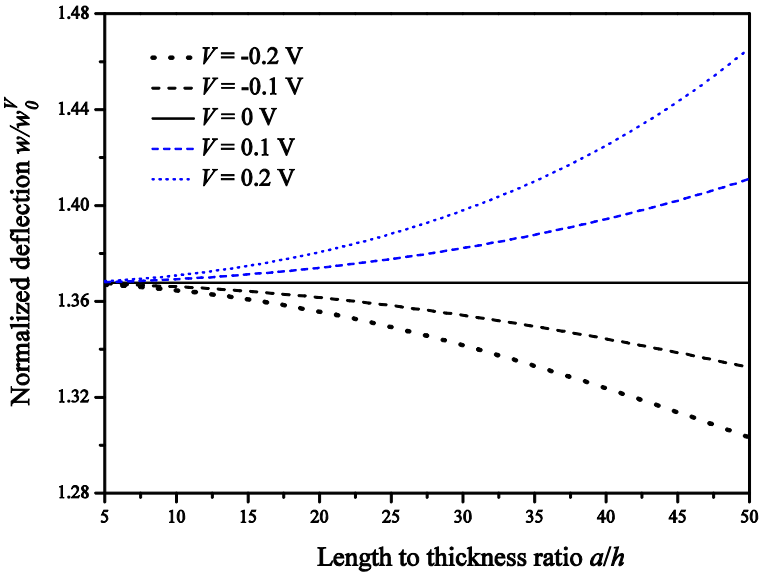

Figure 2.3: Variation of normalized maximum deflection with length to thickness ratio under different voltage ($a = b$).

It is expected that the consideration of the strain gradients and the polarization gradients will influence the electric field distribution. For the plates with different thickness, for example, h = 20 nm or 200 nm, figures 2.4(a) and 2.4(b) plot the distribution of the electric field density E along the thickness direction at the middle of

the plate (x = 0.5a, y = 0.5b) when the applied voltage V = -0.1 V. For the plate with smaller thickness, the flexoelectricity has a significant effect upon the electric field distribution as evidenced by the discrepancy between the current and the classical solutions in figure 2.4(a). However, when the plate thickness becomes larger (h = 200 nm for example), the flexoelectricity has negligible influence upon the electric field distribution except near the surfaces of the plate as shown in figure 2.4(b). The discrepancy of the electric field near the surfaces with the consideration of the flexoelectricity is a typical boundary behavior for a gradient theory also observed for a plate with polarization gradient (Mindlin, 1969) and a circular cylindrical shell with electric field gradient (Yang *et al*., 2004).

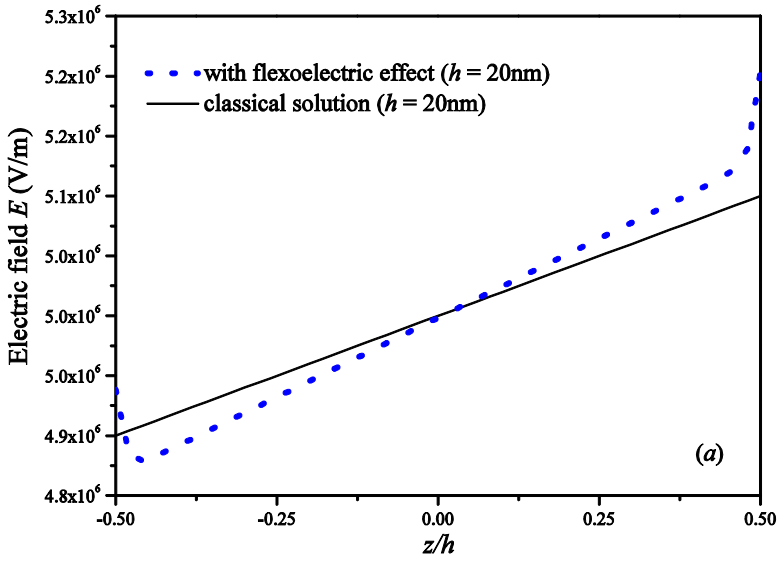

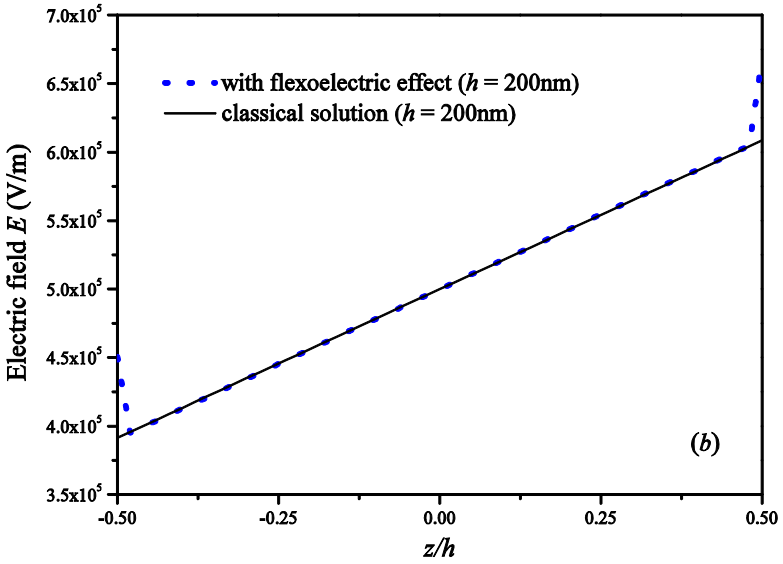

Figure 2.4: Electric field distribution along thickness direction at the middle of the plate with different thickness (*a*) *h* = 20 nm and (*b*) *h* = 200 nm.

As discussed in the previous section, a spontaneous electric polarization along the plate thickness direction will be induced by the strain gradient in the PNP, which is indicated in equation (2.9c). Within the range of the thickness considered in this work, the varying terms along the thickness are relatively negligible compared with the other fixed terms. Thus we can assume that the polarization is constant across the plate thickness. Figure 2.5 plots the in-plane distribution of the polarization for a square plate ($a = b = 50h$, $h = 20$ nm) under a negative applied voltage (V = -0.1 V). Without the consideration of the flexoelectricity, the polarization uniformly distributes in the plate as indicated by the flat plane in this figure, which is purely induced by the applied electric voltage. However, the flexoelectricity significantly influences the in-plane distribution of the polarization, resulting in a non-uniform profile. For example, the polarization

increases near the sides of the plate, while it decreases when approaching the center area of the plate under the current loading condition. However, if the applied voltage changes its direction, an opposite trend for the in-plane polarization distribution is observed, but not shown here. In order to show the dependence of flexoelectricity on the size of the plate, the variation of the polarization for some particular points of a square plate ($a = b = 50h$) against its thickness is plotted in figure 2.6. As indicated in both figures 2.6(a) and 2.6(b), the flexoelectricity has greater influences on the polarization of the plate with smaller thickness. Such an effect diminishes when the plate thickness is getting bigger and eventually the results approach those of the conventional Kirchhoff plate model without the consideration of the flexoelectricity. It is also observed from figures 2.6(a) and 2.6(b) that the flexoelectric effect upon the polarization depends on the direction of the applied voltage, which plays an opposite role in determining the magnitude of the polarization. For example, for a particular point at the end of the plate ($x = 0,\ y = 0.5b$), the flexoelectricity increases the magnitute of polarization with a negative applied voltage. However, the polarization is reduced by the flexoelectricity at the same point when the applied voltage becomes positive. From the results in all these figures, it could be concluded that the effect of the flexoelectricity upon the electroelastic fields of the bending plate depends on both its size and the applied electrical load including amplitude and direction.

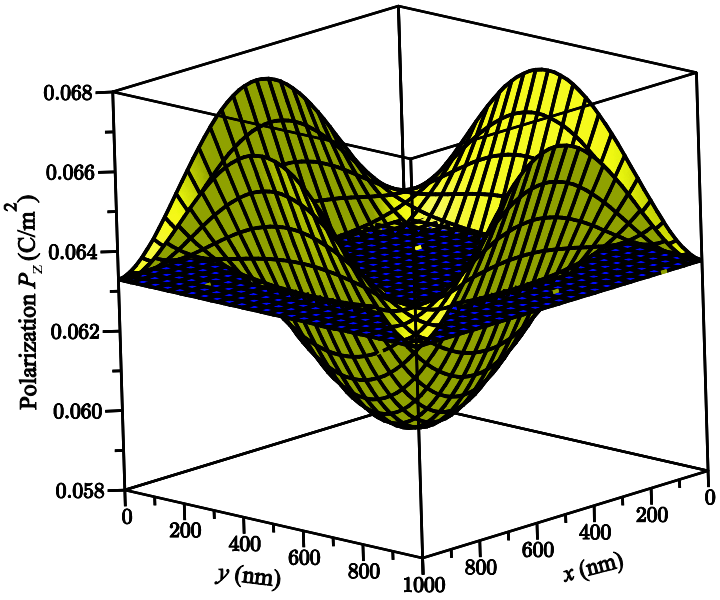

Figure 2.5: In-plane distribution of polarization in a PNP under V = -0.1 V (h = 20 nm), Blue flat surface: classical solution without flexoelectricity; Yellow curved surface: with flexoelectricity.

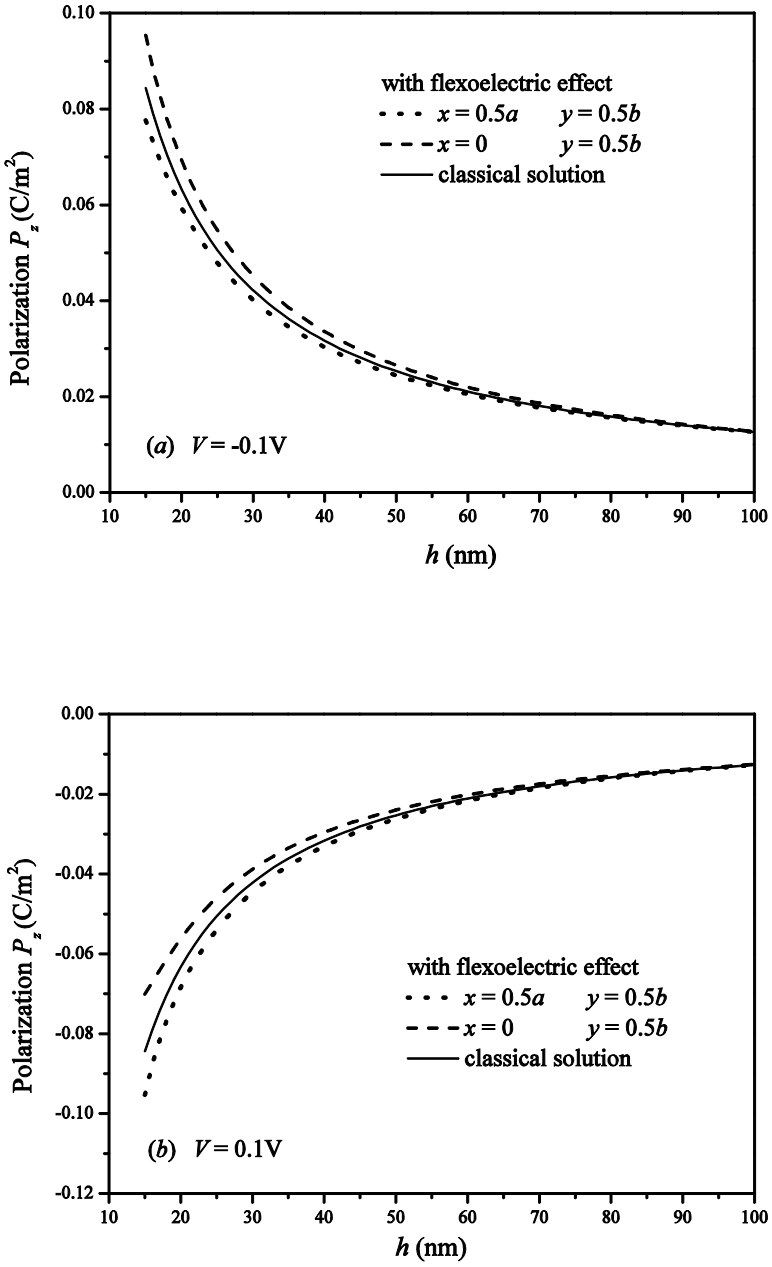

Figure 2.6: Variation of polarization with plate thickness at different locations of the plate under different voltage (*a*) V = -0.1 V and (*b*) V = 0.1 V.

In order to investigate the effect of the flexoelectricity on the vibrational behavior of the PNP, its fundamental resonant frequency is examined. Figure 2.7 depicts the variation of the normalized resonant frequency of a square nanoplate ($a = b = 50h$) with the plate thickness h under different applied electrical loads. ω_0 is the resonant frequency of the nanoplate without considering both the flexoelectric effect and the applied voltage. As revealed in this figure, the flexoelecricity decreases the resonant frequency of the plate significantly for the plate with smaller thickness, indicating the necessity of incorporating the flexoelectric effect in characterizing the vibrational behavior of the PNP. However, with the increase of the plate thickness, the flexoelectric effect upon the resonant frequency diminishes and the normalized resonant frequency tends to approach a constant. It is also observed in this figure that flexoelectric effect upon the resonant frequency is dependent on the applied electrical load, i.e., a positive electric potential enhances the flexoelectric effect upon the resonant frequency while such a trend is reversed when a negative electric potential is applied. The discrepancy among the curves in this figure suggests a possible way for frequency tuning of the PNP by adjusting the applied electrical loads, which has been well discussed in Refs. (Yan and Jiang, 2012a; 2012b). Such a frequency tuning concept originates from the intrinsic electromechanical coupling of the piezoelectric materials, while it is significantly influenced by the flexoelectricity. Thus, the flexoelectricity may modify the frequency tuning process of the PNP-based resonators. Exclusion of the flexoelectric effect in the design of PNP as resonators may lead substantial errors.

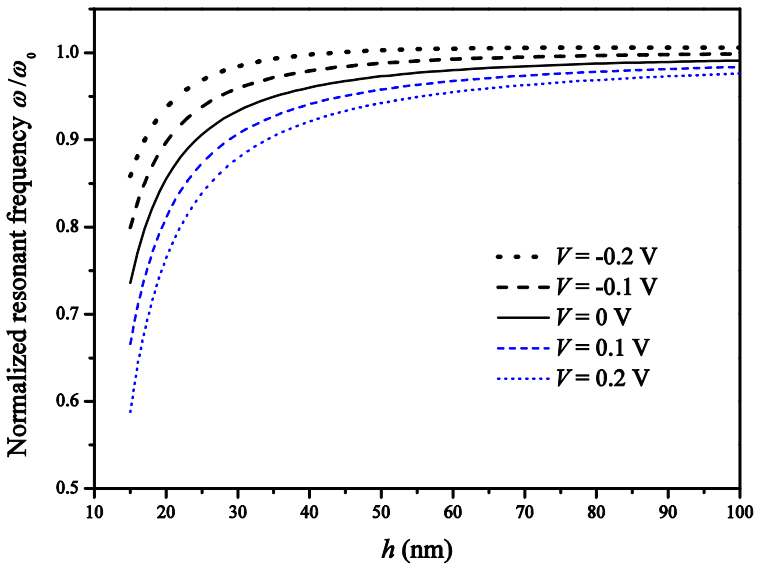

Figure 2.7: Variation of normalized resonant frequency with plate thickness for a plate under different voltage ($a = b = 50h$).

In order to see how the flexoelectric effect varies with the in-plane dimension aspect ratio of the plate, the normalized resonant frequency ω / ω_0^V of a PNP versus the plate thickness h under different applied voltage (V = -0.2 V, 0 V, and 0.2 V, for example) is plotted in figure 2.8 for the plate ($a = 50h$) with different in-plane dimensions a/b. ω_0^V is the resonant frequency for the plate without the consideration of the flexoelectricity. For the case when the plate is subject to a negative voltage, it is observed in figure 2.8 (a) that with the increase of the in-plane aspect ratio a/b, i.e., the plate is becoming narrower when a is fixed, the influence of the flexoelectricity is getting bigger. Once the plate aspect ratio a/b is sufficient large, $a/b > 10$ for example, the flexoelectric effect upon the resonant frequency of the plate will not change with the aspect ratio. Under this

situation, the plate reduces to a beam model and its resonant frequency is independent of its width (i.e., the dimension b for the plate), which is consistent with the formulation (20) in Ref. (Yan and Jiang, 2013b). However, when the plate is subject to a positive voltage, the flexoelectricity has more influence upon the vibration of a plate than a beam as indicated in figure 2.8 (*b*). Without any applied voltage, the flexoelectricity effect on the resonant frequency does not change with the plate in-plane aspect ratio as expected in figure 2.8 (*c*). Therefore, it is concluded from the results in figures 2.7 and 2.8 that the influence of the flexoelectricity upon the resonant frequency of the PNP depends on both the plate size and applied electrical load.

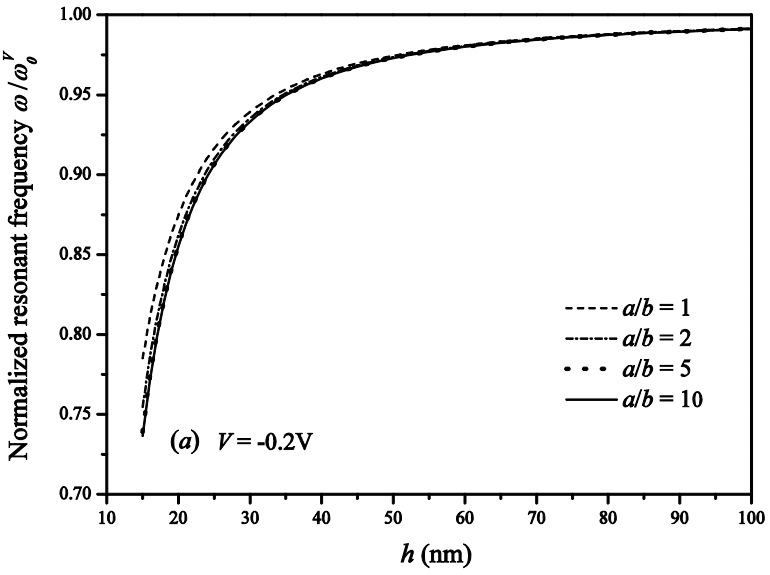

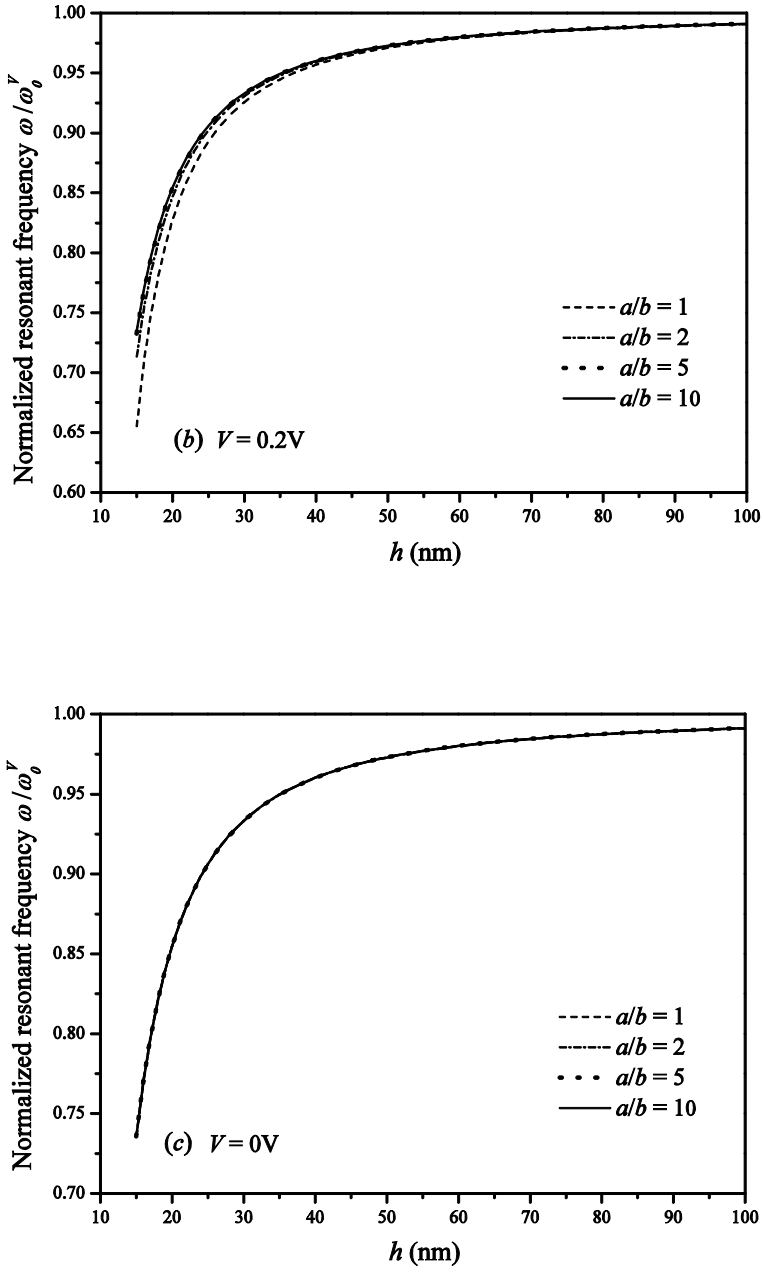

Figure 2.8: Variation of normalized resonant frequency with plate thickness for the plate with different aspect ratio a/b under different voltage ($a = 50h$) (*a*) V = -0.2 V, (*b*) V = 0.2 V and (*c*) V = 0 V.

2.4 Conclusions

In this work, a modified piezoelectric plate model based on the conventional Kirchhoff plate theory and the extended linear piezoelectricity theory with the consideration of the flexoelectric effect is developed to investigate the electroelastic responses and the vibrational behaviors of a piezoelectric nanoplate (PNP). Simulation results indicate that the flexoelectric effect upon the electroelastic fields and the resonant frequency of the PNP is more prominent for thinner plates with smaller thickness while it decays with the increase of the plate thickness. It is also observed that the influence of the flexoelectricity upon the static and dynamic behaviors of the PNP is sensitive to the applied electrical loading and the plate in-plane dimensions. The variation of the resonant frequency of the plate with the applied electric voltage proposes a possible approach for frequency tuning of the PNP-based resonators, which could be modified by the flexoelectric effect. Without considering the surface effects and some other higher order coupling terms in the extended linear piezoelectricity theory, the current work can be claimed as helpful for understanding the trend of the pure static flexoelectric effect upon the size-dependent physical and mechanical properties of the piezoelectric nanoplates, suggesting that the flexoelectricity could modify both the static and dynamic performance of the PNP-based nanodevices.

References

Catalan, G., Noheda, B., McAneney, J., Sinnamon, L. J. and Gregg, J. M., 2005. Strain gradients in epitaxial ferroelectrics. Phys. Rev. B **72** 020102.

Catalan, G., Sinnamon, L. J.and Gregg, J. M., 2004. The effect of flexoelectricity on the dielectric properties of inhomogeneously strained ferroelectric thin films. J. Phys.: Condens. Matter **16** 2253-2264.

Chen, H. T. and Soh, A. K., 2012. Influence of flexoelectric effects on multiferroic nanocomposite thin bilayer films. J. Appl. Phys. **112** 074104.

Chu, M. W., Szafraniak, I., Scholz, R., Harnagea, C., Hesse, D., Alexe, M. and Gösele, U., 2004. Impact of misfit dislocations on the polarization instability of epitaxial nanostructured ferroelectric perovskites. *Nature Mater.* **3** 87-90.

Eliseev, E. A., Morozovska, A. N., Glinchuk, M. D. and Blinc, R., 2009. Spontaneous flexoelectric/flexomagnetic effect in nanoferroics. Phys. Rev. B **79** 165433.

Fousek, J., Cross, L. E. and Litvin, D. B., 1999. Possible piezoelectric composites based on the flexoelectric effect. Mater. Lett. **39** 287-291.

Fu, J. Y., Zhu, W. Y., Li, N., Smith, N. B. and Cross, L. E., 2007. Gradient scaling phenomenon in microsize flexoelectric piezoelectric composites. Appl. Phys. Lett. **91** 182910.

Giannakopoulos, A. E. and Suresh, S., 1999. Theory of indentation of piezoelectric materials. Acta Mater. **47** 2153-2164.

Hlinka, J. and Marton, P., 2006. Phenomenological model of a 90° domain wall in $BaTiO_3$-type ferroelectrics. Phys. Rev. B **74** 104104.

Hu, S. L. and Shen, S. P., 2010. Variational principles and governing equations in nano-dielectrics with the flexoelectric effect. Sci. China, Ser. G **53** 1497-1504.

Lee, D., Yoon, A., Jang, S.Y., Yoon, J. G., Chung, J. S., Kim, M., Scott, J. F. and Noh, T. W., 2011. Giant flexoelectric effect in ferroelectric epitaxial thin films. Phys. Rev. Lett. **107** 057602.

Li, Y. H., Fang, B., Zhang, J. Z. and Song, J. Z., 2011. Surface effects on the wrinkling of piezoelectric films on compliant substrates. J. Appl. Phys. **110** 114303.

Liu, C. C., Hu, S. L. and Shen, S. P., 2012. Effect of flexoelectricity on electrostatic potential in a bent piezoelectric nanowire. Smart Mater. Struct. **21** 115024.

Lu, H., Bark, C. W., de los Ojos, D. E., Alcala, J., Eom, C. B., Catalan, G. and Gruverman, A., 2012. Mechanical writing of ferroelectric polarization. Science **336** 59-61.

Ma, W. H. and Cross, L. E., 2001. Observation of the flexoelectric effect in relaxor Pb (Mg 1/3 Nb 2/3) O 3 ceramics. Appl. Phys. Lett. **78** 2920-2921.

Ma, W. H. and Cross, L. E., 2002. Flexoelectric polarization of barium strontium titanate in the paraelectric state. Appl. Phys. Lett. **81** 3440-3442.

Ma, W. H. and Cross, L. E., 2003. Strain-gradient-induced electric polarization in lead zirconate titanate ceramics. Appl. Phys. Lett. **82** 3293-3295.

Ma, W. H. and Cross, L. E., 2005. Flexoelectric effect in ceramic lead zirconate titanate. Appl. Phys. Lett. **86** 072905.

Ma, W. H. and Cross, L. E., 2006. Flexoelectricity of barium titanate. Appl. Phys. Lett. **88** 232902.

Majdoub, M. S., Maranganti, R. and Sharma, P., 2009. Understanding the origins of the intrinsic dead layer effect in nanocapacitors. Phys. Rev. B **79** 115412.

Majdoub, M. S., Sharma, P. and Cagin, T., 2008. Enhanced size-dependent piezoelectricity and elasticity in nanostructures due to the flexoelectric effect. Phys. Rev. B **77** 125424.

Maranganti, R., Sharma, N. D. and Sharma, P., 2006. Electromechanical coupling in nonpiezoelectric materials due to nanoscale nonlocal size effects: Green's function solutions and embedded inclusions. Phys. Rev. B **74** 014110.

Maranganti, R. and Sharma, P., 2009. Atomistic determination of flexoelectric properties of crystalline dielectrics. Phys. Rev. B **80** 054109.

Mindlin, R. D., 1969. Continuum and lattice theories of influence of electromechanical coupling on capacitance of thin dielectric films. Int. J. Solids Struct. **5** 1197-1208.

Nguyen, T. D., Mao, S., Yeh, Y. W., Purohit, P. K. and McAlpine, M. C., 2013. Nanoscale flexoelectricity. Adv. Mater. **25** 946-974.

Ponomareva, I., Tagantsev, A. K. and Bellaiche, L., 2012. Finite-temperature flexoelectricity in ferroelectric thin films from first principles. Phys. Rev. B **85** 104101.

Quang, H. L. and He, Q. C., 2011. The number and types of all possible rotational symmetries for flexoelectric tensors. Proc. R. Soc. London, Ser. A **467** 2369-2386.

Rao, S. S., 2007. Vibration of continuous systems, New York: Wiley.

Reddy, J. N., 2007. Theory and analysis of elastic plates and shells, Boca Raton, FL:

CRC Press.

Sharma, N.D., Landis, C. M. and Sharma, P. 2010, Piezoelectric thin-film superlattices without using piezoelectric materials. J. Appl. Phys. **108** 024304.

Sharma, N. D., Maranganti, R. and Sharma, P., 2007. On the possibility of piezoelectric nanocomposites without using piezoelectric materials. J. Mech. Phys. Solids **55** 2328-2350.

Shen, S. P. and Hu, S. L., 2010. A theory of flexoelectricity with surface effect for elastic dielectrics. J. Mech. Phys. Solids **58** 665-677.

Shu, L. L., Wei, X. Y., Pang, T., Yao, X., and Wang, C. L., 2011. Symmetry of flexoelectric coefficients in crystalline medium. J. Appl. Phys. **110** 104106.

Stengel, M., 2013. Microscopic response to inhomogeneous deformations in curvilinear coordinates. Nat. Commun. **4** 2693.

Tagantsev, A. K., 1986. Piezoelectricity and flexoelectricity in crystalline dielectrics. Phys. Rev. B **34** 5883-5889.

Tagantsev, A. K. and Gerra, G., 2006. Interface-induced phenomena in polarization response of ferroelectric thin films. J.Appl. Phys. **100** 051607.

Tagantsev, A. K. and Yurkov, A. S., 2012. Flexoelectric effect in finite samples. J. Appl. Phys. **112** 044103.

Toupin, R. A., 1956. The elastic dielectric. J. Ration. Mech. Anal. **5** 849-915.

Wang, Z. L., 2007. The new field of nanopiezotronics. Mater. Today **10** 20-28.

Yan, Z. and Jiang, Y. L. 2011. The vibrational and buckling behaviors of piezoelectric nanobeams with surface effects. Nanotechnology **22** 245703.

Yan, Z. and Jiang, L. Y., 2012a. Vibration and buckling analysis of a piezoelectric nanoplate considering surface effects and in-plane constraints. Proc. R. Soc. A **468** 3458-3475.

Yan, Z. and Jiang, L. Y., 2012b. Surface effects on the vibration and buckling of piezoelectric nanoplates. EPL **99** 27007.

Yan, Z. and Jiang, L. Y., 2013a. Flexoelectric effect on the electroelastic responses of bending piezoelectric nanobeams. J. Appl. Phys. **113** 194102.

Yan, Z. and Jiang, L. Y., 2013b. Size-dependent bending and vibration behaviour of piezoelectric nanobeams due to flexoelectricity. J. Phys. D: Appl. Phys. **46** 355502.

Yang, J. S., 2006. A review of a few topics in piezoelectricity. Appl. Mech. Rev **59** 335-345.

Yang, X. M., Hu, Y. T. and Yang, J. S., 2004. Electric field gradient effects in anti-plane problems of polarized ceramics. Int. J. Solids Struct. **41** 6801-6811.

Yudin, P. V. and Tagantsev, A. K., 2013. Fundamentals of flexoelectricity in solids. Nanotechnology **24** 432001.

Zhao, M. H., Qian, C. F., Lee, S. W. R., Tong, P., Suemasu, H. and Zhang, T. Y., 2007. Electro-elastic analysis of piezoelectric laminated plates. Adv. Compos. Mater. **16** 63-81.

Zhu, W. Y., Fu, J. Y., Li, N. and Cross, L., 2006. Piezoelectric composite based on the enhanced flexoelectric effects. Appl. Phys. Lett. **89** 192904.

Zubko, P., Catalan, G. and Tagantsev, A. K., 2013. Flexoelectric effect in solids. Annu. Rev. Mater. Res. **43** 387-421.

Chapter 3

3 Size effects on electromechanical coupling fields of a bending piezoelectric nanoplate due to surface effects and flexoelectricity

3.1 Introduction

Recently, piezoelectric nanostructures have attracted a surge of interests in research communities for the potential applications as transistors, sensors and energy harvesters in the nanoelectromechanical systems (NEMS) due to their high electromechanical coupling and unique features at the nano-scale (Wang *et al*., 2006; Lao *et al*., 2007; Park *et al*., 2010). In order to fulfill these applications of piezoelectric nanostructures, it is essential to get a thorough and comprehensive understanding on the electromechanical coupling behaviors of piezoelectric materials at the nano-scale.

It has been reported from experimental observations and atomistic simulations that the elastic properties and the piezoelectric coefficients of piezoelectric materials are size-dependent when their characteristic size scales down to the nano-scale, which distinguishes them from their macroscopic bulk counterparts (Stan *et al*., 2007; Zhao *et al*., 2004; Chen *et al*., 2006; Kulkarni *et al*., 2005; Zhang *et al*., 2010). It is thus of great importance to understand the origin and the underlying mechanisms of such size dependence in order to accurately characterize the electromechanical coupling of the piezoelectric nanostructures. Due to the large ratio of surface area to volume typically

presented in nanomaterials, surface effects have been commonly believed to contribute to their size-dependent properties. Based on the linear surface elasticity theory developed by Gurtin and Murdoch (1975), the size-dependent properties of nanostructures originating from the surface effects have been widely investigated by the modified continuum models from both static and dynamic perspectives (Miller and Shenoy, 2000; Song *et al*., 2011; Wang *et al*., 2007; 2009; Wang and Feng, 2007; He and Lilley, 2008a; 2008b; Lu *et al*., 2006; Assadi *et al*., 2010). However, for piezoelectric nanomaterials, such a surface elasticity model may fail to accurately predict their size-dependent properties due to the negligence of the surface piezoelectricity. Huang and Yu (2006) did pioneering work for developing the framework of a surface piezoelectricity model with the incorporation of the surface piezoelectricity in addition to the residual surface stress and the surface elasticity. Based on this model, Yan and Jiang and others (zhang *et al*., 2012; Yan and Jiang, 2011a; 2011b; 2012a; 2012b; Li *et al*., 2011) have systematically conducted theoretical modeling to explore the size-dependent static and dynamic responses of piezoelectric nanobeams, nanofilms and nanoplates. It was reported from these studies that the electromechanical responses, bending, wrinkling, vibrational and buckling behaviors of the piezoelectric nanostructures are size-dependent and are significantly influenced by the surface effects.

In addition to the surface effects, flexoelectricity which refers to a spontaneous polarization induced by strain gradients is also believed to play an important role in characterizing the size-dependent properties of dielectrics at the nano-scale. It was interpreted that the strain gradients or non-uniform strain fields can locally break the inversion symmetry of the materials and thus induce the polarization in the structures

(Maranganti and Sharma, 2009). Therefore, the flexoelectricity is a universal effect in all dielectrics even in centrosymmetric crystals. In general, such flexoelectric effect is rather insignificant relative to the piezoelectric effect for macro-scale piezoelectric materials. However, due to the large strain gradients typically exhibited in nanomaterials, the flexoelectricity becomes manifest and may significantly influence the electromechanical behaviors of nano-scale piezoelectrics. A thorough and comprehensive review of the physical fundamentals, effects and possible applications of the flexoelectricity in solids has been conducted by Nguyen *et al* (2013), Yudin and Tagantsev (2013) and Zubko *et al* (2013). In recent years, efforts have been made by researchers to provide increased understanding on this delicate effect from both experimental and theoretical aspects. For example, a series of experiments have been conducted by Ma and Cross (2001; 2002; 2005; 2006) to quantitatively investigate the flexoelectricity by measuring the flexoelectric coefficients of ferroelectric ceramics, which were found to scale with their dielectric permittivity. In addition, some pioneering theoretical frameworks have been established to account for the flexoelectricity (Maranganti *et al*., 2006; Hu and Shen, 2010) by extending from the linear piezoelectricity developed by Toupin (1956). Based on these fundamental frameworks, the flexoelectric effect on the electromechanical coupling behaviors of piezoelectric nanostructures has been investigated and it was found that the flexoelectricity is responsible for the size-dependent electroelastic responses of piezoelectric nanomaterials (Majdoub, 2008; Yan and Jiang, 2013a; 2013b; Ma and Cross, 2003; Liu *et al*., 2012; Chen and Soh, 2012). Therefore, the flexoelectricity is another significant factor needed to be considered for characterizing the electromechanical coupling of piezoelectric nanomaterials.

In order to capture all these nano-scale structure features as discussed above, Hu and Shen (2010) have successfully established a theoretical framework by proposing an electric enthalpy variational principle for nanosized dielectrics, in which the surface effects, the flexoelectricity and the electrostatic force were considered. Nevertheless, to the authors' best knowledge, theoretical studies of modeling the effects of both the surface and flexoelectricity upon the electromechanical coupling behaviors of piezoelectric nanostructures are very limited. Until recently, Xu *et al*. (2014) investigated the static bending of a piezoelectric nanobeam by a modified Euler-Bernoulli beam model with the consideration of the combined effects of the surface and the flexoelectricity. It was found that the size-dependent properties of the piezoelectric beams may not be accurately characterized when the influence of either the surface effects or the flexoelectricity is ignored. However the study of the effects of the flexoelectricity and the surface upon two-dimensional piezoelectric nanostructures has not been reported thus far. Therefore, the objective of the current work is to develop a modified Kirchhoff plate model incorporating the effects of the residual surface stress, the surface elasticity, the surface piezoelectricity and the flexoelectricity to predict the electroelastic responses and the vibrational behaviors of a bending piezoelectric nanoplate (PNP). We aim to provide increased understanding on the size-dependent properties of piezoelectric nanostructures.

3.2 Formulation and solution of the problem

The problem envisaged in the current work is a clamped PNP with length a, width b and thickness h as depicted in figure 3.1. A Cartesian coordinate system is used to describe the plate with xy-plane in the undeformed midplane of the plate and z-axis along the

thickness direction. The poling direction of the plate is along the *z*-axis. The plate is under an electric voltage *V* between the upper and lower surfaces. When considering the static bending of the plate, it is also subjected to a uniformly distributed mechanical load q. Firstly, we will introduce the fundamental theories describing the electromechanical coupling behaviors of the piezoelectric plates at the nano-scale.

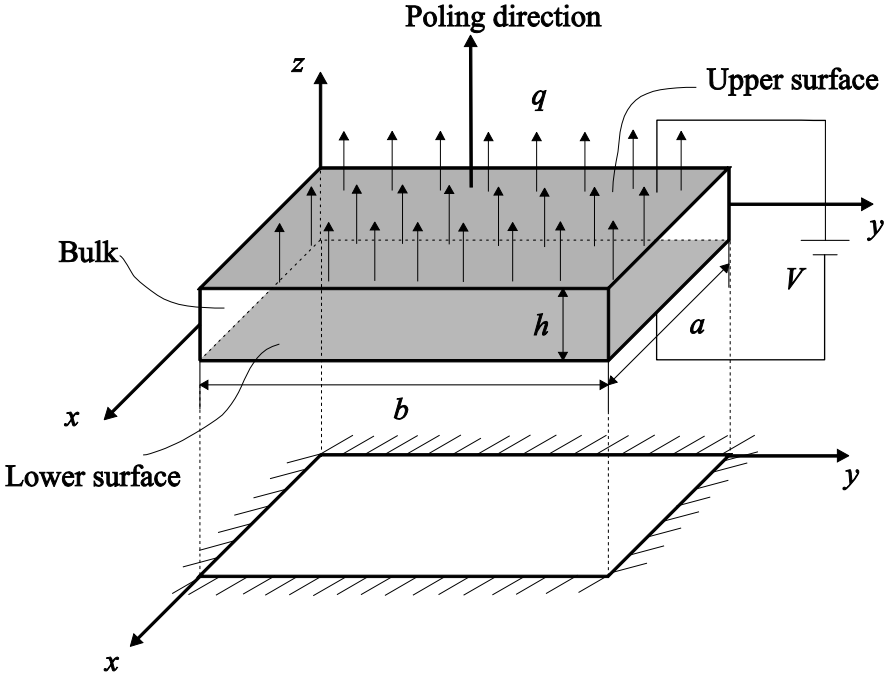

Figure 3.1: Schematic of a clamped piezoelectric nanoplate composed of bulk and surfaces, subjected to electrical and mechanical loads.

3.2.1 Extended linear piezoelectricity theory with surface effects and flexoelectricity

As concluded in Shen and Hu's framework (2010), in order to take the surface effects into consideration, the plate itself is decomposed into a bulk part and surface layers with negligible thickness as shown in figure 3.1. Meanwhile, the flexoelectric effect is

incorporated into the extended linear theory of piezoelectricity by the coupling between the strain gradient and the polarization, the coupling between the polarization gradient and the strain and the product of the polarization gradient and polarization gradient (Yudin and Tagantsev, 2013; Majdoub *et al*., 2008; Sharma *et al*., 2012). Thus the general expression of the bulk internal energy density U_b can be expressed as:

$$U_b = \frac{1}{2}a_{kl}P_kP_l + \frac{1}{2}c_{ijkl}\varepsilon_{ij}\varepsilon_{kl} + d_{ijk}\varepsilon_{ij}P_k + \frac{1}{2}b_{ijkl}P_{i,j}P_{k,l} + f_{ijkl}u_{i,jk}P_l + e_{ijkl}\varepsilon_{ij}P_{k,l}. \quad (3.1)$$

The first three terms in equation (3.1) represent the conventional electromechanical coupling where P_i is the polarization tensor and ε_{ij} is the strain tensor defined as $\varepsilon_{ij} = \frac{1}{2}(u_{i,j} + u_{j,i})$ with u_i being the displacement vector; a_{ij} , c_{ijkl} and d_{ijk} are the conventional material constant tensors which stand for the reciprocal dielectric susceptibility, elastic constant and piezoelectric constant, respectively. Different from the conventional linear piezoelectricity, the extra terms in equation (3.1) represent the higher order couplings. In particular, b_{ijkl} stands for the higher-order coupling between the polarization gradient and the polarization gradient; f_{ijkl} and e_{ijkl} are the effective flexocoupling coefficient tensors renormalized by the surface contribution which always arise from a linear combination of both effects of bulk flexoelectricity and surface piezoelectricity (Stengel, 2013) with f_{ijkl} representing the strain gradient and polarization coupling (direct flexoelectricity) and e_{ijkl} representing the strain and polarization gradient coupling (converse flexoelectricity). According to Refs. (Shen and Hu, 2010; Sharma *et al*., 2012), these two flexocoupling coefficient tensors were justified to satisfy $f_{ijkl} = -e_{ijkl}$. It should be noted that in the current work, the effects of the higher-order couplings between the strain and the strain gradient, the strain gradient and the strain gradient, and

the strain gradient and the polarization gradient are neglected for simplicity as assumed in the Refs. (Zubko *et al*., 2013; Majdoub *et al*., 2008; Yan and Jiang, 2013a; Sharma *et al*., 2012).

Correspondingly, the constitutive equations for the bulk can be derived from the internal energy density as (Hu and Shen, 2010; Shen and Hu, 2010)

$$\sigma_{ij} = \frac{\partial U_b}{\partial \varepsilon_{ij}} = c_{ijkl}\varepsilon_{kl} + d_{ijk}P_k + e_{ijkl}P_{k,l}, \tag{3.2a}$$

$$\sigma_{ijm} = \frac{\partial U_b}{\partial u_{i,jm}} = f_{ijmk}P_k, \tag{3.2b}$$

$$E_i = \frac{\partial U_b}{\partial P_i} = a_{ij}P_j + d_{jki}\varepsilon_{jk} + f_{jkli}u_{j,kl} \tag{3.2c}$$

$$E_{ij} = \frac{\partial U_b}{\partial P_{i,j}} = b_{ijkl}P_{k,l} + e_{klij}\varepsilon_{kl} \tag{3.2d}$$

where σ_{ij} and E_i represent the conventional stress and electrical field tensors. However, these conventional quantities are influenced by the flexoelectricity, i.e. the direct flexoelectric effect contributes to the electrical field while the converse flexoelectric effect contributes to the stress field. The flexoelectric effect is also demonstrated by the development of higher order stress tensor (or moment stress tensor) σ_{ijm} and the higher order local electrical force E_{ij}, which disappear in the conventional linear piezoelectricity theory.

Manipulating equations (3.1) and (3.2), the bulk internal energy density U_b can be rewritten as

$$U_b = \frac{1}{2}E_k P_k + \frac{1}{2}\varepsilon_{ij}\sigma_{ij} + \frac{1}{2}E_{ij}P_{i,j} + \frac{1}{2}u_{i,jm}\sigma_{ijm}. \tag{3.3}$$

According to Toupin's work (1956), the bulk electric enthalpy density can be separated into the bulk internal energy density and a remainder, which was expressed in (Shen and Hu, 2010) as

$$H_b = U_b - \frac{1}{2}\kappa\Phi_{,i}\Phi_{,i} + \Phi_{,i}P_i. \tag{3.4}$$

With the consideration of the surface effects, i.e., the residual surface stress, the surface elasticity and the surface piezoelectricity, the surface internal energy density U_s can be expressed as a function in terms of the surface strain and the surface polarization from the framework of (Shen and Hu, 2010), i.e.,

$$U_s = U_{s0} + \frac{1}{2}a^s_{\alpha\beta}P^s_\alpha P^s_\beta + \frac{1}{2}c^s_{\alpha\beta\gamma\kappa}\varepsilon^s_{\alpha\beta}\varepsilon^s_{\gamma\kappa} + d^s_{\alpha\beta\gamma}\varepsilon^s_{\alpha\beta}P^s_\gamma + \Gamma_{\alpha\beta}\varepsilon^s_{\alpha\beta} \tag{3.5}$$

which is similar to the formulation adopted in Refs. (Huang and Yu, 2006; Liang *et al*., 2014). P^s_α is the surface polarization tensor and $\varepsilon_{\alpha\beta}$ is the surface strain tensor which is defined as $\varepsilon^s_{\alpha\beta} = \frac{1}{2}(u^s_{\alpha,\beta} + u^s_{\beta,\alpha})$ with u^s_α being the surface displacement. $a^s_{\alpha\beta}$, $c^s_{\alpha\beta}$, and $d^s_{\alpha\beta\gamma}$ are the surface reciprocal dielectric susceptibility tensor, the surface elastic constant tensor and the surface piezoelectric constant tensor, respectively. $\Gamma_{\alpha\beta}$ is the residual surface stress tensor which takes $\Gamma_{\alpha\beta} = \sigma^0\delta_{\alpha\beta}$ according to the surface elasticity theory (Shen and Hu, 2010; Liang *et al*., 2014). It should be noted that the surface flexoelectricity (both direct and converse) are ignored in equation (3.5). However, as discussed in (Yudin and Tagantsev, 2013), for materials with higher dielectric constants

(e.g. $BaTiO_3$), the contribution of the surface flexoelectricity is of minor importance and thus it is reasonable to ignore it in the formulation. In this paper, the Greek indices run from 1 to 2 representing the quantities in the surface while the Latin indices run from 1 to 3 representing the corresponding ones in the bulk.

Correspondingly, the constitutive equations for the surface part take the form of

$$\sigma_{\alpha\beta}^{s} = \frac{\partial U_s}{\partial \varepsilon_{\alpha\beta}^{s}} = \Gamma_{\alpha\beta} + c_{\alpha\beta\gamma\kappa}^{s}\varepsilon_{\gamma\kappa}^{s} + d_{\alpha\beta\gamma}^{s}P_{\gamma}^{s}, \tag{3.6a}$$

$$E_{\alpha}^{s} = \frac{\partial U_s}{\partial P_{\alpha}} = a_{\alpha\beta}^{s}P_{\beta}^{s} + d_{\beta\gamma\alpha}^{s}\varepsilon_{\beta\gamma}^{s}, \tag{3.6b}$$

where $\sigma_{\alpha\beta}^{s}$ is the surface stress tensor and E_{α}^{s} is the surface electric field vector.

Combining equations (3.5), (3.6a) and (3.6b), the surface internal energy density can be rewritten as

$$U_s = U_{s0} + \frac{1}{2}E_{\alpha}^{s}P_{\alpha}^{s} + \frac{1}{2}\varepsilon_{\alpha\beta}^{s}\sigma_{\alpha\beta}^{s} + \frac{1}{2}\Gamma_{\alpha\beta}\varepsilon_{\alpha\beta}^{s}. \tag{3.7}$$

Similar to the corresponding bulk electric enthalpy, the surface electric enthalpy can be determined as (Shen and Hu, 2010),

$$H_s = U_s + \Phi_{,\kappa}^{s}P_{\kappa}^{s}, \tag{3.8}$$

where Φ^{s} is the surface electric potential which is continuous cross the surface.

3.2.2 Modified Kirchhoff plate model

In this section, the modified Kirchhoff plate theory with the consideration of the surface effects and the flexoelectricity is developed to investigate the size-dependent bending behaviors of the clamped piezoelectric nanoplate. For a clamped plate, it is reasonable to set the midplane displacement, generally induced by the electromechanical coupling, as zero (Zhao *et al*., 2007). Therefore, the in-plane displacements of the plate can be expressed in terms of the transverse displacement $w(x, y, t)$ according to the Kirchhoff plate theory as

$$u(x,y,z,t) = -z\frac{\partial w(x,y,t)}{\partial x}, \tag{3.9a}$$

$$v(x,y,z,t) = -z\frac{\partial w(x,y,t)}{\partial y}, \tag{3.9b}$$

where $u(x,y,z,t)$ and $v(x,y,z,t)$ are the in-plane displacements of the plate along the x-axis and y-axis, respectively. Thus the non-zero strains can be obtain as

$$\varepsilon_{xx} = -z\frac{\partial^2 w}{\partial x^2}, \tag{3.10a}$$

$$\varepsilon_{yy} = -z\frac{\partial^2 w}{\partial y^2}, \tag{3.10b}$$

$$\varepsilon_{xy} = -z\frac{\partial^2 w}{\partial x \partial y}. \tag{3.10c}$$

Since the thickness of the Kirchhoff plate is much smaller than the in-plane dimensions, the strain gradients along the x and y directions are negligible compared to the strain gradients along the thickness direction similarly to the Euler beam model in Yan and

Jiang's work (2013a). Correspondingly, the nonzero components for the strain gradients can be expressed as

$$\varepsilon_{xx,z} = -\frac{\partial^2 w}{\partial x^2}, \tag{3.11a}$$

$$\varepsilon_{yy,z} = -\frac{\partial^2 w}{\partial y^2}, \tag{3.11b}$$

$$\varepsilon_{xy,z} = -\frac{\partial^2 w}{\partial x \partial y}. \tag{3.11c}$$

In order to present the formulation in a simple way, the contracted notation for the subscripts of the material constant tensors is adopted here, i.e., c_{11}=c_{1111}, c_{66}=c_{1212}, d_{31}=d_{311}, a_{3333}=a_{33} and b_{3333}=b_{33}. According to the relationship between the flexocoupling coefficient tensor f_{ijkl} and the flexoelectric coefficient tensor μ_{ijkl} (Yan and Jiang, 2013a; Sharma *et al*., 2012), i.e., $f_{ijkl} = a_{lm}(\mu_{ijkm} + \mu_{ikjm} - \mu_{jkim})$, and the provided number of the non-zero and independent flexoelectric coefficient elements μ_{ijkl} in a matrix form for a given symmetry class of materials in Refs. (Shu *et al*., 2011; Quang and He, 2011), the corresponding flexocoupling coefficient tensor of the example material of tetragonal $BaTiO_3$ (point group 4mm) can be obtained. Following the same subscript transformation in Ref. (Shu *et al*., 2011), $f_{1133} = f_{2233}$ can be represented by f_{19}. Substituting equations (3.10) and (3.11) into equations (3.2c) and (3.2d), the electric field E_i which is assumed to exist in the z direction only (Zhao *et al*., 2007) and the higher order electric field E_{ij} for a transversely isotropic material can be derived as

$$E_z = a_{33}P_z + d_{31}(-z\frac{\partial^2 w}{\partial x^2} - z\frac{\partial^2 w}{\partial y^2}) + f_{19}(-\frac{\partial^2 w}{\partial x^2} - \frac{\partial^2 w}{\partial y^2}), \tag{3.12a}$$

$$E_{zx} = b_{3133} P_{z,z}, \tag{3.12b}$$

$$E_{zy} = b_{3233} P_{z,z}, \tag{3.12c}$$

$$E_{zz} = b_{33} P_{z,z} - f_{19}(-z\frac{\partial^2 w}{\partial x^2} - z\frac{\partial^2 w}{\partial y^2}). \tag{3.12d}$$

When the plate is subjected to an electric potential Φ across its thickness, the equilibrium equation involving the electric potential Φ, electric field E_i and the higher order electric field E_{ij} should be satisfied as (Shen and Hu, 2010),

$$E_z + \frac{\partial \Phi}{\partial z} - E_{zx,x} - E_{zy,y} - E_{zz,z} = 0. \tag{3.13}$$

In the absence of free electric charges, the Gauss's law requires

$$-\kappa \Phi_{,zz} + P_{z,z} = 0, \tag{3.14}$$

where $\kappa = \kappa_0 \kappa_b$ with the consideration of the so-called background permittivity for ferroelectrics (Tagantsev and Gerra, 2006). $\kappa_0 = 8.85 \times 10^{-12} C \cdot V^{-1} \cdot m^{-1}$ is the permittivity of the air, and $\kappa_b = 6.62$ is the background permittivity for the example material $BaTiO_3$ when its electric field is parallel to the polarization (Tagantsev and Gerra, 2006).

By means of equations (3.12)-(3.14) and the electric boundary conditions $E_{ij} n_j = 0$, $\Phi(\frac{h}{2}) = V$ and $\Phi(-\frac{h}{2}) = 0$ for the current case, the electric potential, the polarization and the electric field can be derived in terms of the plate transverse displacement w and the applied voltage V as,

$$\Phi = \frac{d_{31}}{2(1+a_{33}\kappa)}(\frac{\partial^2 w}{\partial x^2}+\frac{\partial^2 w}{\partial y^2})(\mathrm{z}^2-\frac{1}{4}h^2)+\frac{V}{h}z+\frac{V}{2}$$
$$+\frac{f_{19}}{1+a_{33}\kappa}(\frac{\partial^2 w}{\partial x^2}+\frac{\partial^2 w}{\partial y^2})z-\frac{f_{19}h}{2(1+a_{33}\kappa)}(\frac{\partial^2 w}{\partial x^2}+\frac{\partial^2 w}{\partial y^2})\frac{e^{\lambda z}-e^{-\lambda z}}{e^{\frac{h}{2}\lambda}-e^{-\frac{h}{2}\lambda}}, \tag{3.15}$$

$$E_z = -\frac{d_{31}}{1+a_{33}\kappa}(\frac{\partial^2 w}{\partial x^2}+\frac{\partial^2 w}{\partial y^2})z-\frac{V}{h}+\frac{a_{33}\kappa f_{19}}{1+a_{33}\kappa}(\frac{\partial^2 w}{\partial x^2}+\frac{\partial^2 w}{\partial y^2})$$
$$-\frac{a_{33}f_{19}h}{2\lambda b_{33}}(\frac{\partial^2 w}{\partial x^2}+\frac{\partial^2 w}{\partial y^2})\frac{e^{\lambda z}+e^{-\lambda z}}{e^{\frac{h}{2}\lambda}-e^{-\frac{h}{2}\lambda}}, \tag{3.16}$$

$$P_z = \frac{d_{31}\kappa}{1+a_{33}\kappa}(\frac{\partial^2 w}{\partial x^2}+\frac{\partial^2 w}{\partial y^2})\mathrm{z}-\frac{V}{a_{33}h}+\frac{f_{19}(1+2a_{33}\kappa)}{a_{33}(1+a_{33}\kappa)}(\frac{\partial^2 w}{\partial x^2}+\frac{\partial^2 w}{\partial y^2})$$
$$-\frac{f_{19}h}{2\lambda b_{33}}(\frac{\partial^2 w}{\partial x^2}+\frac{\partial^2 w}{\partial y^2})\frac{e^{\lambda z}+e^{-\lambda z}}{e^{\frac{h}{2}\lambda}-e^{-\frac{h}{2}\lambda}}, \tag{3.17}$$

where $\lambda = \sqrt{\frac{1+\kappa a_{33}}{\kappa b_{33}}}$.

After the derivation of these electric fields, the traditional stresses can be determined from the constitutive equation (3.2a) in terms of the applied voltage and the transverse displacement, i.e.,

$$\sigma_{xx} = (-c_{11}+\frac{d_{31}^2\kappa}{1+a_{33}\kappa})z\frac{\partial^2 w}{\partial x^2}+(-c_{12}+\frac{d_{31}^2\kappa}{1+a_{33}\kappa})z\frac{\partial^2 w}{\partial y^2}-\frac{d_{31}V}{a_{33}h}$$
$$+(\frac{d_{31}f_{19}}{a_{33}}-\frac{d_{31}f_{19}h}{2\lambda b_{33}}\frac{e^{\lambda z}+e^{-\lambda z}}{e^{\frac{h}{2}\lambda}-e^{-\frac{h}{2}\lambda}}+\frac{f_{19}^2 h}{2b_{33}}\frac{e^{\lambda z}-e^{-\lambda z}}{e^{\frac{h}{2}\lambda}-e^{-\frac{h}{2}\lambda}})(\frac{\partial^2 w}{\partial x^2}+\frac{\partial^2 w}{\partial y^2}), \tag{3.18a}$$

$$\sigma_{yy}=(-c_{12}+\frac{d_{31}^2\kappa}{1+a_{33}\kappa})z\frac{\partial^2 w}{\partial x^2}+(-c_{11}+\frac{d_{31}^2\kappa}{1+a_{33}\kappa})z\frac{\partial^2 w}{\partial y^2}-\frac{d_{31}V}{a_{33}h}$$
$$+(\frac{d_{31}f_{19}}{a_{33}}-\frac{d_{31}f_{19}h}{2\lambda b_{33}}\frac{e^{\lambda z}+e^{-\lambda z}}{e^{\frac{h}{2}\lambda}-e^{-\frac{h}{2}\lambda}}+\frac{f_{19}^2 h}{2b_{33}}\frac{e^{\lambda z}-e^{-\lambda z}}{e^{\frac{h}{2}\lambda}-e^{-\frac{h}{2}\lambda}})(\frac{\partial^2 w}{\partial x^2}+\frac{\partial^2 w}{\partial y^2}), \tag{3.18b}$$

$$\sigma_{xy}=-2c_{66}z\frac{\partial^2 w}{\partial x\partial y}. \tag{3.18c}$$

Additionally, the surface stresses can also be derived in terms of the applied voltage and the transverse deflection from the surface constitutive equation (3.6a) as

$$\sigma_{xx}^s=\sigma^0+(-c_{11}^s+\frac{d_{31}d_{31}^s\kappa}{1+a_{33}\kappa})z\frac{\partial^2 w}{\partial x^2}+(-c_{12}^s+\frac{d_{31}d_{31}^s\kappa}{1+a_{33}\kappa})z\frac{\partial^2 w}{\partial y^2}-\frac{d_{31}^s V}{a_{33}h}$$
$$+(\frac{d_{31}^s f_{19}(1+2a_{33}\kappa)}{a_{33}(1+a_{33}\kappa)}-\frac{d_{31}^s f_{19}h}{2\lambda b_{33}}\frac{e^{\lambda z}+e^{-\lambda z}}{e^{\frac{h}{2}\lambda}-e^{-\frac{h}{2}\lambda}})(\frac{\partial^2 w}{\partial x^2}+\frac{\partial^2 w}{\partial y^2}), \tag{3.19a}$$

$$\sigma_{yy}^s=\sigma^0+(-c_{12}^s+\frac{d_{31}d_{31}^s\kappa}{1+a_{33}\kappa})z\frac{\partial^2 w}{\partial x^2}+(-c_{11}^s+\frac{d_{31}d_{31}^s\kappa}{1+a_{33}\kappa})z\frac{\partial^2 w}{\partial y^2}-\frac{d_{31}^s V}{a_{33}h}$$
$$+(\frac{d_{31}^s f_{19}(1+2a_{33}\kappa)}{a_{33}(1+a_{33}\kappa)}-\frac{d_{31}^s f_{19}h}{2\lambda b_{33}}\frac{e^{\lambda z}+e^{-\lambda z}}{e^{\frac{h}{2}\lambda}-e^{-\frac{h}{2}\lambda}})(\frac{\partial^2 w}{\partial x^2}+\frac{\partial^2 w}{\partial y^2}), \tag{3.19b}$$

$$\sigma_{xy}^s=-2c_{66}^s z\frac{\partial^2 w}{\partial x\partial y}. \tag{3.19c}$$

It is worth mentioning that the expressions of all the bulk electroelastic fields are consistent with those according to the classical piezoelectricity theory if the flexoelectricity and the surface effects are excluded.

In order to determine the transverse displacement in the electroelastic fields for both the bulk and surfaces of the plate, Hamilton's principle is adopted in the current work (Yan and Jiang, 2013b; Rao, 2007), i.e.,

$$\delta\int_{t_1}^{t_2}(-\int_{\Omega}Hd\Omega+K+W)dt=0 \tag{3.20}$$

where H is the electric enthalpy including both the bulk and surface components, i.e., $H=H_b+H_s$. According to equations (3.3), (3.4), (3.7) and (3.8), the bulk and the surface electric enthalpy of the plate can be reduced to $H_b=\frac{1}{2}(\sigma_{xx}\varepsilon_{xx}+\sigma_{yy}\varepsilon_{yy}+2\sigma_{xy}\varepsilon_{xy}+\sigma_{xxz}\varepsilon_{xx,z}+\sigma_{yyz}\varepsilon_{yy,z}+E_zP_z+\mathrm{E}_{zz}\mathrm{P}_{z,z})-\frac{1}{2}\kappa\Phi_{,z}\Phi_{,z}+\Phi_{,z}P_z$ and $H_s=U_{s0}+\frac{1}{2}(\varepsilon_{xx}^s\sigma_{xx}^s+\varepsilon_{yy}^s\sigma_{yy}^s+2\varepsilon_{xy}^s\sigma_{xy}^s+\sigma^0\varepsilon_{xx}^s+\sigma^0\varepsilon_{yy}^s)$, respectively. K is the kinetic energy defined as $K=\frac{1}{2}\iint[\rho\frac{h^3}{12}\left(\left(\frac{\partial\dot{w}}{\partial x}\right)^2+\left(\frac{\partial\dot{w}}{\partial y}\right)^2\right)+\rho h\dot{w}^2]dxdy$ for the plate, where ρ is the mass density and the dot "." represents the derivation with respect to time *t*. Additionally, *W* is the work done by the external forces. For the clamped PNP with four edges fixed, *W* takes the form of $W=\iint qwdxdy-\frac{1}{2}\iint[N_{xx}^*(\frac{\partial w}{\partial x})^2+N_{yy}^*(\frac{\partial w}{\partial y})^2+2N_{xy}^*(\frac{\partial w}{\partial x}\frac{\partial w}{\partial y})]dxdy$, where N_{xx}^*, N_{yy}^* and N_{xy}^* are the generalized resultant in-plane forces defined as $N_{ij}^*=N_{ij}+(\sigma_{ij}^s)^u+(\sigma_{ij}^s)^l$ with N_{ij} being the resultant in-plane forces for the bulk component and the superscripts "*u* " and "*l*" representing the upper and lower surfaces, respectively. The in-plane forces for the bulk can be expressed as

$$N_{xx}=\int_{-\frac{h}{2}}^{\frac{h}{2}}\sigma_{xx}dz=\frac{d_{31}f_{19}h}{a_{33}(1+\kappa a_{33})}(\frac{\partial^2w}{\partial x^2}+\frac{\partial^2w}{\partial y^2})-\frac{d_{31}}{a_{33}}V,$$

$N_{yy}=\int_{-\frac{h}{2}}^{\frac{h}{2}}\sigma_{yy}dz=\frac{d_{31}f_{19}h}{a_{33}(1+\kappa a_{33})}(\frac{\partial^2w}{\partial x^2}+\frac{\partial^2w}{\partial y^2})-\frac{d_{31}}{a_{33}}V$ and $N_{xy}=\int_{-\frac{h}{2}}^{\frac{h}{2}}\sigma_{xy}dz=0$. Obviously, the generalized resultant in-plane forces are induced by the electric voltage due to the conventional electromechanical coupling. For the nano-scale plates, both the surface

effects and the flexoelectricity contribute to these in-plane forces which may become compressive depending on the direction and magnitude of the electric potential, the residual surface stress and the flexoelectricity.

By conducting the variational principle of equation (3.20), the governing equation of the piezoelectric plate including the surface effects and the flexoelectricity can be derived as,

$$\begin{aligned}
&D_{11}\left(\frac{\partial^4 w}{\partial x^4}+\frac{\partial^4 w}{\partial y^4}\right)+2(D_{12}+2D_{66})\frac{\partial^4 w}{\partial^2 x\partial^2 y}+\left(\frac{d_{31}}{a_{33}}V+\frac{2d_{31}^s V}{a_{33}h}-2\sigma^0\right)\left(\frac{\partial^2 w}{\partial x^2}+\frac{\partial^2 w}{\partial y^2}\right)\\
&+2\left(\frac{d_{31}f_{19}h+2f_{19}d_{31}^s(1+2\kappa a_{33})}{a_{33}(1+\kappa a_{33})}-\frac{f_{19}hd_{31}^s}{\lambda b_{33}}\frac{e^{\frac{h}{2}\lambda}+e^{-\frac{h}{2}\lambda}}{e^{\frac{h}{2}\lambda}-e^{-\frac{h}{2}\lambda}}\right)\left(\frac{\partial^2 w}{\partial x\partial y}\right)^2\\
&-2\left(\frac{d_{31}f_{19}h+2f_{19}d_{31}^s(1+2\kappa a_{33})}{a_{33}(1+\kappa a_{33})}-\frac{f_{19}hd_{31}^s}{\lambda b_{33}}\frac{e^{\frac{h}{2}\lambda}+e^{-\frac{h}{2}\lambda}}{e^{\frac{h}{2}\lambda}-e^{-\frac{h}{2}\lambda}}\right)\frac{\partial^2 w}{\partial x^2}\frac{\partial^2 w}{\partial y^2}\\
&-\frac{\rho h^3}{12}\left(\frac{\partial^2 \ddot{w}}{\partial x^2}+\frac{\partial^2 \ddot{w}}{\partial y^2}\right)+\rho h\ddot{w}-q=0,
\end{aligned} \tag{3.21}$$

with

$$\begin{aligned}
D_{11}\equiv&\left(c_{11}-\frac{d_{31}^2\kappa}{(1+\kappa a_{33})}\right)\frac{h^3}{12}-\frac{f_{19}^2 h}{a_{33}(1+\kappa a_{33})}-\frac{f_{19}^2h^2}{2\lambda b_{33}}\frac{e^{\frac{h}{2}\lambda}+e^{-\frac{h}{2}\lambda}}{e^{\frac{h}{2}\lambda}-e^{-\frac{h}{2}\lambda}}+\frac{b_{33}d_{31}^2\kappa^2 h}{(1+\kappa a_{33})^2}\\
&+\left(c_{11}^s-\frac{d_{31}^s d_{31}k}{1+\kappa a_{33}}\right)\frac{h^2}{2},
\end{aligned} \tag{3.22a}$$

$$\begin{aligned}
D_{12}\equiv&\left(c_{12}-\frac{d_{31}^2\kappa}{(1+\kappa a_{33})}\right)\frac{h^3}{12}-\frac{f_{19}^2 h}{a_{33}(1+\kappa a_{33})}-\frac{f_{19}{}^2h^2}{2\lambda b_{33}}\frac{e^{\frac{h}{2}\lambda}+e^{-\frac{h}{2}\lambda}}{e^{\frac{h}{2}\lambda}-e^{-\frac{h}{2}\lambda}}+\frac{b_{33}d_{31}^2\kappa^2 h}{(1+\kappa a_{33})^2}\\
&+\left(c_{12}^s-\frac{d_{31}^s d_{31}k}{1+\kappa a_{33}}\right)\frac{h^2}{2},
\end{aligned} \tag{3.22b}$$

$$D_{66} \equiv \frac{c_{66}}{12} h^3 + \frac{c_{66}^s}{2} h^2 . \tag{3.22c}$$

It is identified from the expressions of D_{11} and D_{12} that the flexoelectricity decreases the effective bending rigidity while the surface effects increase it. With the given values of the material property constants of the example material $BaTiO_3$, when the thickness of the plate is small, e.g. at nanometers, the contribution of the flexoelectricity and surface effects on the effective bending rigidity becomes significant. Thus the exclusion of these effects might result in inaccuracy when investigating the bending behaviors of the PNP. However, the bending rigidity needs to be positive to ensure the stability of the plate. It should be pointed out that without the consideration of the surface effects and the flexoelectricity, the governing equation (3.21) can be reduced to the motion equation for a classical piezoelectric Kirchhoff plate.

In addition, the mechanical boundary conditions for the clamped PNP can also be derived by the means of the variational principle as

$$w = 0 \text{ and } \frac{\partial w}{\partial x} = 0 \quad \text{at } x = 0 \text{ and } x = a ; \tag{3.23a}$$

$$w = 0 \text{ and } \frac{\partial w}{\partial y} = 0 \quad \text{at } y = 0 \text{ and } y = b . \tag{3.23b}$$

Thus the deflection, the corresponding electroelastic fields, and the dynamic responses of the bending PNP can be determined by solving the nonlinear partial differential equation (3.21) with the mechanical boundary conditions listed in equations (3.23).

3.2.3 Electroelastic responses of a static bending PNP

For the static bending analysis of the PNP, the inertial terms are neglected and the governing equation (3.21) can be rewritten as

$$\begin{aligned}
&D_{11}\left(\frac{\partial^4 w}{\partial x^4}+\frac{\partial^4 w}{\partial y^4}\right)+2(D_{12}+2D_{66})\frac{\partial^4 w}{\partial^2 x\partial^2 y}+\left(\frac{d_{31}}{a_{33}}V+\frac{2d_{31}^s V}{a_{33}h}-2\sigma^0\right)\left(\frac{\partial^2 w}{\partial x^2}+\frac{\partial^2 w}{\partial y^2}\right)\\
&+2\left(\frac{d_{31}f_{19}h+2f_{19}d_{31}^s(1+2\kappa a_{33})}{a_{33}(1+\kappa a_{33})}-\frac{f_{19}hd_{31}^s}{\lambda b_{33}}\frac{e^{\frac{h}{2}\lambda}+e^{-\frac{h}{2}\lambda}}{e^{\frac{h}{2}\lambda}-e^{-\frac{h}{2}\lambda}}\right)\left(\frac{\partial^2 w}{\partial x\partial y}\right)^2\\
&-2\left(\frac{d_{31}f_{19}h+2f_{19}d_{31}^s(1+2\kappa a_{33})}{a_{33}(1+\kappa a_{33})}-\frac{f_{19}hd_{31}^s}{\lambda b_{33}}\frac{e^{\frac{h}{2}\lambda}+e^{-\frac{h}{2}\lambda}}{e^{\frac{h}{2}\lambda}-e^{-\frac{h}{2}\lambda}}\right)\frac{\partial^2 w}{\partial x^2}\frac{\partial^2 w}{\partial y^2}\\
&-q=0.
\end{aligned}\tag{3.24}$$

When the plate undergoes infinitesimal deformation within the considered range of the material properties, the plate dimensions and applied mechanical and electrical loads, the distribution of the nonlinear terms $2\left(\frac{d_{31}f_{19}h+2f_{19}d_{31}^s(1+2\kappa a_{33})}{a_{33}(1+\kappa a_{33})}-\frac{f_{19}hd_{31}^s}{\lambda b_{33}}\frac{e^{\frac{h}{2}\lambda}+e^{-\frac{h}{2}\lambda}}{e^{\frac{h}{2}\lambda}-e^{-\frac{h}{2}\lambda}}\right)\left(\frac{\partial^2 w}{\partial x\partial y}\right)^2$ and $2\left(\frac{d_{31}f_{19}h+2f_{19}d_{31}^s(1+2\kappa a_{33})}{a_{33}(1+\kappa a_{33})}-\frac{f_{19}hd_{31}^s}{\lambda b_{33}}\frac{e^{\frac{h}{2}\lambda}+e^{-\frac{h}{2}\lambda}}{e^{\frac{h}{2}\lambda}-e^{-\frac{h}{2}\lambda}}\right)\frac{\partial^2 w}{\partial x^2}\frac{\partial^2 w}{\partial y^2}$ in equation (3.24) is checked and it is found that these terms could be neglected as compared with the other terms. Accordingly, the nonlinear partial differential equation (3.24) could be simplified as a linear one, i.e.,

$$\begin{aligned}
&D_{11}\left(\frac{\partial^4 w}{\partial x^4}+\frac{\partial^4 w}{\partial y^4}\right)+2(D_{12}+2D_{66})\frac{\partial^4 w}{\partial^2 x\partial^2 y}\\
&+\left(\frac{d_{31}}{a_{33}}V+\frac{2d_{31}^s V}{a_{33}h}-2\sigma^0\right)\left(\frac{\partial^2 w}{\partial x^2}+\frac{\partial^2 w}{\partial y^2}\right)-q=0.
\end{aligned}\tag{3.25}$$

In order to investigate how the surface effects and the flexoelectricity influence the static bending of the PNP, the Ritz method (Reddy, 2007) is adopted to get the approximate solution of equation (3.25), in which the weak form of the variational statement of equation (3.25) is expressed as,

$$\begin{aligned}&\iint \{D_{11}[\frac{\partial^2 w}{\partial x^2}\frac{\partial^2(\delta w)}{\partial x^2}+\frac{\partial^2 w}{\partial y^2}\frac{\partial^2(\delta w)}{\partial y^2}]+D_{12}[\frac{\partial^2 w}{\partial x^2}\frac{\partial^2(\delta w)}{\partial y^2}+\frac{\partial^2 w}{\partial y^2}\frac{\partial^2(\delta w)}{\partial x^2}]\\&+4D_{66}\frac{\partial^2 w}{\partial x\partial y}\frac{\partial^2(\delta w)}{\partial x\partial y}-(\frac{d_{31}}{a_{33}}V+\frac{2d_{31}^s V}{a_{33}h}-2\sigma^0)[\frac{\partial w}{\partial x}\frac{\partial(\delta w)}{\partial x}+\frac{\partial w}{\partial y}\frac{\partial(\delta w)}{\partial y}]\\&-q(\delta w)\}dxdy=0.\end{aligned} \tag{3.26}$$

According to the Ritz method, the transverse deflection can be approximated as (Reddy, 2007),

$$w(x,y)\approx\sum_{i=1}^{m}\sum_{j=1}^{n}A_{ij}X_i(x)Y_j(y) \tag{3.27}$$

where A_{ij} are unknown constants to be determined, and $X_i(x)$ and $Y_j(y)$ are coordinate functions which should satisfy the mechanical boundary conditions of the plate. Thus for the clamped plate, $X_i(x)$ and $Y_j(y)$ are chosen as (Reddy, 2007)

$$X_i(x)=\left(\frac{x}{a}\right)^{i+1}-2\left(\frac{x}{a}\right)^{i+2}+\left(\frac{x}{a}\right)^{i+3}, \tag{3.28a}$$

$$Y_j(y)=\left(\frac{y}{b}\right)^{j+1}-2\left(\frac{y}{b}\right)^{j+2}+\left(\frac{y}{b}\right)^{j+3}. \tag{3.28b}$$

Substituting equations (3.27) and (3.28) into equation (3.26) yields,

$$[R]\{A\}=\{F\} \tag{3.29}$$

with

$$
\begin{aligned}
R_{(ij)(kl)} = \iint \Bigg[& D_{11}\left(\frac{\partial^2 X_i}{\partial x^2} Y_j \frac{\partial^2 X_k}{\partial x^2} Y_l + \frac{\partial^2 Y_j}{\partial y^2} X_i \frac{\partial^2 Y_l}{\partial y^2} X_k\right) \\
& + D_{12}\left(\frac{\partial^2 X_i}{\partial x^2} Y_j \frac{\partial^2 Y_l}{\partial y^2} X_k + \frac{\partial^2 Y_j}{\partial y^2} X_i \frac{\partial^2 X_k}{\partial x^2} Y_l\right) \\
& + 4D_{66} \frac{\partial X_i}{\partial x} \frac{\partial Y_j}{\partial y} \frac{\partial X_k}{\partial x} \frac{\partial Y_l}{\partial y} \\
& - \left(\frac{d_{31}}{a_{33}} V + \frac{2 d_{31}^s V}{a_{33} h} - 2\sigma^0\right)\left(\frac{\partial X_i}{\partial x} Y_j \frac{\partial X_k}{\partial x} Y_l + \frac{\partial Y_j}{\partial y} X_i \frac{\partial Y_l}{\partial y} X_k\right)\Bigg] dxdy,
\end{aligned}
\tag{3.30}
$$

and $$F_{kl} = \iint q X_k Y_l dxdy. \tag{3.31}$$

The unknown constants A_{ij} can be determined by solving the linear algebraic equation (3.29). Thus the corresponding deflection, the electroelastic fields can be obtained according to equations (3.27), (3.16) and (3.17).

3.2.4 Free vibration of a PNP

For the analysis of the free vibration of the PNP with the consideration of the surface effects and the flexoelectricity, the governing equation (3.24) can be similarly reduced by neglecting the nonlinear terms as

$$
\begin{aligned}
& D_{11}\left(\frac{\partial^4 w}{\partial x^4} + \frac{\partial^4 w}{\partial y^4}\right) + 2(D_{12} + 2D_{66}) \frac{\partial^4 w}{\partial^2 x \partial^2 y} \\
& + \left(\frac{d_{31}}{a_{33}} V + \frac{2 d_{31}^s V}{a_{33} h} - 2\sigma^0\right)\left(\frac{\partial^2 w}{\partial x^2} + \frac{\partial^2 w}{\partial y^2}\right) - \frac{\rho h^3}{12}\left(\frac{\partial^2 \ddot{w}}{\partial x^2} + \frac{\partial^2 \ddot{w}}{\partial y^2}\right) + \rho h \ddot{w} = 0.
\end{aligned}
\tag{3.32}
$$

The harmonic solution of equation (3.32) can be expressed as

$$w(x,y,t) = W(x,y)e^{i\omega t} \tag{3.33}$$

where ω is the resonant frequency and $W(x, y)$ is the vibration mode. Substituting equation (3.33) into equation (3.32) yields

$$\begin{aligned} &D_{11}\left(\frac{\partial^4 W}{\partial x^4}+\frac{\partial^4 W}{\partial y^4}\right)+2(D_{12}+2D_{66})\frac{\partial^4 W}{\partial^2 x\partial^2 y}+\frac{\rho h^3}{12}\omega^2\left(\frac{\partial^2 W}{\partial x^2}+\frac{\partial^2 W}{\partial y^2}\right) \\ &+\left(\frac{d_{31}}{a_{33}}V+\frac{2d_{31}^s V}{a_{33}h}-2\sigma^0\right)\left(\frac{\partial^2 W}{\partial x^2}+\frac{\partial^2 W}{\partial y^2}\right)-\rho h\omega^2 W=0. \end{aligned} \tag{3.34}$$

Similarly, Ritz method is also adopted to get the approximate solution of equation (3.34) starting from the weak form of the variational statement of equation (3.34), i.e.,

$$\begin{aligned} &\iint\left\{D_{11}\left[\frac{\partial^2 W}{\partial x^2}\frac{\partial^2(\delta W)}{\partial x^2}+\frac{\partial^2 W}{\partial y^2}\frac{\partial^2(\delta W)}{\partial y^2}\right]+D_{12}\left[\frac{\partial^2 W}{\partial x^2}\frac{\partial^2(\delta W)}{\partial y^2}+\frac{\partial^2 W}{\partial y^2}\frac{\partial^2(\delta W)}{\partial x^2}\right]\right. \\ &+4D_{66}\frac{\partial^2 W}{\partial x\partial y}\frac{\partial^2(\delta W)}{\partial x\partial y}-\rho h\omega^2 W\delta W-\frac{\rho h^3}{12}\omega^2\left[\frac{\partial W}{\partial x}\frac{\partial(\delta W)}{\partial x}+\frac{\partial W}{\partial y}\frac{\partial(\delta W)}{\partial y}\right] \\ &\left.-\left(\frac{d_{31}}{a_{33}}V+\frac{2d_{31}^s V}{a_{33}h}-2\sigma^0\right)\left[\frac{\partial W}{\partial x}\frac{\partial(\delta W)}{\partial x}+\frac{\partial W}{\partial y}\frac{\partial(\delta W)}{\partial y}\right]\right\}dxdy=0. \end{aligned} \tag{3.35}$$

According to the Ritz method, the approximate form of the mode shape of the vibration is expressed as

$$W(x,y)\approx\sum_{i=1}^{m}\sum_{j=1}^{n}A_{ij}X_i(x)Y_j(y) \tag{3.36}$$

with $X_i(x)$ and $Y_j(y)$ given in the previous section, which should satisfy the mechanical boundary conditions of the clamped PNP. Substituting equation (3.36) into equation (3.35) results in

$$([R]-\omega^2[B])\{A\}=\{0\} \tag{3.37}$$

with $R_{(ij)(kl)}$ derived in the previous section and

$$B_{(ij)(kl)}=\iint\left[\rho h X_i Y_j X_k Y_l+\frac{\rho h^3}{12}\left(\frac{\partial X_i}{\partial x}Y_j\frac{\partial X_k}{\partial x}Y_l+\frac{\partial Y_j}{\partial y}X_i\frac{\partial Y_l}{\partial y}X_k\right)\right]dxdy. \tag{3.38}$$

Thus the resonant frequency can be determined from the characteristic equation (3.37).

It should be mentioned that the so-called dynamic flexoelectric effect (Yudin and Tagantsev, 2013; Tagantsev, 1986) is not considered here. Therefore, the modeling in the current work could be claimed to provide a qualitative prediction on the trend of the influence of the surface effects and the static flexoelectricity upon the electromechanical coupling fields of the PNP. In the following section, the analysis of how the flexoelectricity and the surface effects influence the size-dependent properties of a bending PNP will be conducted. It is worth mentioning that all the equations derived above can be reduced to the ones of the classical piezoelectric plate if the higher order couplings in the internal energy expression and the surface effects are excluded.

3.3 Results and discussions

For case study, $BaTiO_3$ is taken as an example material to investigate how the flexoelectricity and the surface effects influence the size-dependent bending behaviors of a piezoelectric nanoplate. The bulk material properties of $BaTiO_3$ under the plane strain condition can be obtained as c_{11}=167.55 GPa, c_{12}=78.15 GPa, $c_{66}=44.7$ GPa, $a_{33}=0.79\times10^{8}$ V·m/C and d_{31}=3.5×10^{8} V/m based on the information given in Ref. (Giannakopoulos and Suresh, 1999). $b_{33}=1\times10^{-9}$ $\mathrm{Jm^3}$ /$\mathrm{C^2}$ is chosen according to Ref (Maranganti *et al*., 2006). However the surface parameters for $BaTiO_3$ are not completely available due to the lack of sufficient atomistic calculations and experiments. In the current work, the surface piezoelectricity is adopted as $d_{31}^{s}=-0.056$ C/m according to Ref. (Dai *et al*., 2011). Using the same approximation scheme adopted in (Huang and Yu, 2006), the other surface elasticity constants are estimated as $c_{11}^{s}=9.72$ N/m, $c_{12}^{s}=4.35$ N/m and $c_{66}^{s}=2.68$ N/m. The residual surface stress may alter from a negative value to a positive value depending on the crystal plane direction (He and Lilley, 2008a). Thus we use the varying values for the residual surface stress from a negative one $\sigma^{0}=-1$ N/m to a positive one $\sigma^{0}=1$ N/m, respectively (He and Lilley, 2008a; Yan and Jiang, 2012a). In addition, the distributed load q is set as 0.1 $\mathrm{pN/nm^2}$ to ensure the small deformation assumption. In current work, three terms for the coordinate functions are used in the Ritz method to approximate the transverse displacement (e.g. m = 3, n = 3) to ensure the convergence of the solution.

The influence of the flexoelectricity and the surface effects on the static bending of a PNP is investigated first. Figure 3.2 depicts the variation of the normalized maximum deflection (w/w_0^V) at the middle ($x = 0.5a$, $y = 0.5b$) of a square plate ($a = b = 50h$) with the plate thickness h under an electric voltage (V = -0.1 V) and a mechanical load q, where w_0^V is the maximum deflection of the plate subjected to the same external loads without considering the flexoelectricity and the surface effects. It is found that both the flexoelectricity and the surface effects contribute to the size-dependent bending responses of the PNP. For example, the pure flexoelectricity softens the PNP resulting in a larger deflection. However, the surface effects may soften or stiffen the plate depending on the sign of the residual surface stress. It was explained in (Yan and Jiang, 2012b) that the residual surface stress induces in-plane forces which in turn affect the effective bending rigidity of the plate. It is thus concluded that it might lead to substantial errors if only the influence of the flexoelectricity or the surface effects is considered when investigating the electroelastic responses of a bending plate. It is also found that the influence of the surface effects and the flexoelectricity decays with the increase of the plate thickness as all the curves tend to approach unit. Additionally, this figure shows that within the considered range of surface properties in the current work, the effects of surface elasticity and surface piezoelectricity on the static bending of the plate are not significant compared to the effect from the residual surface stress, especially for the plate with a relative large length to thickness ratio, $a = b = 50h$ for example.

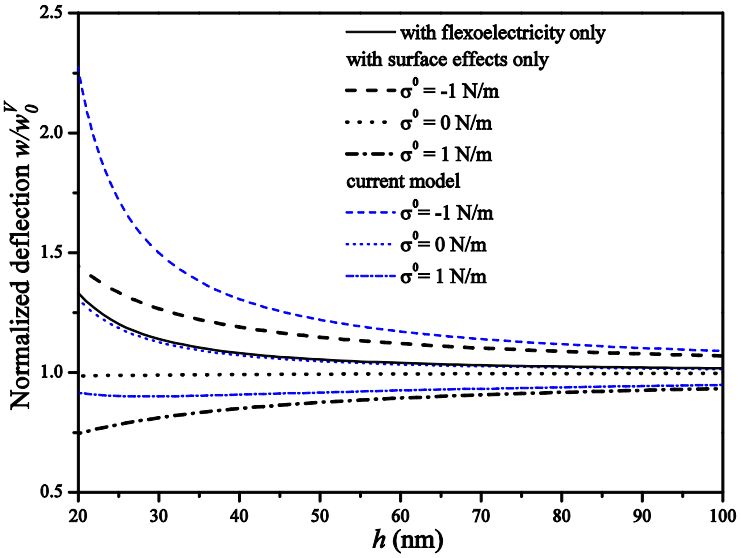

Figure 3.2: Variation of normalized maximum deflection with plate thickness (a = b = 50h, V = -0.1 V).

In order to investigate how the combined effects of the flexoelectricity and the surface upon the static bending of a PNP are influenced by the plate length to thickness ratio and the applied electric voltage, figure 3.3 shows the variation of the normalized maximum deflection of a square plate (a = b) with length to thickness ratio (a/h) under different voltage and residual surface stress. The thickness of the plate is set as h = 20 nm. It can be concluded from the figure that the applied voltage influences the combined effects of the flexoelectricity and the surface on the static bending of the PNP. For example, when a positive voltage is applied, the combined effects are magnified by increasing the magnitude of the applied voltage, while an opposite trend is observed for a negative applied voltage. Figure 3.3(a) also demonstrates that the combined effects are enhanced with the increase of length to thickness ratio when the residual surface stress is

negative. When the residual surface stress becomes positive, it is interesting to point out that a critical length to thickness ratio $(a/h)_{cr}$ exists where the combined effects of the flexoelectricity and the surface disappear as indicated by the interception of these three curves associated with different applied voltages at unity in figure 3.3(*b*). The observations in figures 3.3(*a*) and 3.3(*b*) could be explained by the fact that the flexoelectricity always softens the bending of the PNP within the considered range of the material properties, the plate aspect ratio and the applied voltage, while the surface effects are enhanced with the increase of the plate length to thickness ratio as discussed in (Yan and Jiang, 2012b). Therefore, the softening behavior induced by a negative residual surface stress is magnified with the increase of the plate length to thickness ratio, which is additive to the softening behavior caused by the flexoelectricity. However, a positive residual surface stress always stiffens the bending of the plate, which gives an opposite effect upon the bending of the plate compared to the flexoelectricity. When the plate length to thickness ratio is less than the critical value, the softening behavior due to the flexoelectricity is dominant over the stiffening behavior induced by the surface effects, while this trend is reversed when the length to thickness ratio is greater than the critical value. Therefore, a transition exists with no size-dependency. From figures 3.3(*a*) and 3.3(*b*), it is also observed that for the plate with fixed thickness, the flexoelectricity plays more significant role in the static bending of the plate for the plate with smaller length to thickness ratio a/h. However, with the increase of the length to thickness ratio, the influence of the surface effects is getting larger. The results in figure 3.2 and figure 3.3 concludes that the combined effects of the flexoelectricity and the surface on the bending properties of a PNP depend on the plate thickness, the plate length to thickness ratio, the applied voltage and the residual surface stress. Thus it is necessary to take both the

flexoelectricity and the surface effects into consideration when predicting the static bending of a PNP.

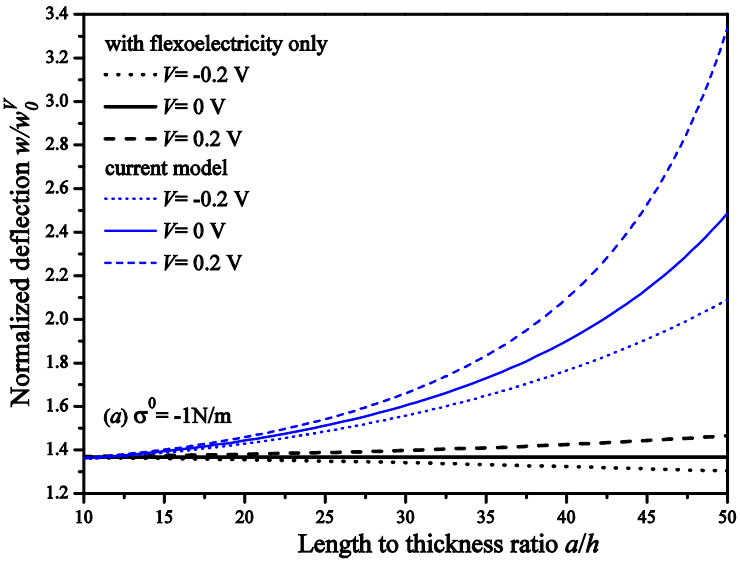

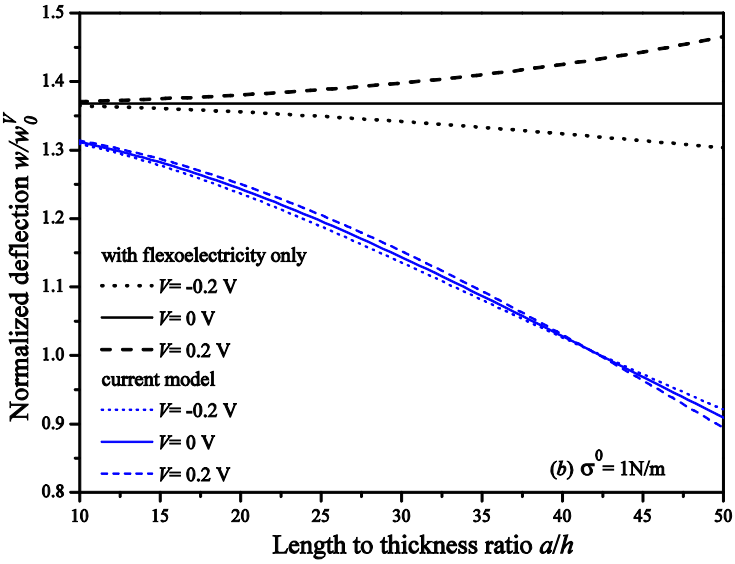

Figure 3.3: Variation of normalized maximum deflection with plate length to thickness ratio under different voltage and residual surface stress (*a*) $\sigma^0 = -1$ N/m and (*b*) $\sigma^0 = 1$ N/m.

As indicated by the expression of the electric field in equation (3.16), the incorporation of surface effects, the strain gradients and the polarization gradients will influence the distribution of the electric field. Figure 3.4 plots the distribution of the electric field at the middle of the plate (x = 0.5a, y = 0.5b) along the plate thickness direction under an applied voltage (V = -0.1 V) with different residual surface stress values. When the plate is very thin, e.g. h = 20 nm, the combined effects of the flexoelectricity and the surface have significant contribution to the electric field as indicated by the difference between the curves representing the current model and the classical solution. In addition, the electric field may be increased or decreased by the combined effects depending on the sign of the residual surface stress. It should be

mentioned that the jump of the distribution of the electric field near the surfaces is due to the account for the flexoelectricity, which is a typical boundary behavior for a gradient theory and this phenomenon was also reported in Ref. (Mindlin, 1969) for a plate with polarization gradient and Ref. (Yang *et al.*, 2004) for a circular cylindrical shell with electric field gradient.

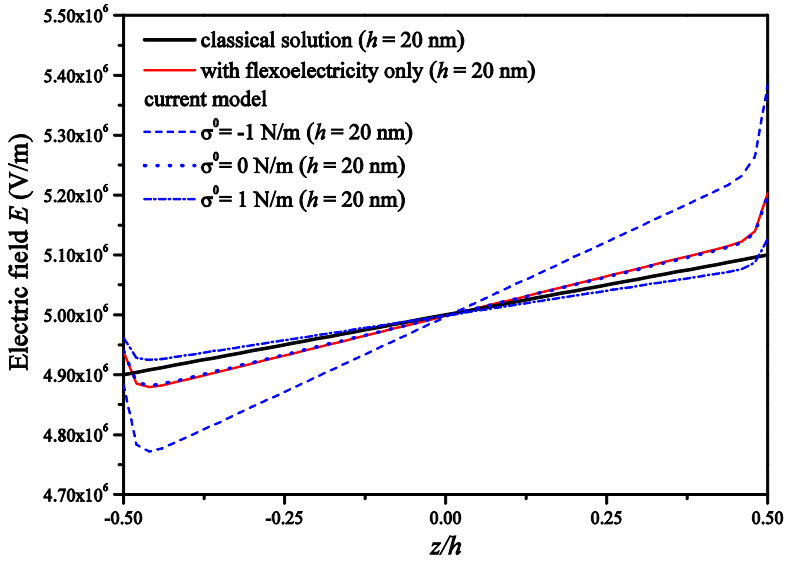

Figure 3.4: Electric field distribution along the plate thickness direction at the middle of the plate.

The combined effects of the flexoelectricity and the surface on the polarization in the plate are also demonstrated in the current work. By checking equation (3.17), it is found that the varying terms with plate thickness are relatively negligible in comparison to the other fixed terms within the considered range of the plate thickness. Thus we can assume that the polarization is uniform across the plate thickness. For different residual

surface stresses, figures 3.5(*a*) and 3.5(*b*) depict the variation of the polarization at different location of the plate against the plate thickness *h* when a negative voltage (*V* = -0.1 V) is applied. It is found that the combined effects on the polarization are more significant for the plate with smaller thickness. When the thickness increases, these effects will eventually disappear as indicated by the fact that all the results approach those from the classical solution where the polarization uniformly distributes in the plate. As indicated by figures 3.5(*a*) and 3.5(*b*), the combined effects of the flexoelectricity and the surface significantly alter the distribution of the polarization. For example, under such an applied voltage, the polarization is increased at a particular point along the side of the plate ($x = 0$, $y = 0.5b$ for example) while it is decreased in the middle of the plate ($x = 0.5a$, $y = 0.5b$ for example). Comparing the results from the current model with both the flexoelectricity and the surface effects and those only considering the flexoelectricity, it can be concluded that both the flexoelectricity and the surface effects contribute to the polarization and neglecting any individual effect will lead to inaccurate prediction. It is also found that the influence of the surface effects upon the polarization depends on the value of the residual surface stress. For example, for a particular point at the middle of the plate, the surface effects decrease the polarization with a negative residual surface stress ($\sigma^0 = -1$ N/m for example) but increase the polarization with a positive residual surface stress ($\sigma^0 = 1$ N/m for example). Thus figures 3.4 and 3.5 indicate the importance of considering both the flexoelectricity and the surface effects in studying the electroelastic responses of the piezoelectric plate at the nano-scale.

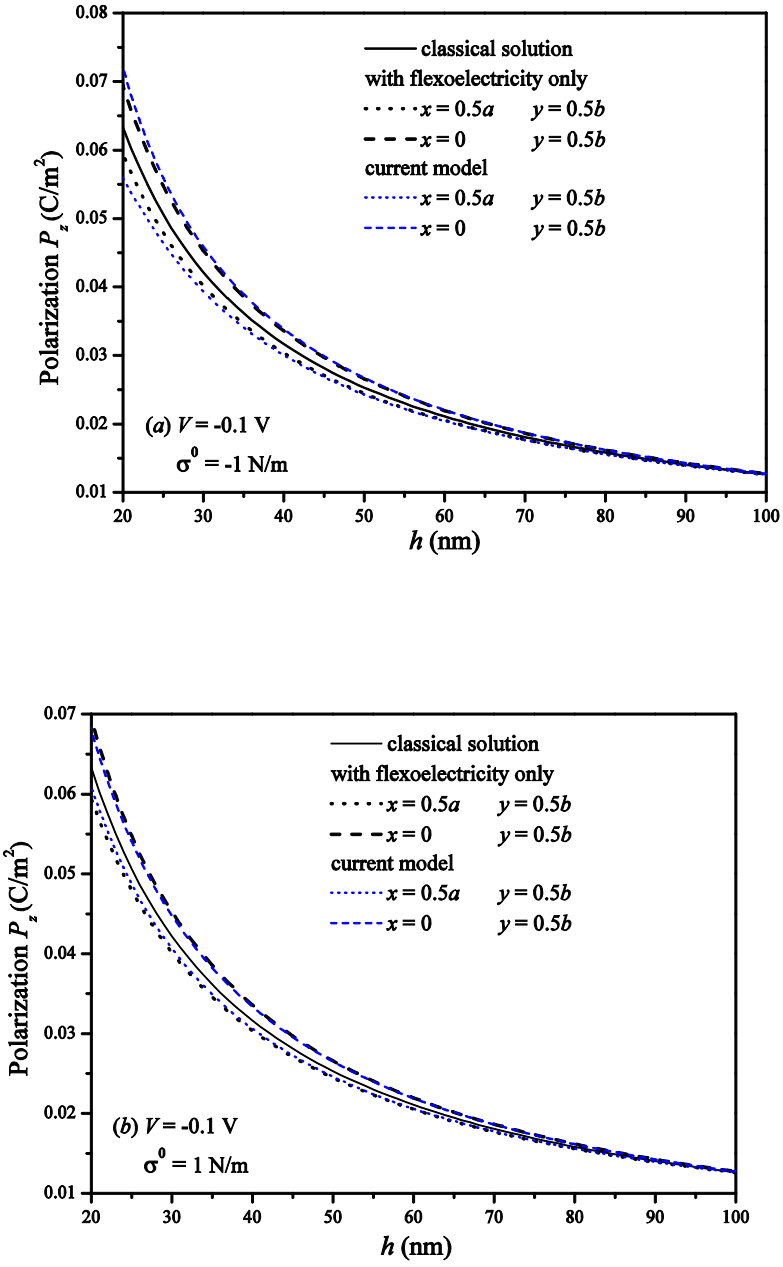

Figure 3.5: Variation of polarization with plate thickness at different locations of the plate under different residual surface stress (*a*) V = -0.1 V, $\sigma^0 = -1$ N/m and (*b*) V = -0.1 V, $\sigma^0 = 1$ N/m.

The vibrational behaviors of a PNP with the consideration of both the flexoelectricity and the surface effects is also an important issue needed to be investigated. For a square plate ($a = b = 50h$) subjected to a negative voltage (V = -0.1 V), the variation of the normalized fundamental resonant frequency ω / ω_0^V of the plate with the plate thickness h is plotted in figure 3.6. ω_0^V is the resonant frequency of the plate without considering both the flexoelectricity and the surface effects. It can be concluded that with the considered surface material parameters and the flexocoupling coefficients, both the surface effects and the flexoelectricity influence the resonant frequency significantly. For example, the flexoelectricity decreases the resonant frequency while the surface effects may enhance the resonant frequency with a positive residual surface stress but reduce the resonant frequency with a negative one. In addition, the effects of the surface elasticity and the surface piezoelectricity on the resonant frequency are not prominent for a plate with such a relatively large length to thickness ratio, a/h = 50 for example, as indicated by the curve representing the surface effects without considering the residual surface stress, i.e., $\sigma^0 = 0$ N/m. Due to the opposite trends of the flexoelectricity and the positive residual surface stress upon the resonant frequency, the size-dependent vibration may disappear. Otherwise, the combined effects are more pronounced for the thinner plates with smaller thickness and diminish with the increasing plate thickness as indicated by all the curves tending to approach a unity. Thus it is necessary to incorporate both the flexoelectricity and surface effects in investigating the dynamic response of piezoelectric devices at the nano-scale.

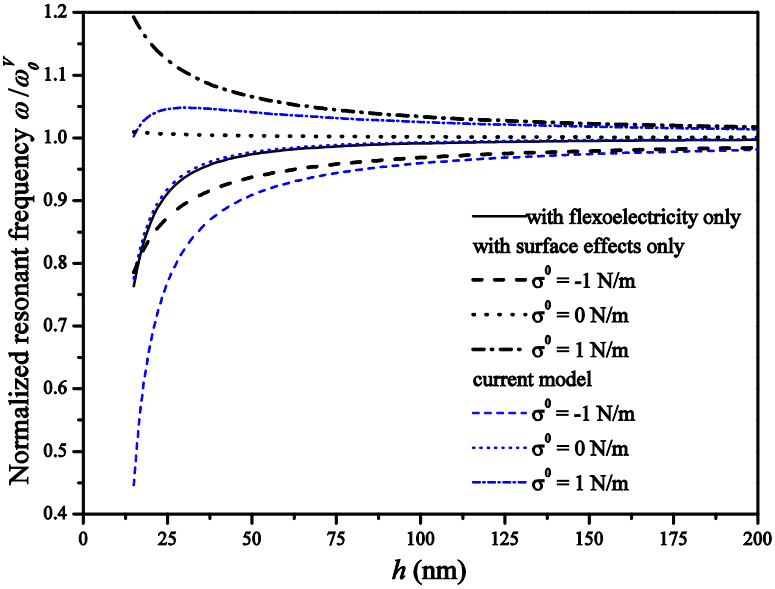

Figure 3.6: Variation of normalized resonant frequency with plate thickness h ($a = b = 50h$, $V = -0.1$ V).

Figure 3.7 depicts the variation of the normalized resonant frequency of a square piezoelectric plate ($a = b = 50h$) against the plate thickness h under different applied electrical loads with ω_0 being the resonant frequency calculated by neglecting the flexoelectricity, the surface effects and the applied voltage. The residual surface stress is set as $\sigma^0 = 1$ N/m. As indicated in the figure, the combined effects of the flexoelectricity and surface on the resonant frequency are dependent on the applied electric potential. For example, when the plate is subjected to a negative voltage, the combined effects increase the resonant frequency and such effects are enhanced with the increase of the magnitude of the applied voltage. However, when a positive voltage is applied to the plate, the combined effects may decrease or increase the resonant frequency depending on the magnitude of the applied voltage and the plate thickness. The discrepancy of the curves

in this figure suggests a possible way for frequency tuning by means of the applied voltage as discussed in Refs. (Yan and Jiang, 2012a; 2012c). However, such a frequency tuning process in the design of PNP resonators may be altered by the combined effects of the flexoelectricity and the surface.

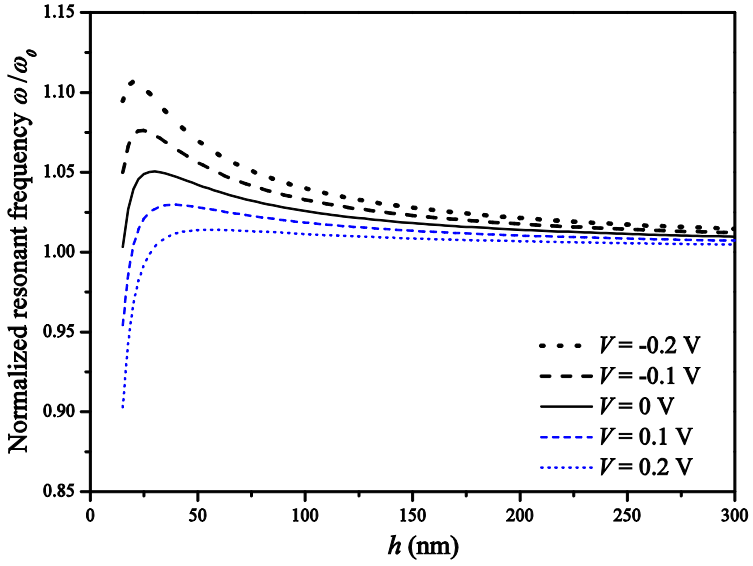

Figure 3.7: Variation of normalized resonant frequency with plate thickness for a plate under different voltage ($a = b = 50h$).

In order to investigate how the in-plane aspect ratio influences the combined effects of the flexoelectricity and the surface upon the vibrational behaviors of the PNP, the variation of the normalized resonant frequency ω/ω_0^V of the plate (a = 50h) against the plate thickness h for the plate with different aspect ratio a/b and under different voltage (e.g. V = -0.2 V, V = 0 V and V = 0.2 V) is depicted in figure 3.8. As revealed in the figure, for a fixed residual surface stress (σ^0 =1N/m for example), the combined effects

of the flexoelectricity and the surface may decrease or increase the resonant frequency depending on the plate in-plane dimensions. For example, when the plate is a square (*a/b* = 1), the combined effects increase the resonant frequency with more prominent surface effects. However, with the increase of the in-plane aspect ratio a/b, i.e., the plate is becoming narrower when a is fixed, the combined effects will reduce the resonant frequency as the flexoelectricity becomes dominant. In addition, when the aspect ratio *a/b* is sufficiently large, i.e., $a/b > 10$, the combined effects of the flexoelectricity and the surface on the resonant frequency will slightly change with the aspect ratio. Since a is fixed, large aspect ratio will reduce the current model to the Euler beam model. It was justified by equation (20) in Ref. (Yan and Jiang, 2013b) and equation (22) in Ref. (Yan and Jiang, 2011a) that the beam resonant frequency is independent of the beam width when the individual influence of the flexoelectricity or the surface effects are considered. Therefore, it can be concluded from figures 3.6, 3.7 and 3.8 that the plate dimensions, the residual surface stress and the applied electric voltage contribute to the combined effects of the flexoelectricity and the surface upon the resonant frequency of the PNP.

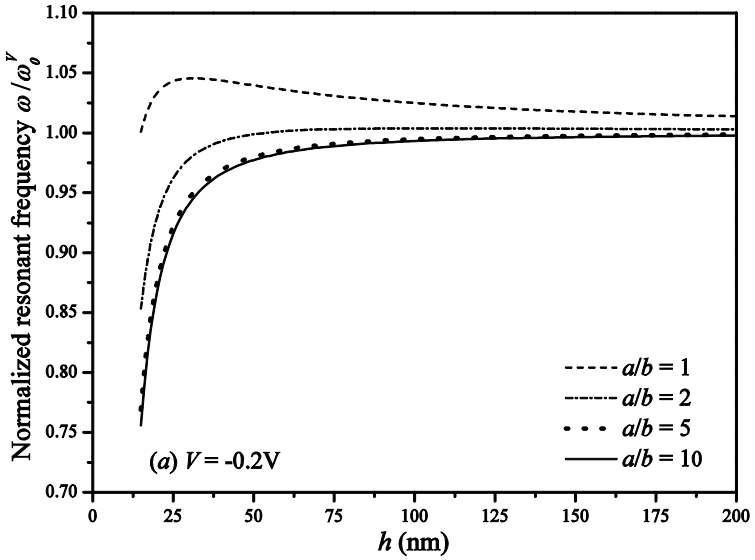
Normalized resonant frequency ω/ω_o^V
1.10
1.05
1.00
0.95
0.90
0.85
0.80
0.75
0.70
0
25
50
75
100
125
150
175
200
h (nm)
(a) V = -0.2V
a/b = 1
a/b = 2
a/b = 5
a/b = 10

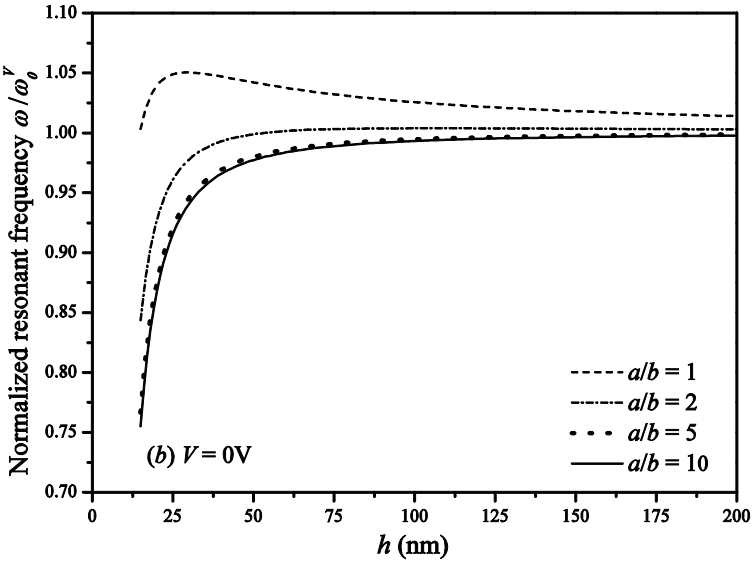
Normalized resonant frequency ω/ω_o^V
1.10
1.05
1.00
0.95
0.90
0.85
0.80
0.75
0.70
0
25
50
75
100
125
150
175
200
h (nm)
(b) V = 0V
a/b = 1
a/b = 2
a/b = 5
a/b = 10

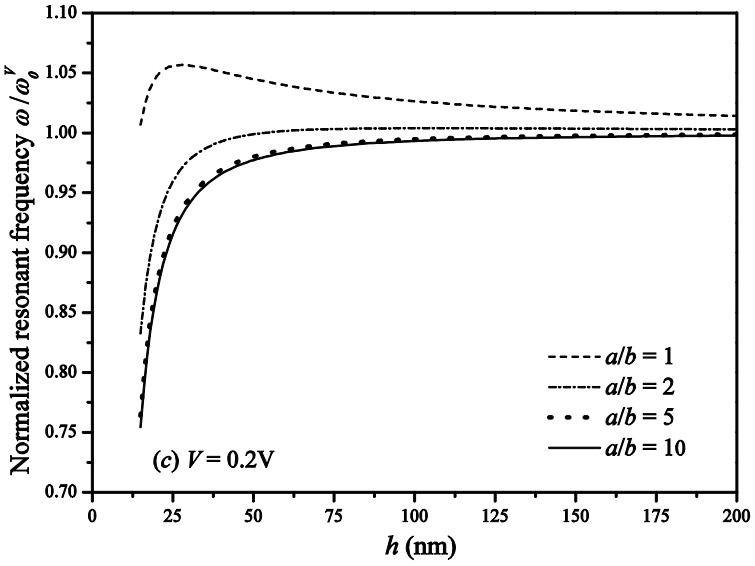

Figure 3.8: Variation of normalized resonant frequency with plate thickness for a plate with different aspect ratio a/b and under different voltage ($a = 50h$) (a) $V = -0.2$ V, (b) $V = 0$ V and (c) $V = 0.2$ V.

3.4 Conclusions

In this work, a modified Kirchhoff plate model incorporating the surface effects and the flexoelectricity is developed to investigate the size-dependent properties of a bending piezoelectric nanoplate (PNP). The simulation results indicate that the combined flexoelectricity and surface effects have significant influence upon the electroelastic responses and the free vibration of the PNP. Such effects are size-dependent and decrease with the increase of the plate thickness. Neglecting any individual effect may induce inaccurate characterization of the electromechanical coupling of the PNP. It can also be concluded that the combined effects of the surface and the flexoelectricity on the

electromechanical coupling behaviors of a PNP are sensitive to the values of surface material constants, the applied electric potential and the plate dimensions. Additionally, the results suggest that the frequency tuning of PNP-based resonators by adjusting the applied electric voltage could be modified by the flexoelectricity and the surface effects. This work is claimed to be helpful for further understanding the fundamental physics of the size-dependent electromechanical coupling behaviors of piezoelectric nanomaterials and provide basic guidelines for the design and applications of piezoelectric nanodevices.

References

Assadi, A., Farshi, B. and Alinia-Ziazi, A., 2010. Size dependent dynamic analysis of nanoplates. J. Appl. Phys. **107** 124310.

Chen, C. Q., Shi, Y., Zhang, Y. S., Zhu, J. and Yan, Y. J., 2006. Size dependence of Young's modulus in ZnO nanowires. Phys. Rev. Lett. **96** 075505.

Chen, H. T. and Soh, A. K., 2012. Influence of flexoelectric effects on multiferroic nanocomposite thin bilayer films. J. Appl. Phys. **112** 074104.

Dai, S. X., Gharbi, M., Sharma, P. and Park, H. S., 2011. Surface piezoelectricity: Size effects in nanostructures and the emergence of piezoelectricity in non-piezoelectric materials. J.Appl. Phys. **110** 104305.

Giannakopoulos, A. E., and Suresh, S., 1999. Theory of indentation of piezoelectric materials. Acta Mater. **47** 2153-2164.

Gurtin, M. E. and Murdoch, A. I., 1975. A continuum theory of elastic material surfaces. Arch. Ration. Mech. Anal. **57** 291-323

He, J. and Lilley, C. M., 2008a. Surface effect on the elastic behavior of static bending nanowires. Nano Lett. **8** 1798-1802.

He, J. and Lilley, C. M., 2008b. Surface stress effect on bending resonance of nanowires with different boundary conditions. Appl. Phys. Lett. **93** 263108.

Huang, G. Y. and Yu, S. W., 2006. Effect of surface piezoelectricity on the electromechanical behavior of a piezoelectric ring. Phys. Status Solidi B—Basic Solid State Phys. **243** R22-R24.

Hu, S. L. and Shen, S. P., 2010. Variational principles and governing equations in nano-dielectrics with the flexoelectric effect. Sci. China, Ser. G **53** 1497-1504.

Kulkarni, A. J., Zhou, M. and Ke, F. J., 2005. Orientation and size dependence of the elastic properties of zinc oxide nanobelts. Nanotechnology **16** 2749-2756.

Lao, C. S., Kuang, Q., Wang, Z. L., Park, M. C. and Deng, Y. L., 2007. Polymer functionalized piezoelectric-FET as humidity/chemical nanosensors. Appl. Phys. Lett. **90** 262107.

Li, Y. H., Fang, B., Zhang, J. Z. and Song, J. Z., 2011. Surface effects on the wrinkling of piezoelectric films on compliant substrates. J. Appl. Phys. **110** 114303.

Liang, X., Hu, S. L. and Shen, S. P., 2014. Effects of surface and flexoelectricity on a piezoelectric nanobeam. Smart Mater. Struct. **23** 035020.

Liu, C. C., Hu, S. L. and Shen, S. P., 2012. Effect of flexoelectricity on electrostatic potential in a bent piezoelectric nanowire. Smart Mater. Struct. **21** 115024.

Lu, P., He, L. H., Lee, H. P. and Lu, C., 2006. Thin plate theory including surface effects. Int. J. Solids Struct. **43** 4631-4647.

Ma, W. H. and Cross, L. E., 2001. Observation of the flexoelectric effect in relaxor Pb (Mg 1/3 Nb 2/3) O 3 ceramics. Appl. Phys. Lett. **78** 2920-2921.

Ma, W. H. and Cross, L. E., 2002. Flexoelectric polarization of barium strontium titanate in the paraelectric state. Appl. Phys. Lett. **81** 3440-3442.

Ma, W. H. and Cross, L. E., 2003. Strain-gradient-induced electric polarization in lead zirconate titanate ceramics. Appl. Phys. Lett. **82** 3293-3295.

Ma, W. H. and Cross, L. E., 2005. Flexoelectric effect in ceramic lead zirconate titanate. Appl. Phys. Lett. **86** 072905.

Ma, W. H. and Cross, L. E., 2006. Flexoelectricity of barium titanate. Appl. Phys. Lett. **88** 232902.

Majdoub, M. S., Sharma, P. and Cagin, T., 2008. Enhanced size-dependent piezoelectricity and elasticity in nanostructures due to the flexoelectric effect. Phys. Rev. B **77** 125424.

Maranganti, R., Sharma, N. D. and Sharma, P., 2006. Electromechanical coupling in nonpiezoelectric materials due to nanoscale nonlocal size effects: Green's function solutions and embedded inclusions. Phys. Rev. B **74** 014110.

Maranganti, R. and Sharma, P. 2009. Atomistic determination of flexoelectric properties of crystalline dielectrics. Phys. Rev. B **80** 054109.

Miller, R. E. and Shenoy, V. B., 2000. Size-dependent elastic properties of nanosized structural elements. Nanotechnology **11** 139-147.

Mindlin, R. D., 1969. Continuum and lattice theories of influence of electromechanical coupling on capacitance of thin dielectric films. Int. J. Solids Struct. **5** 1197-1208.

Nguyen, T. D., Mao, S., Yeh, Y. W., Purohit, P. K. and McAlpine, M. C., 2013. Nanoscale Flexoelectricity. Adv. Mater. **25** 946-974.

Park, K. I., Xu, S., Liu, Y., Hwang, G. T., Kang, S. J. L., Wang, Z. L. and Lee, K. J., 2010. Piezoelectric BaTiO3 thin film nanogenerator on plastic substrates. Nano Lett. **10** 4939-4943.

Quang, H. L. and He, Q. C., 2011. The number and types of all possible rotational symmetries for flexoelectric tensors. Proc. R. Soc. London, Ser. A **467** 2369-2386.

Rao, S. S., 2007. Vibration of continuous systems, New York: Wiley.

Reddy, J. N., 2007. Theory and analysis of elastic plates and shells, Boca Raton, FL:

CRC Press.

Shu, L. L., Wei, X. Y., Pang, T., Yao, X., and Wang, C. L., 2011. Symmetry of flexoelectric coefficients in crystalline medium. J. Appl. Phys. **110** 104106.

Sharma, N. D., Landis, C. M. and Sharma, P., 2012. Piezoelectric thin-film superlattices without using piezoelectric materials. J. Appl. Phys. **108** 024304.

Shen, S. P. and Hu, S. L., 2010. A theory of flexoelectricity with surface effect for elastic dielectrics. J. Mech. Phys. Solids **58** 665-677.

Song, F., Huang, G. L., Park, H. S. and Liu, X. N., 2011. A continuum model for the mechanical behavior of nanowires including surface and surface-induced initial stresses. Int. J. Solids Struct. **48** 2154-2163.

Stan, G., Ciobanu, C. V., Parthangal, P. M. and Cook, R. F., 2007. Diameter-dependent radial and tangential elastic moduli of ZnO nanowires. Nano Lett. **7** 3691-3697.

Stengel, M., 2013. Microscopic response to inhomogeneous deformations in curvilinear coordinates. Nat. Commun. **4** 2693.

Tagantsev, A. K., 1986. Piezoelectricity and flexoelectricity in crystalline dielectrics. *Phys. Rev. B* **34** 5883-5889.

Tagantsev, A. K. and Gerra, G., 2006. Interface-induced phenomena in polarization response of ferroelectric thin films. J.Appl. Phys. **100** 051607.

Toupin, R. A., 1956. The elastic dielectric. J. Ration. Mech. Anal. **5** 849-915.

Wang, X. D., Zhou, J., Song, J. H., Liu, J., Xu, N. S. and Wang, Z. L., 2006. Piezoelectric Field Effect Transistor and Nanoforce Sensor Based on a Single ZnO Nanowire. Nano Lett. **6** 2768-2772.

Wang, G. F. and Feng, X. Q., 2007. Effects of surface elasticity and residual surface tension on the natural frequency of microbeams. Appl. Phys. Lett. **90** 231904.

Wang, G. F. and Feng, X. Q., 2009. Surface effects on buckling of nanowires under uniaxial compression. Appl. Phys. Lett. **94** 141913.

Wang, G. F., Feng, X. Q. and Yu, S. W., 2007. Surface buckling of a bending microbeam due to surface elasticity. Europhys. Lett. **77** 44002.

Yan, Z. and Jiang, Y. L., 2011a. The vibrational and buckling behaviors of piezoelectric nanobeams with surface effects. Nanotechnology **22** 245703.

Yan, Z. and Jiang, L. Y., 2011b. Surface effects on the electromechanical coupling and bending behaviours of piezoelectric nanowires. J. Phys. D: Appl. Phys. **44** 075404.

Yan, Z. and Jiang, L. Y., 2012a. Surface effects on the vibration and buckling of piezoelectric nanoplates. EPL **99** 27007.

Yan, Z. and Jiang, L. Y., 2012b. Surface effects on the electroelastic responses of a thin piezoelectric plate with nanoscale thickness. J. Phys. D: Appl. Phys. **45** 255401.

Yan, Z. and Jiang, L. Y., 2012c. Vibration and buckling analysis of a piezoelectric nanoplate considering surface effects and in-plane constraints. Proc. R. Soc. A **468** 3458-3475.

Yan, Z. and Jiang, L. Y., 2013a. Flexoelectric effect on the electroelastic responses of bending piezoelectric nanobeams. J. Appl. Phys. **113** 194102.

Yan, Z. and Jiang, L. Y., 2013b. Size-dependent bending and vibration behaviour of piezoelectric nanobeams due to flexoelectricity. J. Phys. D: Appl. Phys. **46** 355502.

Yang, X. M., Hu, Y. T. and Yang, J. S., 2004. Electric field gradient effects in anti-plane problems of polarized ceramics. Int. J. Solids Struct. **41** 6801-6811.

Yudin, P. V. and Tagantsev, A. K., 2013. Fundamentals of flexoelectricity in solids. Nanotechnology **24** 432001.

Zhang, J., Wang, C. Y. and Adhikari, S., 2012. Surface effect on the buckling of piezoelectric nanofilms. J. Phys. D: Appl. Phys. **45** 285301.

Zhang, Y. H., Hong, J. W., Liu, B. and Fang, D. N., 2010. Strain effect on ferroelectric behaviors of BaTiO3 nanowires: a molecular dynamics study. Nanotechnology **21** 015701.

Zhao, M. H., Qian, C. F., Lee, S. W. R., Tong, P., Suemasu, H. and Zhang, T. Y., 2007. Electro-elastic analysis of piezoelectric laminated plates. Adv. Compos. Mater. **16** 63-81.

Zhao, M., H., Wang, Z. L. and Mao, S. X., 2004. Piezoelectric characterization of individual Zinc Oxide nanobelt probed by piezoresponse force microscope. Nano Lett. **4** 587-590.

Zubko, P., Catalan, G. and Tagantsev, A. K., 2013. Flexoelectric effect in solids. Annu. Rev. Mater. Res. **43** 387-421.

Chapter 4

4 Conclusions and recommendations

4.1 Conclusions

Piezoelectric nanostructures have recently attracted much attention with the development of nanotechnology for their potential applications as sensors, actuators, energy harvesters and etc. in nanoelectromechanical systems (NEMS) due to their intrinsic electromechanical coupling and unique features at the nano-scale. Existing studies have shown that those nanostructures present size-dependent physical and mechanical properties. Therefore, it is essential to explore the origins and underlying physics of such size effects of piezoelectric nanostructures and understand how these size effects influence the electromechanical coupling behaviors of the nanostructures. In this thesis, the size-dependent static bending and vibrational behaviors of a piezoelectric nanoplate have been examined by the modified continuum mechanics modeling approaches for the sake of efficiency and simplicity.

The size-dependent responses of a piezoelectric nanostructural element can be understood by resorting to the effect of the flexoelectricity as large strain gradients typically present in the nanosized structures. However, continuum modeling of such effect on the size-dependent properties of piezoelectric nanostructures is very scarce, particularly for two-dimensional piezoelectric nanostructure. Therefore this thesis first attempted to develop a modified Kirchhoff plate model accounting for the pure

flexoelectricity to qualitatively predict the electromechanical coupling behaviors of the piezoelectric nanoplate.

As is well addressed in the literature, the surface effects play a significant role in determining the size-dependent properties of nanostructures due to their large surface to volume ratio. Thus it is essential to incorporate the surface effects in the investigation of the static and dynamic behaviors of a piezoelectric nanoplate in addition to the flexoelectricity. Based on the surface piezoelectricity model and the extended linear piezoelectricity theory, this thesis established a modified Kirchhoff plate model with the consideration of both the surface effects and the flexoelectricity to capture the size effects on the electromechanical coupling fields of a bending piezoelectric nanoplate. The surface effects include the residual surface stress, surface elasticity, and surface piezoelectricity.

From the simulation results, it can be concluded that both the surface effects and the flexoelectricity play significant role in the static bending and vibrational behaviors of the piezoelectric plate. Such size effects upon the electroelastic responses and the vibrational behaviors are more pronounced with the decrease of the plate thickness. In addition, the influence of the surface effects and the flexoelectricity are sensitive to the surface material parameters, applied electric voltage and the plate dimensions. It also suggests a possible way for frequency tuning of piezoelectric nanoplate-based resonators by altering the applied electrical loading, which can be modified by either the flexoelectricity or the surface effects.

4.2 Recommendations for future work

This thesis has provided a theoretical prediction on how the surface effects and the flexoelectricity influence the size-dependent physical and mechanical properties of the piezoelectric nanostructures. However there are some limitations and issues for the current work that need to be addressed and some other issues needed to be further explored.

In the current work, some factors that might contribute to the size effects are neglected for the mathematically tractable purpose, for example, the higher order coupling between the strain and strain gradient, and the coupling between the strain gradient and strain gradient. If those factors are considered, more complex governing equations and boundary conditions will be derived to solve this problem. Therefore numerical solution technique has to be pursued for these cases in the future.

In addition, this thesis focuses on investigating the effects of the surface and the flexoelectricity upon the static bending and vibrational behavior of a clamped piezoelectric plate with four edges fixed. However, the piezoelectric nanoplates with other boundary conditions are necessarily needed to be studied. From the variational principle, the in-plane displacements and the transverse displacement are coupled. In addition, the mechanical boundary conditions for those plates are more complicated than the classical mechanical boundary conditions as they are altered by the flexoelectricity and the surface effects. Thus it is very difficult, if not impossible, to find the approximate analytical solutions for the plates. One may resort to the numerical techniques to get the solutions for such cases.

Moreover, the current work focuses on investigating the electromechanical couplings of a fundamental building block, i.e., plate structure. However, from the application point of view, the piezoelectricity-based nanodevices are complex structures, which may be multi-layered nanocomposites. Due to mathematical difficulty, the derivation of the analytical solutions of such piezoelectric nanostructures becomes a great challenge. Numerical solution technique must be resorted to investigate the influence of the surface effects and the flexoelectricity upon the performance of those complex nanodevices.

Curriculum Vitae

Name: Zhengrong Zhang

Post-secondary Education and Degrees:
Wuhan University of Technology
Wuhan, Hubei, China
2008-2012 B.E.

The University of Western Ontario
London, Ontario, Canada
2012-2014 M.E.Sc

Related Work Experience
Teaching Assistant
The University of Western Ontario
2012-2014

Research Assistant
The University of Western Ontario
2012-2014

Publications:

Zhang, Z. R., Yan, Z. and Jiang, L. Y., 2014. Flexoelectric effect on the electroelastic responses and vibrational behaviors of a piezoelectric nanoplate. J. Appl. Phys. **116** 014307

Zhang, Z. R. and Jiang, L. Y., 2014. Size effects on electromechanical coupling fields of a bending piezoelectric nanoplate due to surface effects and flexoelectricity. Submitted for publication.